THE INVESTIGATION ON THE MECHANISM OF NEUROPROTECTION BY ADENOSINE IN 1,3-DINITROBENZENE TOXICITY

by

Yipei Wang

A dissertation submitted in partial fulfillment
of the requirements for the degree of
Doctor of Philosophy
(Toxicology)
in The University of Michigan
2012

Doctoral Committee:

Professor Martin A. Philbert, Chair
Professor Richard A. Altschuler
Professor Richard F. Keep
Professor Raoul Kopelman
Assistant Professor Niladri Basu

© Yipei Wang

2012

DEDICATION

To my family and friends,

ACKNOWLEDGEMENTS

First and foremost, I would like to thank all members of my committee. I thank my mentor, Dr. Martin Philbert, for all of his support and guidance. I appreciate the opportunity to work under his mentorship and all his efforts to develop me as an independent research. I also thank Dr. Richard Keep, Dr. Nil Basu, Dr. Richard Altschuler and Dr. Raoul Kopelman for providing support and valuable suggestions.

I also want to give special thanks to Dr. Richardson and Dr. Fierke, who are equally important to my professional development. It was a great pleasure working with them on my first publication.

I want to acknowledge all the past and present members of the Philbert Lab including Dr. Stephen Steiner, Dr. Hao Xu, Dr. James Miller, Stephanie Runkle, Dr. Gwangseong Kim, Dr. Sonja Capracotta, Jen Fernandez, Dr. Angela Dixon, Laura Maurer, Ian Speirs and Kristen Russ. Special thanks to three undergrads that worked closely with me in various time: Brandon Schneider, Caitlin Parsons and Rebecca Gentner. I enjoyed working with you all and sincerely wish the best for your future endeavor.

I would like to thank faculties, administrative staff and my peer students outside of Philbert Lab. To mention a few: Dr. Loch Caruso, Dr. Craig Harris, Lauren Tetz, Cassandra Korte, Dr. Jaclyn Goodrich, Kelly Bakulski, Justin Colacino, Dr.

Nichole Hein, Sue Crawford, and Patrice Sommerville. The helpful discussions and shared emotions have made this journey more fun and enjoyable.

And I am grateful for having great friends outside of SPH, who have witnessed and shared struggles, happiness and growth with me. They are Dr. Jinjin Ma, Dr. Jing Chen, Dr. Tracy Xiao Liu, Xin Liu, Dr. Wenjing Chen, Chenxi Shen, Penny Bo Peng, Dr. Liuling Gong, Dr. Lyra Chang, Dr. Jiaying Tan, Xiaomei Chen, Nan Zhao, Zhenzhong Jia, Jie Cheng, Xiaojian You, Gang Su, and Youjian Chi. And for my friends (Panger, Wawa, Zhangting, Koukou, Xiaomubiaoer, Qiangqiang, Laomusisi, Tuantuan and Huahua, Han, Lulu, Huli) in China, US and Germany, I cannot tell how grateful I am to have known you in college and middle school. Our friendship shall always last.

Last but not least, I would like to thank my family Mom, Dad, and Grandpa for their financial and spiritual support throughout all five years. Without you, I cannot achieve any of it. To you, I dedicate this dissertation.

TABLE OF CONTENTS

DEDICATION ..... **ii**

ACKNOWLEDGEMENTS ..... **iii**

LIST OF EQUATIONS ..... **ix**

LIST OF FIGURES ..... **x**

LIST OF TABLES ..... **xii**

LIST OF ABBREVIATIONS ..... **xiii**

ABSTRACT ..... **xvi**

CHAPTER 1 INTRODUCTION **1**

1.1 OBJECTIVES 1

1.2 NITRO COMPOUNDS 2

1.2.1 Industrial application 2

1.2.2 Public health concerns 2

1.2.3 Individual nitro–substituted-benzenes 3

1.3 METABOLISM OF NITROBENZENE 4

1.3.1 Oxidation of nitrobenzene 4

1.3.2 Reduction of nitrobenzene 4

1.4 ACUTE ENERGY DEPRIVATION SYNDROMES 7

1.4.1 Histopathological analysis of AEDS 7

1.4.2 Causes of AEDS 7

1.5 MECHANISM OF 1,3-DNB TOXICITY 11

1.5.1 Systematic toxicity 11

1.5.2 Biochemical and molecular toxicity 13

1.6 KNOWLEDGE GAPS 16

1.6.1 Differential cellular sensitivity 16

1.6.2 Mechanism of neuroprotection 17

1.7 HYPOTHESIS 19

1.8 SPECIFIC AIMS 19

1.8.1 Specific aim 1: Test if 1,3-DNB exposure increases the extracellular adenosine level and the mechanism 20

1.8.2 Specific aim 2: Test if adenosine mediates neuroprotective effects in 1,3-DNB and the mechanism 20

1.9 FIGURES 21

1.10 TABLES 25
1.11 REFERENCES 30

CHAPTER 2 MIXED INHIBITION OF ADENOSINE DEAMINASE ACTIVITY BY 1,3-DINITROBENZENE: A MODEL FOR UNDERSTANDING CELL-SELECTIVE NEUROTOXICITY IN CHEMICALLY INDUCED ENERGY DEPRIVATION SYNDROMES IN BRAIN 37

2.1 ABSTRACT 37
2.2 INTRODUCTION 38
2.3 MATERIALS AND METHODS 42
2.3.1 Chemicals. 42
2.3.2 Purity of purchased adenosine deaminase (ADA). 43
2.3.3 Extinction coefficients of adenosine and inosine. 43
2.3.4 Adenosine deaminase (ADA) assay. 44
2.3.5 DI TNC-1 Cell Culture. 44
2.3.6 Measurement of adenosine and inosine from DI TNC-1 conditioned media. 45
2.3.7 Aggregation based inhibition. 45
2.3.8 Time dependence. 46
2.3.9 Native gel electrophoresis. 46
2.3.10 Measurement of particle size using dynamic light scattering (DLS). 47
2.3.11 Kinetics studies of 1,3-DNB inhibition of adenosine deaminase. . 47
2.3.12 Molecular modeling. 48
2.3.13 Cell fractionation. 50
2.3.14 Western blot analysis 51
2.3.15 Statistical analysis. 51
2.4 RESULTS 52
2.4.1 The purity and molecular weight of purchased ADA 52
2.4.2 Extinction coefficient of adenosine and inosine 52
2.4.3 1,3-DNB inhibits ADA activity 52
2.4.4 Effect of 1,3-DNB on the extracellular adenosine and inosine level in conditioned media 53
2.4.5 Aggregation based inhibition test 53
2.4.6 Time dependence 54
2.4.7 Denaturation experiment 55
2.4.8 Kinetics and curve fitting 55

2.4.9 ADA has multiple potential 1,3-DNB binding sites: the active site and peripheral sites 56
2.4.10 A_1R and ADA both exist on DI TNC-1 cells 57
2.5 DISCUSSION 57
2.6 ACKNOWLEDGEMENTS 64
2.7 EQUATIONS 66
2.8 FIGURES 67
2.9 TABLES 81
2.10 REFERENCES 86

CHAPTER 3 THE NEUROPROTECTIVE EFFECTS OF ADENOSINE IN 1,3-DINITROBENZENE TOXICITY IN RAT PRIMARY NEURONS 90

3.1 ABSTRACT 90
3.2 INTRODUCTION 92
3.3 MATERIALS AND METHODS 95
3.3.1 Chemicals and Supplies 95
3.3.2 Single Device Fabrication 97
3.3.3 Primary cortical neuron and primary astrocyte isolation 98
3.3.4 Purity test for primary neurons and primary astrocytes by immunocytochemistry of MAP-2 and GFAP 99
3.3.5 Adenosine level measurement in primary astrocytes 100
3.3.6 ATP level of primary neurons 100
3.3.7 Membrane integrity of primary neurons 101
3.3.8 Measurement of Fluo4-AM fluorescence in single well device .. 101
3.3.9 Quantification of cytoplasmic Ca2+ concentration 102
3.3.10 Statistical analysis 103
3.4 RESULTS 103
3.4.1 Primary cortical neuron and astrocytes purity 103
3.4.2 Extracellular adenosine increased in 1,3-DNB-exposed-astrocytes 104
3.4.3 ATP level in primary astrocytes 104
3.4.4 ATP level in primary neuron 104
3.4.5 Membrane integrity of primary neurons 105
3.4.6 Potassium induced cytoplasmic Ca^{2+} increased was suppressed by A1R agonist 105
3.5 DISCUSSION 106

3.6 ACKNOWLEDGEMENTS 111
3.7 EUQATION 112
3.8 FIGURES 113
3.9 REFERENCES 123

CHAPTER 4 CONCLUSION 128

4.1 OBJECTIVES 128
4.2 MAJOR RESULTS AND DISCUSSION 129
4.2.1 1,3-DNB is a mixed inhibitor of ADA 130
4.2.2 Extracellular adenosine levels increase in 1,3-DNB exposed primary astrocytes 132
4.2.3 Adenosine suppresses neuroexcitability and increases neuronal survival in 1,3-DNB toxicity 134
4.3 FUTURE DIRECTION 137
4.3.1 Metabolism and distribution of 1,3-DNB in brain 137
4.3.2 Docking 1,3-DNB onto other proteins 138
4.3.3 Microdialysis 138
4.3.4 Protein expression 138
4.4 REFERENCES 140
4.5 FIGURES 153

LIST OF EQUATIONS

Equation 2-1.Calculate IC_{50} in cooperative inhibition. 66
Equation 2-2. Global fitting for mixed inhibition mechanism. 66
Equation 2-3. Global fitting for noncompetitive inhibition mechanism. 66
Equation 2-4. Calculate positive cooperativity in k_{cat} and k_{cat} / K_M conditions 66

Equation 3-1. Calculate the fluorescence in neurons. 112

LIST OF FIGURES

Figure 1.1. The oxidative metabolism pathway of nitrobenzene. 21
Figure 1.2. Two electron transfer nitroreduction scheme. 22
Figure 1.3. One electron transfer nitroreduction scheme. 23
Figure 1.4. Summary of known affected components in AEDS. 24

Figure 2.1. Model describing inhibition of adenosine deaminase (E, ADA) catalyzed deamination of adenosine (S) to form inosine (P) by 1,3-dinitrobenzene (I, 1,3-DNB). 67
Figure 2.2. Characterization of purchased ADA. 68
Figure 2.3. Extinction coefficients of adenosine and inosine. 69
Figure 2.4. Structural and sequence alignments of 1,3-DNB and ADA. 70
Figure 2.5. 1,3-DNB inhibits the activity of ADA. 72
Figure 2.6. Extracellular adenosine (Ado) level, and extracellular inosine (Ino) plus hypoxanthine (HX) level in DMSO- and 1,3-DNB-treated DI TNC cells. 73
Figure 2.7. Evaluation of 1,3-DNB as an aggregation-based inhibitor. 74
Figure 2.8. Time-dependence of inhibition. 75
Figure 2.9. Native electrophoretic gel stained by Coomassie blue and rendered in grayscale. 76
Figure 2.10. Kinetics of inhibition of ADA by 1,3-DNB. 77
Figure 2.11. Docking studies reveal multiple energetically favorable binding sites in ADA. 78
Figure 2.12. Expression of ADA by western blot. 79
Figure 2.13. The proposed mechanism of increased adenosine level in 1,3-DNB toxicity. 80

Figure 3.1. Time course of 1,3-DNB neurotoxicity 113
Figure 3.2. Purity of primary astrocytes (A, B, C) and primary neurons (D, E, F) isolated from cortex pair from embryonic day 18 rat. 114
Figure 3.3. Extracellular adenosine level in DMSO and 1,3-DNB treated primary astrocytes. 115
Figure 3.4. Relative ATP levels measured by luminescence in primary astrocytes exposed to 1,3-DNB for 12 h. 116
Figure 3.5. ATP levels of primary neurons. 117
Figure 3.6. Ado and increased primary neuron membrane integrity measured by fluorescence in 1,3-DNB 12 h exposure. 119
Figure 3.7. Potassium induced cytoplasmic Ca^{2+} increase in intact primary neurons exposed to different chemicals for 12 h. 120
Figure 3.8. Quantification of peak fluorescence and the time to reach peak fluorescence. 122

Figure 4.1. Results summary. 153
Figure 4.2 Targets in 1,3-DNB toxicity. 154
Figure 4.3. Proposed neuroprotection mechanism of adenosine in 1,3-DNB toxicity. 155

LIST OF TABLES

Table 1-1. Comparison of Lesions Caused by Nitrobenzene, Dinitrobenzene and 1,3,5-Trinitrobenzene. 25
Table 1-2. Summary of 1,3-DNB Assess by *in vivo* Studies 26
Table 1-3. The Comparison of Two Reductive Pathways of Nitro Compounds. . 29

Table 2-1. Steady-state Parameters of Adenosine Deaminase in the Presence of 1,3-Dinitrobenzene [a] 81
Table 2-2. List of Steady-State Parameters and Goodness of Fit from the Global Fit of Adenosine Deaminase Activity [a] 82
Table 2-3. Analysis of Docked 1,3-Dinitrobenzene Clusters..... 83
Table 2-4. Estimated 1,3-DNB Concentration upon Administration to Rats in Previous Studies..... 85

LIST OF ABBREVIATIONS

1,3-DNB	1,3-Dinitrobenzene
6-AN	6-aminonicotinamide
6-ANADP	6-aminonicotinamide-adenine-dinucleotide-phosphate
A_1R	Adenosine Receptor 1
$A_{2a}R$	Adenosine Receptor 2a
$A_{2b}R$	Adenosine Receptor 2b
A_3R	Adenosine Receptor 3
ABP	Androgen Binding Protein
ADA	Adenosine Deaminase
ADP	Adenosine Diphosphate
AEDS	Acute Energy Deprivation Syndromes
AK	adenosine kinase
AMP	Adenosine Monoposphate
ANOVA	ANalysis Of VAriance between groups
AR(s)	Adenosine Receptor(s)
ATP	Adenosine Triphosphate
BCL-2	B-cell lymphoma 2
BCNU	1,3-bis(2-chloroethyl)-l-nitrosourea
BkA	Bongkrekic Acid
BSA	Bovine Serum Albumin
BSO	L-Buthionine-(SR)-sulfoximine
BTX	Benzene-Toluene-Xylene
CEB	Cytoplasmic Extraction Buffer

CGS 21680	3-[4-[2-[[6-amino-9-[(2R,3R,4S,5S)-5-(ethylcarbamoyl)-3,4-dihydroxy-oxolan-2-yl]purin-2-yl]amino]ethyl]phenyl]propanoic acid
CI	Confidence Interval
CNS	Central Nervous System
CPA	N6-Cyclopentyladenosine
CsA	Cyclosporin A
CSF	Cerebrospinal Fluid
DAPI	4',6-diamidino-2-phenylindole
DLS	Dynamic Light Scattering
DMEM	Dulbecco Modified Eagle's Medium
DMSO	Dimethyl Sulfoxide
DPBS	Dulbecco's Phosphate Buffered Saline
DPCPX	8-Cyclopentyl-1,3-dipropylxanthine
ENT	Equilibrative Nucleoside Transporters
ESR	Electron Spin Resonance
FBS	Fetal Bovine Serum
GCS	γ-glutamylcysteine synthetase
GFAP	Glial Fibrillary Acidic Protein
GR	Glutathione Reductase
GSH	Glutathione
GSSG	Glutathione Disulfide
HBSS	Hank's Balanced Salt Solution
HEPES	(4-(2-hydroxyethyl)-1-piperazineethanesulfonic acid
IC_{50}	Concentration Inhibiting 50%
k_{cat}	Turnover Number
KCl	Potassium Chloride
K_I	Dissociation Constant (Inhibitor to Enzyme)

K_{IS}	Dissociation Constant (Inhibitor to Enzyme-Substrate Complex)
K_M	Michaelis-Menten Constant
KOH	Potassium Hydroxide
LC/MS/MS	Liquid Chromatography–Mass Spectrometry
LDH	Lactate Dehydrogenase
MAP-2	Microtubule-Associated Protein-2
MEB	Membrane Extraction Buffer
mtPTP	Mitochondrial Permeability Transition Pore
NADP	Nicotinamide Adenine Dinucleotide Phosphate
NADPH	reduced Nicotinamide Adenine Dinucleotide Phosphate
NBT	Nitroblue Tetrazolium
NGS	Normal Goat Serum
NMDA	N-Methyl-D-aspartic Acid
PDHc	Pyruvate Dehydrogenase complex
PDL	Poly-D-lysine
PDMS	Polydimethylsiloxane
PLL	Poly-L-lysine
PSG	Penicillin, Streptomycin, Glutamate
ROS	Reactive Oxygen Species
SDH	Succinate Dehydrogenase
SDS	Sodium Dodecyl Sulfate
TCA	Tri-Carboxylic Acid
TMRM	Tetramethylrhodamine
TPP	Thiamine Pyrophosphate
V_{max}	Maximum Velocity

ABSTRACT

Used as an intermediate in plastic and explosive industries, 1,3-dinitrobenzene (1,3-DNB) causes cell-specific lesions in brain stem. *In vivo* studies have shown that reduced neuronal activity decreases dependence upon glucose metabolism and reduces neuronal damage in rats. However the molecular mechanism of this neuroprotection has remained elusive. This dissertation hypothesizes that 1,3-DNB is an inhibitor of adenosine deaminase (ADA), and that inhibition of ADA increases local extracellular adenosine levels. Elevated extracellular adenosine provides neuroprotection by binding to the inhibitory adenosine receptor 1 (A_1R) to suppress the excitability of neurons.

Firstly, using spectrophotometry, we showed that 1,3-DNB inhibited ADA with an IC_{50} of 284 µM. Computational modeling and kinetics studies suggest mixed inhibition with one and four 1,3-DNB molecules binding to active and peripheral sites of one human ADA molecule, respectively. Second, we examined whether inhibition of ADA increases extracellular adenosine concentration ($[Ado]_e$) in primary astrocyte-conditioned media using enzyme-based sensors. We found that $[Ado]_e$ elevated significantly to 4-6 µM in primary astrocytes, a two or three magnitude increase compared to physiological conditions. Finally we assessed adenosine-mediated neuroprotection in cultures of rat primary neurons. Results show that addition of exogenous adenosine (10 and 100 µM) to 1,3-DNB

exposed neurons increased ATP levels by 25% and 50% respectively. 100 µM CPA (an A_1R agonist) increased membrane integrity of neurons by approximately 100%. Adenosine 5 µM also significantly delayed onset and reduced the magnitude of cytoplasmic Ca^{2+} increases by binding to A_1R. Both neuroprotection and suppressed excitability are mediated by activation of A_1R, as demonstrated by application of AR agonists and antagonists.

This work advances understanding of the effects of 1,3-DNB and similar environmental/industrial chemicals on enzymes in the energy metabolism pathway and provides a mechanistic explanation for the observed mixed inhibition of ADA. The role of adenosine-mediated neuroprotection through modulation of cytoplasmic Ca^{2+} increase elicited by exogenous KCl stimulation is explored using pharmacologic agonists and antagonists of the A_1R.

CHAPTER 1

INTRODUCTION

1.1 OBJECTIVES

This dissertation examines the mechanisms of cell specific injury and protection by using a prototypical neurotoxicant, 1,3-dinitrobenzene (1,3-DNB). Findings in cultured cells and isolated enzyme preparations are confirmed by the employment of *in silico* methods. **It is hypothesized that 1,3-DNB is an inhibitor of adenosine deaminase (ADA), and that inhibition of ADA increases local extracellular adenosine levels. Elevated extracellular adenosine binds in turn to the inhibitory adenosine receptor 1 (A_1R) and suppresses the excitability of neurons, leading to reduced energy consumption and neuroprotection.**

This work advances understanding of the effects of 1,3-DNB and similar environmental/industrial chemicals on enzymes in the energy metabolism pathway and provides a mechanistic explanation for the observed mixed inhibition of ADA. Additionally, this study assesses adenosine-mediated neuroprotection in cultures of rat primary neurons. The role of adenosine-mediated neuroprotection through modulation of cytoplasmic Ca^{2+} increase elicited by exogenous KCl stimulation is explored using pharmacologic agonists and antagonists of the A_1R.

This research provides basic mechanistic information that may be incorporated into the development of therapeutic strategies for mitigating occupational or accidental exposure to nitro- and related compounds that induce energy deprivation syndromes in brain.

1.2 NITRO COMPOUNDS

1.2.1 Industrial application

Nitro compounds have extensive industrial applications in the manufacture of specialized products such as explosives, plastics and pharmaceuticals. Nitro compounds provide a commercially viable source of nitrogen atoms affixed to an aromatic ring for the synthesis of a wide variety of compounds. Approximately 5% of total benzene-toluene-xylene (BTX) is used to produce nitro compounds worth in excess of $2 billion annually. These nitro compounds are further derivatized into downstream consumer and other products with a 1985 reported value of $12-15 billion worldwide (Rickert, 1985).

1.2.2 Public health concerns

The value and size of this industry suggest the potential for a significant risk for occupational exposure and for coincidental exposures for those living near or adjacent to these sites. Exposure typically occurs by breathing contaminated air, drinking contaminated water or contact with contaminated food or soil (U.S. Department of Health and Human Services, 1995, U.S. Environmental Protection Agency, 1997, 2009)

1.2.3 Individual nitro–substituted-benzenes

Nitrobenzene, dinitrobenzene and trinitrobenzene have been reported to be toxic to multiple organs and systems in human and animal subjects. Clinical manifests include methemoglobinemia, neurological symptoms (e.g. paralysis, ataxia and nausea) and liver damage (Parke, 1961, Ikeda and Kita, 1964, Cody et al., 1981a, Beauchamp et al., 1982, Morgan et al., 1985, Philbert et al., 1987).

A comparison of the toxicities and lesions caused by these three kinds of chemicals is provided in Table 1-1. A summary of toxicity and histopathological examination of 1,3-DNB, is provided in

.

1.3 METABOLISM OF NITROBENZENE

It has been suggested that the toxicity of nitro compounds comes from the generation of free radicals during the process of metabolism (Reeve and Miller, 2002b, Li et al., 2003, Hsu et al., 2007). The metabolism of nitro compounds generates both oxidative and reductive products (Rickert, 1987).

1.3.1 Oxidation of nitrobenzene

The primary oxidation of nitrobenzene, for example, occurs in the endoplasmic reticulum of liver, with the intermediate being *p*- or *m*-nitrophenol. Ensuing secondary conjugation with sulfate or glucuronide results in a molecule that may be readily eliminated in the urine (Figure 1.1) (Rickert, 1987). Hydroxylation of the benzene ring is relatively slow compared to the rates of nitroreduction. However, nitrophenols and their conjugated metabolites were detected in the urine of different species, including humans, mice and rats (Salmowa et al., 1963, Rickert et al., 1983). In Fischer-344 rats, nitrophenols were not detected, but the sulfate and glucuronide conjugated nitrophenols account for approximately 30% of the total urinary excretion (Rickert et al., 1983). This fact suggests that despite of the slow rate, the oxidation pathway is not negligible *in vivo* in rats.

1.3.2 Reduction of nitrobenzene

Compared to nitro oxidation, nitro reductive pathways have been more extensively studied in both *in vivo* and *in vitro* systems and it is generally agreed that biological reduction of nitro groups requires enzymatic catalysis coupled with

the generation of reactive intermediates (Rickert, 1985, Hu et al., 1997a, Hsu et al., 2007). Mutant bacteria lacking nitroreductases are immune to the toxicity of nitro compounds. Ascorbate in relatively high concentrations is the only known non-enzymatic catalyst for the biological reduction of nitroaromatic chemicals (Biaglow et al., 1978).

1.3.2.1 Nitroreductases

Known enzymes with the capacity for nitroreduction include NADPH-cytochrome P450 reductase, xanthine oxidase, and aldehyde oxidase (Mason and Holtzman, 1975, Harada and Omura, 1980). The reductive capabilities of these three enzymes are especially sensitive to oxygen concentrations, with >70% inhibition of the reduction in the presence of air (Mason and Holtzman, 1975, Rickert, 1985). It is believed that oxygen reverses the nitroreduction process by exchanging electron with nitro radicals to convert them back to parent compounds (Mason and Holtzman, 1975). In ambient aerobic conditions, metabolism of 1,3-DNB is inhibited within the first 5 min of incubation (Reeve and Miller, 2002b). The latter finding in combination with the predominantly vascular endothelial distribution of xanthine oxidase in brain (Betz, 1985), correlated well with the observation of hemorrhagic stroke as an early sign of 1,3-DNB toxicity (Cavanagh, 1993).

1.3.2.2 Two reduction mechanisms

Two pathways have been identified for nitroreduction: a) intestinal microfloral and b) the essentially identical somatic microsomal and erythrocytic pathways. The first pathway is a three-steps process, with two-electron transfer in each step, as

shown in Figure 1.2 (Reddy et al., 1976, Levin and Dent, 1982). The second is a six-step process with one electron transfer in each step, as shown in an electron spin resonance (ESR) study (Figure 1.3) (Mason and Holtzman, 1975, Holder, 1999).

The comparison of rat (Fischer-344) hepatic microsomes and cecal microflora suggests that the bacterial catalysis is 200 times faster than the microsomal pathway, and is thus likely to play a more important role in the complete reduction of nitro compounds: especially in the anaerobic environment of the later segments of the gut (Levin and Dent, 1982). Another study comparing the metabolism rates of 1,3-DNB in liver microsomes and liver mitochondria found that liver microsomes had greater capacity for the metabolism of 1,3-DNB (Reeve and Miller, 2002b). Of the reductive metabolites tested, only nitrosonitrobenzene induced similar histological changes as 1,3-DNB in Sertoli cells (Foster, 1989). Interestingly, in a study to assess the capacity of Fischer-344 rat tissues to metabolize 1,3-DNB, only slices from forebrain and brain stem produced nitrosonitrobenzene; the slices from liver slices did not (Hu et al., 1997a). However, no similar studies have been performed in cells of neural origin.

1.3.2.3 The "*futile cycle*"

The generation of nitroaromatic radicals from other compounds such as nitrofurantoin, nitrofurazone and nitrobenzoate has been confirmed experimentally by ESR (Sealy et al., 1978). In the presence of oxygen, the nitroaromatic radicals were quickly converted back to the parent compound with concomitant conversion of oxygen to superoxide (Perez-Reyes et al., 1980,

Holder, 1999). The production of superoxide, the abundance of peroxidases in the brain and the availability of physiological levels of adenine nucleotides provides a plausible molecular mechanism for the sustained production of reactive intermediates that might accelerate free radical mediated damage of DNA and the carcinogenicity of nitrobenzene. However, the exact mechanism of carcinogenicity of nitrobenzenes and related nitroaromatic compounds is not known.

1.4 ACUTE ENERGY DEPRIVATION SYNDROMES

1,3-dinitrobenzene (1,3-DNB) causes pathological changes that resemble the lesions observed in Acute Energy Deprivation Syndromes (AEDS) produced by several known antimetabolites involved in energy metabolism (Cavanagh, 1993).

1.4.1 Histopathological analysis of AEDS

AEDS describes a set of neuropathological changes that involve glio-vascular lesions, with secondary neuronal damage (Cavanagh, 1993). Some commonly observed characteristics include symmetrical brain stem lesions and selective neuronal damage. In the affected regions, light and electron microscopy show that astrocytes retract from neurons and blood vessels with attendant enlarged Virchow-Robin spaces and swollen foot processes (Aschner and Costa, 2005).

1.4.2 Causes of AEDS

AEDS can be caused by chemicals such as (S)-α-chlorohydrin(Cavanagh and Nolan, 1993), 6-aminoicotinamide (Kauffman and Johnson, 1974) and methyl

bromide (Cavanagh, 1992, Squier et al., 1992), or by disease including thiamine deficiency or Leigh's disease (Cavanagh, 1993, Philbert et al., 2000).

1.4.2.1 Idiopathic and mitochondrial genomic diseases

Leigh's Necrotizing Encephalopathy- Leigh's Disease

Leigh disease is an inherited disorder caused by mitochondrial or nuclear gene mutations. The mutations lead to the deficiency of a series of enzymes required for energy metabolism, including pyruvate dehydrogenase and complex I, II and IV [red stars, Figure 1.4; (Brown and Squier, 1996)]. Disturbances in brain energy metabolism affect the most active regions and nuclei of the brain resulting in movement disorders and dystonias (Brown and Squier, 1996, Dahl, 1998). Histopathological evaluation reveals symmetrical cystic lesions in the brain stem (inferior colliculus, cerebellar nuclei and substantia nigra) and basal ganglia. Most of these lesions involve perturbations in the morphology of the capillary bed (Cavanagh and Harding, 1994, Dahl, 1998).

Wernicke's encephalopathy

Wernicke's encephalopathy is also known as thiamine (vitamin B1) deficiency or beriberi. This syndrome can be inherited or result from malnutrition associated with alcoholism (Martin et al., 2003, Bradley, 2008). Like other AEDS, the clinical manifestitation of Wernicke's encephalopathy includes ataxia, nystagmus and confusion. Affected regions in the brain include the mammillary bodies, superior and inferior colliculi and the ocular motor nucleus in humans. The severity and combination of affected regions vary among different species (Cavanagh, 1993).

Thiamine is essential for the formation of thiamine pyrophosphate (TPP) in the tri-carboxylic acid (TCA) cycle, without which the pyruvate dehydrogenase complex (PDHc) cannot decarboxylate pyruvate into acetyl CoA (orange star, Figure 1.4) (Butterworth et al., 1993, Sedel et al., 2008). Again, those areas in the forebrain with the greatest requirement for energy equivalents are the most vulnerable to pathologic change.

1.4.2.2 Chemicals

<u>α-chlorohydrin</u>

In rats, exposure to 50 mg/kg/day or higher doses of α-chlorohydrin for 3-4 days induces lesions in trigeminal, auditory, and vestibular pathways of the brain. More specifically, the affected areas includes mammillary bodies, inferior colliculi, oculomotor nucleus, red nucleus, lateral leminiscus nucleus, substantia nigra, superior olivary nucleus, cochlear, cerebellar roof nuclei and vestibular nulei (Cavanagh and Nolan, 1993).

(S)- α-chlorohydrin together with other chlorosugars can be metabolized to (S)-3-chlorolactaldehyde, a specific inhibitor of glyceraldehyde 3-phosphate dehydrogenase (Stevenson and Jones, 1985). The inhibition of glyceraldehyde 3-phosphate dehydrogenase leads to reduced energy generation (blue star, Figure 1.4).

<u>6-aminonicotinamide (6-AN)</u>

6-Aminonicotinamide also produces lesions in the central nervous system (CNS) in a pattern similar to α-chlorohydrin. 10 mg/kg 6-AN i.p. in rats produces early

neuroglial necrobiosis and secondary neuronal damage (Schneider and Cervos-Navarro, 1974). Light and electron microscopy examination showed cytoplasmic swelling of neuroglial cells and ballooned structure in the neuropil of gray matter, with better preservation of neurons in necrotic regions. Affected regions were constrained to the lower brain stem, including vestibular and cochlear nuclei and the cerebellar roof nuclei (Schneider and Cervos-Navarro, 1974).

Due to the similarity in structure, 6-AN acts as a pseudo substrate and incorporates itself in NADP synthesis, forming 6-ANADP, a product that can only be slowly eliminated from the system. 6-ANADP is a potent inhibitor of the 6-phosphogluconate dehydrogenase, leading to disturbance in energy metabolism (Green star, Figure 1.4) (Meyer-Estorf et al., 1973).

1,3-dinitrobenzene (1,3-DNB) and other nitro compounds

Several nitro compounds have been reported to cause similar neuropathological changes. For example, 1,3-DNB is known to induce focal, bilateral edematous lesions in the vestibular and auditory pathways of the brainstem (Philbert et al., 1987). Drugs, such as nitrofurantoin, misonidazol and metronidazole, also produce similar lesions with a minor difference in inducing neuronal degeneration from the distal axons (Cavanagh, 1993). One common characteristic of these nitro compounds is that they undergo nitroreduction, thus generating free radicals described in Figure 1.3.

1,3-DNB has been used as a model chemical to induce AEDS. Previous results have shown that 1,3-DNB induced mitochondrial depolarization in a dose

dependent manner (Tjalkens et al., 2003) and inhibited the activity of complex II in primary rat astrocytes (Phelka et al., 2003). Recent research of 1,3-DNB has shown that it directly inhibits the activity of pyruvate dehydrogenase complex, resulting in significantly reduced ATP level in C6 glioma cells (Miller et al., 2011a). Another study demonstrated that 1,3-DNB exposure leads to oxidative carbonlyation of F1-ATP synthase beta-subunit [yellow stars, Figure 1.4; (Steiner and Philbert, 2011)].

1.5 MECHANISM OF 1,3-DNB TOXICITY

1.5.1 Systematic toxicity

1.5.1.1 Hematological system

1,3-DNB causes methemoglobinemia in humans and in different animal species (Cody et al., 1981a, Cossum and Rickert, 1987, Philbert et al., 1987, Blackburn et al., 1988a, Kumar et al., 1990). Since methemoglobinemia is not a seminal finding in the complex of AEDS and is not required or sufficient for the formation of neuropathological lesions, it will be not discussed in details in this section.

1.5.1.2 Reproductive system

The reproductive toxicity of 1,3-DNB appears to be gender specific. Female rats received oral administration of 50, 100 or 200 mg/l/day in drinking water for 8 weeks did not present significant lesion in ovaries. Although a decrease of ovary weight was observed, it was proportional to body weight loss (Cody et al., 1981a). At the two highest concentrations, the reduced weight of the testis exceeded the

proportional weight reduction of the body (Cody et al., 1981a). The mechanism for the gender specific injury has been fully understood yet.

1.5.1.3 Neurological system (differential regional sensitivity)

The differential regional sensitivity has been summarized in Table 1-1 and

. In brief, brain stem nuclei are the major affected area, whereas hippocampus or cortex is not affected.

1.5.2 Biochemical and molecular toxicity

Several attempts have been made to explore the molecular mechanism of 1,3-DNB toxicity. The findings, including oxidative stress, mitochondrial damage and enzyme inhibition, are summarized below.

1.5.2.1 Glutathione depletion

Glutathione (GSH) plays a critical role in cellular defense against oxidative stress as an antioxidant and cofactor of glutathione peroxidase in the CNS (Aoyama et al., 2008). The distribution of glutathione in a normal cell is relatively even, except the rough endoplasmic reticulum contains little. When oxidative stress causes GSH depletion, cellular GSH depletes first and mitochondrial GSH reserves last (Ault and Lawrence, 2003).

Exposure to 1,3-DNB induces intracellular GSH depletion in rat primary astrocytes isolated from hippocampus. Glutahtione depletion is dependent upon both time and dose (Romero et al., 1995). A 0.5 mM 1,3-DNB exposure, caused GSH to decrease significantly by 50% within a 2 h exposure, a temporal window that is too soon for vascular damage to develop (Philbert et al., 1987). This result suggests that GSH depletion happens prior to tissue damage in 1,3-DNB toxicity.

When the regeneration of GSH from GSSG was inhibited by 1,3-bis(2-chloroethyl)-l-nitrosourea (BCNU), an inhibitor of glutathione reductase, (GR), 0.5 mM 1,3-DNB caused significant lactate dehydrogenase (LDH) leakage in type I

rat primary astrocytes, while 0.5 mM 1,3-DNB or BCNU by itself did not cause such cytotoxicity (Romero et al., 1996).

In another study, L-Buthionine-SR-sulfoximine (BSO) was injected to ventricles to inhibit the γ-glutamylcysteine synthetase (GCS) in GSH synthesis. Decreased GSH level was detected together with more prominent ataxia and more profound pathologic alterations in brain stem nuclei (Hu et al., 1999).

These results suggest that GSH depletion may contribute to 1,3-DNB toxicity.

1.5.2.2 Mitochondrial damage

1,3-DNB also decreases mitochondrial membrane potential, measured by fluorescent intensity of tetramethylrhodamine (TMRM). The rapid decrease occurred within the first 5 min of exposure and decreased to 20% of the original potential within 40 min (Tjalkens et al., 2000a).

This 1,3-DNB induced mitochondrial depolarization can be prevented by pre-treatment with bongkrekic acid (BkA) (Tjalkens et al., 2003). BkA is a known inhibitor of the mitochondrial permeability transition pore (mtPTP) (Zamzami et al., 1996, Marzo et al., 1998). This prevention effect of BkA indicates that the loss of membrane potential is mediated through mtPTP.

The mitochondrial regulatory protein, B-cell lymphoma 2 (BCL-2) belongs to the BCL-2 family and also regulates apoptosis (Hockenbery et al., 1993, Hengartner, 2000). Overexpression of BCL-2 increased the threshold of 1,3-DNB concentration to induce mtPTP opening in primary astrocytes (Phelka et al., 2006).

1.5.2.3 Oxidative stress

Reactive oxygen species (particularly inorganic and organic peroxides) in 1,3-DNB exposure have been measured in SY5Y neuroblastoma and C6 glioma cells using a redox-sensitive dye (Tjalkens et al., 2000a). Oxidative stress significantly increased 10 min after 1,3-DNB exposure. 50 µM and 500 µM 1,3-DNB caused 4.6 and 6 fold reactive oxygen species (ROS) increase compared to vehicle control groups in SY5Y and C6 cells, respectively (Tjalkens et al., 2000a).

Another study using MitoSOX to measure ROS, found that ROS production reached a peak at 5 h in 1 mM 1,3-DNB exposure (Steiner and Philbert, 2011). The occurrence of maximum ROS was concurrent with mitochondrial depolarization. In addition, pre-treatment with BkA significantly reduced the production of ROS (Steiner and Philbert, 2011), indicating that ROS generation may be related to the loss of membrane potential in 1,3-DNB toxicity.

1.5.2.4 Enzyme inhibition/dysfunction

1,3-Dinitrobenzene directly inhibits or causes dysfunction in several enzymes in the energy metabolism pathway. 100 µM 1,3-DNB temporal inhibited the activity of succinate dehydrogenase (SDH, also known as complex II) in astrocytes. The inhibition occurred fast within 0.5 h (Phelka et al., 2003). Cyclosporin A (CsA) can prevent the opening of mtPTP (Mott et al., 2004). Since adding CsA to primary astrocytes did not reverse the inhibition of SDH, it appears that the inhibition of SDH and opening of mtPTP are two independent mechanisms.

Another important enzyme in ATP metabolism pathway, pyruvate dehydrogenase complex (PDHc) (Figure 1.4), was inhibited directly by 1,3-DNB, assessed by both purified PDHc coincubation with 1,3-DNB and chemical reduction of nitroblue tetrazolium (NBT) in cells (Miller et al., 2011a).

A recent study shows that 1,3-DNB is also a mixed inhibitor of adenosine deaminase (ADA), binding to both ADA and the enzyme-substrate complex (Wang et al., 2012). Computational modeling indicated that the structure of 1,3-DNB overlaps with the adenine group of adenosine, leading to binding in the active site (Wang et al., 2012).

Besides the direct binding and inhibition mechanism mentioned above, 1,3-DNB also carbonylate proteins. Two mitochondrial proteins, mtHsp 70 and F1-ATP synthase beta-subunit have been identified as the carbonxylated protein by LC/MS/MS (Steiner and Philbert, 2011).

1.6 KNOWLEDGE GAPS

1.6.1 Differential cellular sensitivity

Besides gender and brain region specificity, cell specific injury was also observed in the male reproductive and neurological systems. A single dose of 25 mg/kg 1,3-DNB produces lesions, including vacuolation and retraction of Sertoli cell cytoplasm and primary spermatocyte degeneration 12 and 24 h after administration (Blackburn et al., 1988a). A Sertoli cell-specific protein, androgen binding protein (ABP), was detected in the plasma (Reader et al., 1991). Sertoli

cells are the “nursing” cells that provide structural support and nutrients during spermatogenesis (O'Shaughnessy et al., 2009).

Similar selectivity was observed in brain lesion. Edematous alterations such as swelling of astrocyte foot processes and astrocyte necrosis were significant within 12-24 h, while neuronal damage occurred only after 48 h (Philbert et al., 1987, Romero et al., 1991). Astrocytes play an important role in maintaining extracellular and intercellular homeostasis, by removing excitotoxic neurotransmitters and providing antioxidants for neurons (Allaman et al., 2011, Belanger et al., 2011).

It is an interesting fact that in both the male reproductive system and neurological system, the supporting cell types (Sertoli and astrocytes) were the primary targets. The molecular mechanism of this cell specific injury is not fully understood, largely because substantial studies have focused on astrocytes cells, and only limited research of 1,3-DNB toxicity has been performed on neurons. Since neurons cannot regenerate but astrocytes can (Silver and Miller, 2004), understanding the neuroprotective mechanism could potentially enable us to develop therapies for neurological diseases resulting from both occupational exposure and gene deficiency.

1.6.2 Mechanism of neuroprotection

To assess if reduced neuronal activity is associated with less severe lesion in 1,3-DNB toxicity, chemicals that either stimulate or suppress neuronal activity were administered in conjunction with 1,3-DNB. One chemical, Bifenthrin caused

ataxia with 3 x 9 mg/kg 1,3-DNB, a dosage that did not cause ataxia by itself. In contrast, anaesthesia such as isoflurane and urethane led to a milder lesion (Holton et al., 1997). Besides chemicals, surgical modification (one side tympanic membrane rupture) also showed that reduced auditory function coincided with reduced metabolism and attenuated lesion in rats (Ray et al., 1992). These *in vivo* studies suggest that reduced neuronal activity decreases the severity of lesion in 1,3-DNB toxicity.

Although currently there has not been study to address the molecular mechanism of neuroprotection in 1,3-DNB toxicity, several studies have found that adenosine mediates neuroprotection in pathological conditions such as hypoxia/ischemia, excitotoxicity and trauma (Logan and Sweeney, 1997, Sweeney, 1997, de Mendonca et al., 2000, Sperlagh and Vizi, 2011).

The molecular mechanism of adenosine neuroprotection has been well summarized (de Mendonca et al., 2000). In brief, adenosine binds to both presynaptic and postsynaptic adenosine receptor 1 (A_1R). By binding to the presynaptic receptors, adenosine reduces Ca^{2+} influx, leading to reduced glutamate release and decreased NMDA receptor activation. By binding to postsynaptic receptors, adenosine reduces K^+ efflux, leading to hyperpolarization and decreased NMDA receptor activation. All these events result in reduced Ca^{2+} influx and thus contribute to neuroprotection.

With the aid of more advanced visualization tools and a more thorough understanding of the mechanism of adenosine neuroprotection in pathological

conditions, we can further study the molecular mechanism of selective cell injury and the role of adenosine in this mechanism.

1.7 HYPOTHESIS

In response to 1,3-DNB toxicity, primary astrocytes release adenosine. Activation of adenosine 1 receptors (A_1R) by elevated extracellular adenosine level in turn suppresses neuron excitability and promotes neuronal survival in 1,3-DNB toxicity.

1.8 SPECIFIC AIMS

The following specific aims have been conducted to test the aforementioned hypothesis.

1.8.1 Specific aim 1: Test if 1,3-DNB exposure increases the extracellular adenosine level and the mechanism

1.8.1.1 Measure the extracellular adenosine level in 1,3-DNB exposed DI TNC cells

1.8.1.2 Measure the kinetics of adenosine deaminase in the presence of 1,3-DNB

1.8.1.3 Determine the mechanism of inhibition

1.8.2 Specific aim 2: Test if adenosine mediates neuroprotective effects in 1,3-DNB and the mechanism

1.8.2.1 Measure the effects of adenosine on 1,3-DNB exposed primary neurons

1.8.2.2 Measure the excitability of 1,3-DNB exposed neurons with and without the presence of adenosine

1.9 FIGURES

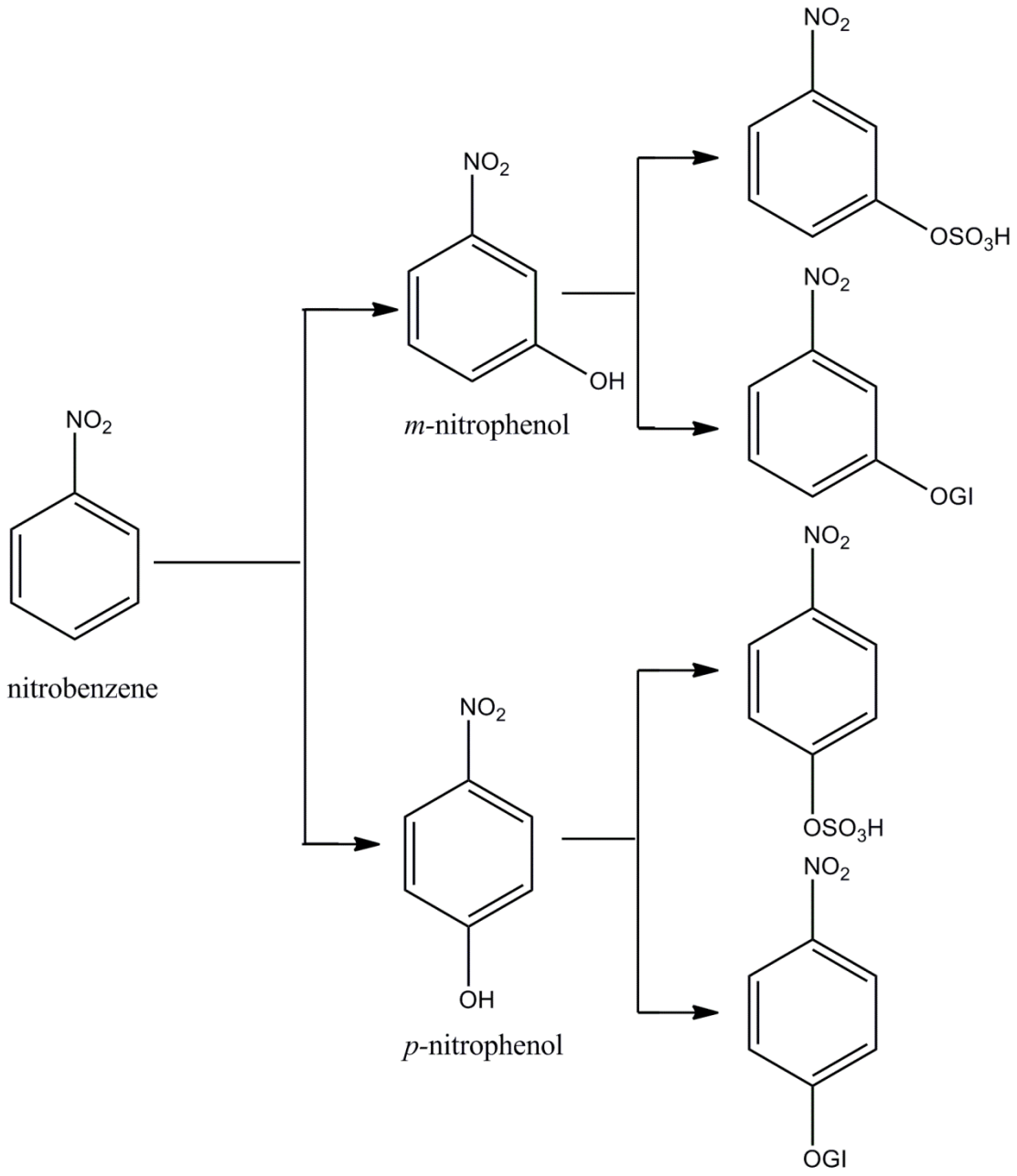

Figure 1.1. The oxidative metabolism pathway of nitrobenzene.

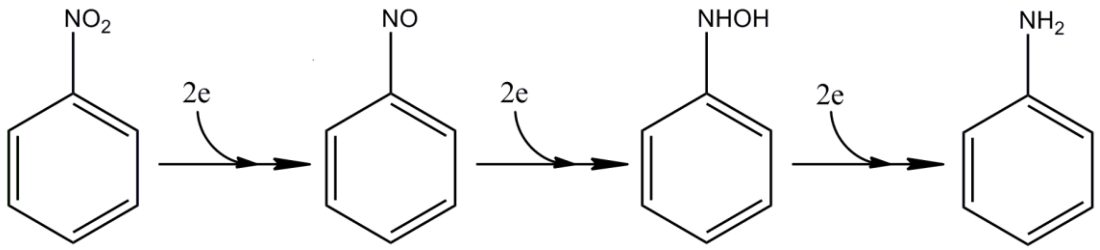

Figure 1.2. Two electron transfer nitroreduction scheme.

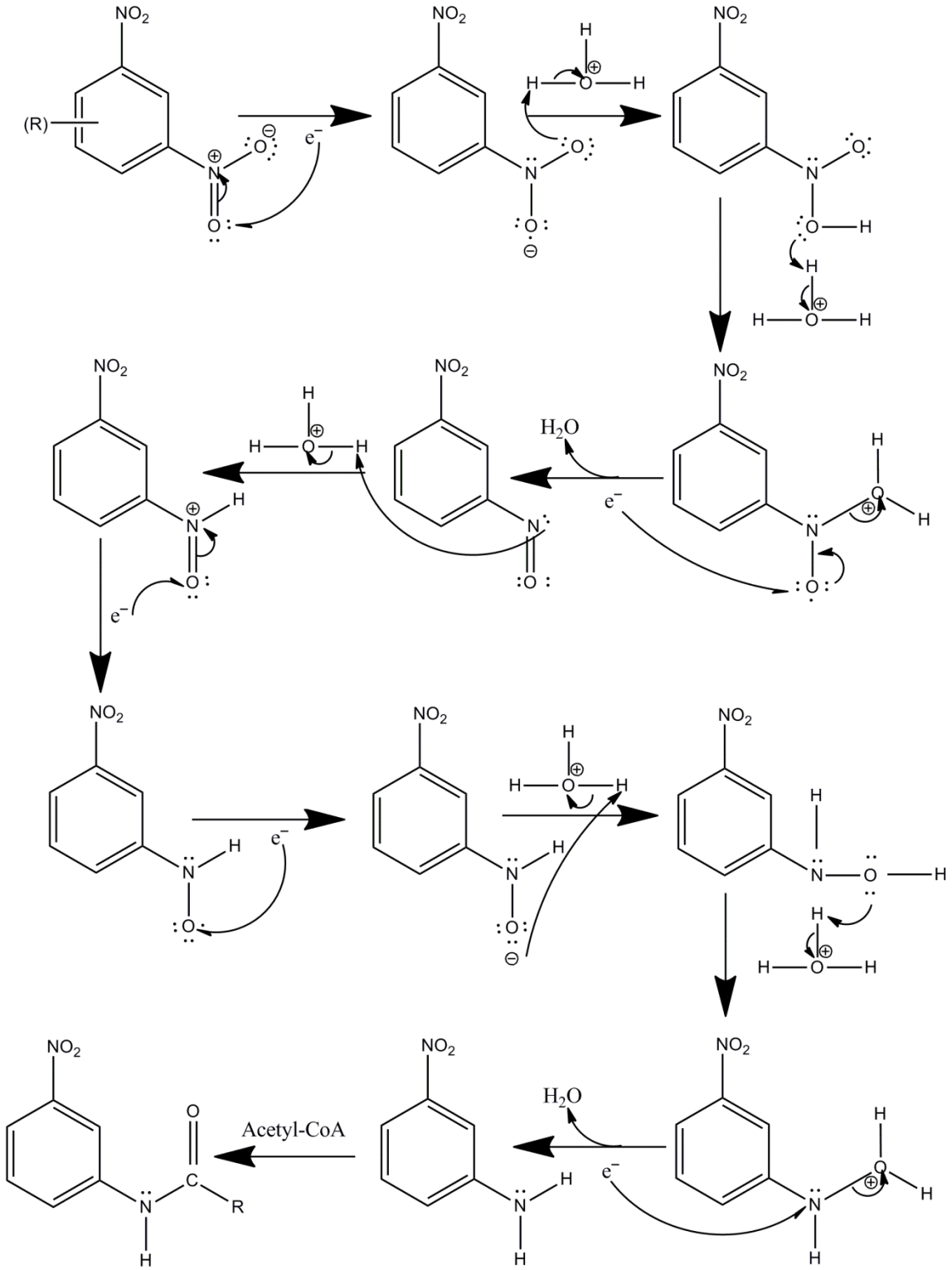

Figure 1.3. One electron transfer nitroreduction scheme.

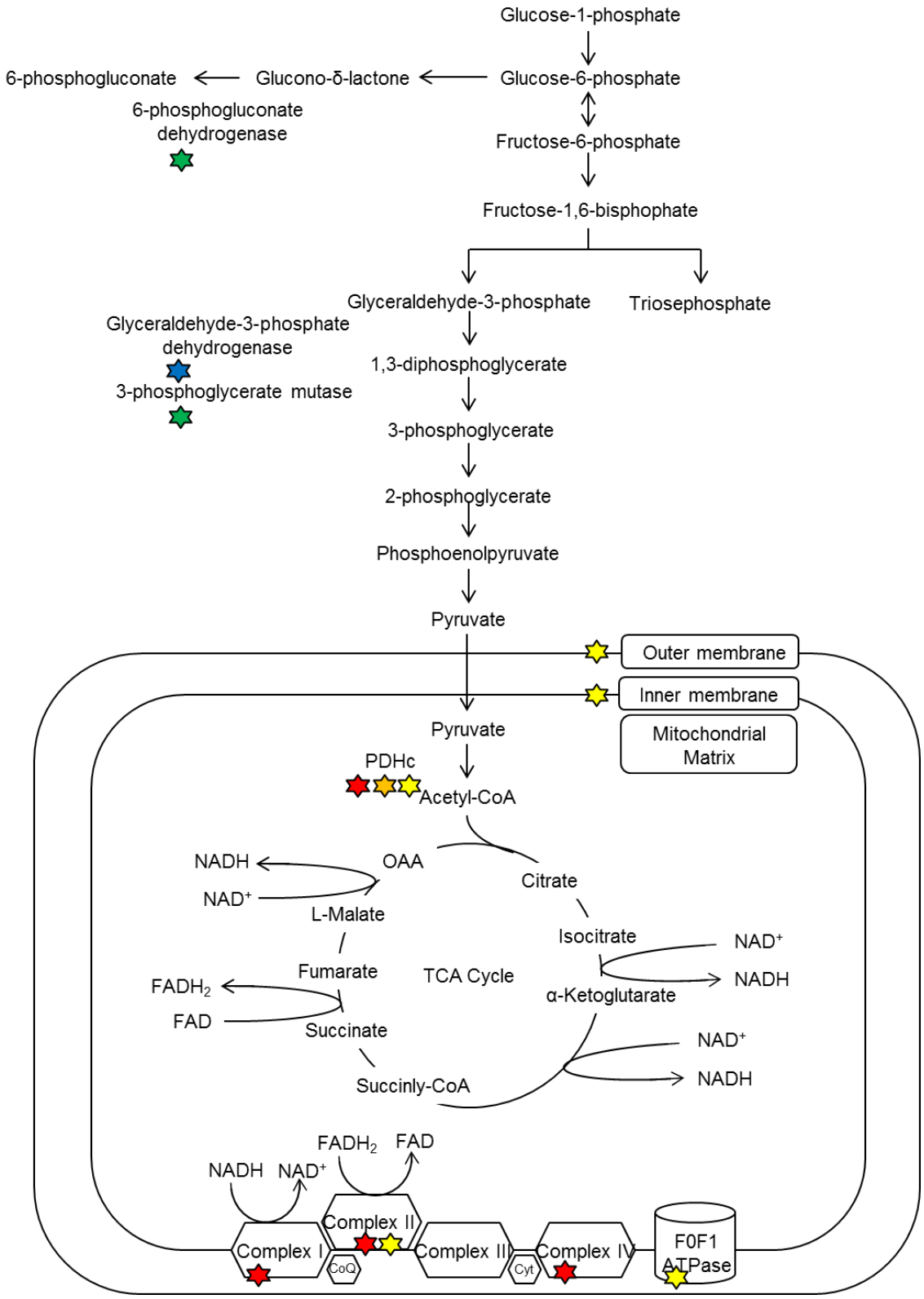

Figure 1.4. Summary of known affected components in AEDS.

1.10 TABLES

Table 1-1. Comparison of Lesions Caused by Nitrobenzene, Dinitrobenzene and 1,3,5-Trinitrobenzene.

Chemical	Animal	Dosage	Time to develop symptoms	Symptoms	Histopathology	Regions
NB [a]	Male Fischer-344 rats	550 mg/kg	Single dose	Ataxia	Hemorrhages in brain stem and cerebellum Bilaterally symmetrical degenerative changes in vestibular nuclei Edematous swelling of bounded tissue compartment	Vestibular nuclei and other nuclei lying near the lateral margins of the fourth ventricles
1,3-DNB [b]	Male Fischer-344 rats	Germ free: Oral dose of 20mg/kg	Single dose	Methaemoglobinaemia and frequently ataxia	Bilaterally symmetrical vacuolated lesions Frequent petechial haemorrhages	Cerebellar roof, vestibular olivary nuclei, superior olivary nuclei and inferior colliculi
		Conventional: Twice-daily oral doses of 10 mg/kg	Four or five doses			
1,3,5-TNB [c]	Male Fischer-344 rats	71 mg/kg	1 day	Pale ears and eyes and dark feet	----	----
			4 days			
			10 days	Pale ears and eyes and dark feet Walking on toes, hunched back and partial disuse of rear legs	Bilaterally symmetrical vacuolated lesions Petechial hemorrhages around the cerebellar peduncles and brain stem	Cerebellar peduncles, inferior colliculi, olivary nuclei, medial and lateral cerebellar nuclei, ventral and dorsal cochlear
		35.5 mg/kg	10 days	Pale ears and eyes and dark feet	----	----

[a] (Morgan et al., 1985) [b] (Philbert et al., 1987) [c] (Chandra et al., 1995)

Table 1-2. Summary of 1,3-DNB Assess by *in vivo* Studies

Ref	Rat strains and Genders [a]		Body Weight	Dosage		Frequency	Length of Study	Timepoints Examined After the 1st Dose [b]	Observations / Results [c]
1	F344	F	250-300g	10mg/kg DNB in DMSO	tail vein injection	once/day	1d	blood sample: 0.5, 1,2,4,8,18h DNB sample: 6,12,24h,2,4,6,8,14d	1. dose threshold: 2 µM 2. time threshold: (T_m that [DNB] above 2 µM) 22.7 h criteria: vacuolar lesions w/ scattered hemorrhage in inferior colliculi, cerebellar roof, vestibular, superior olivary and cochlear nuclei
2	F344	M	180-210g	20mg/kg DNB in PEG600	oral	once/day	1d	24h (3/12), 48h (3/12), 72h (3/12) after dosing	lesion: - (12/12) signs: normal (12/12)
							3d	72h	lesion: +++ (6/6) signs: circling and ataxia (5/6), normal (1/6)
				10mg/kg DNB in PEG600	i.p.	4h interval, twice/day	2d	48h after dosing	lesion: +++ signs: ataxia (3/7) normal (3/7) moribund (1/7)
							3d	54h after dosing	lesion: +++ signs: ataxia (3/7) normal (3/7) moribund (1/7) <u>lesion summary</u>: hindbrain and cerebellum, cerebellar rood nuclei,

3	F344	M	180-250g	10mg/kg DNB in DMSO (10mg DNB / ml DMSO)	i.p.	0, 4, 24h		after the final dose: 6h	increased cerebral bloood flow
								after the final dose: 12h	increasing incidence of petechial haemorrhages in inferior colliculi, cerebellar roof, vestibular, superior olivary periarteriolar oedema and pr leakage, astrocyte swellling
								after the final dose: 24h	signs: +, ++ ataxia
4	F344	M	6-8 week	10mg/kg DNB in DMSO (10mg DNB / ml DMSO)	i.p.	0, 4, 24h	1d	+GSH depletion	ataxia, vacuolation
				7.5mg/kg DNB		once/day	4d	after the final dose: 24h	histology: DNB alone caused no visible damage
5	F344	M	220-270g, 6-10 week	10mg/kg DNB in DMSO (10mg DNB / ml DMSO)	i.p.	0, 4, 24h	1d		
				7.5mg/kg DNB		once/day	4d		

6	F344	M		20mg/kg DNB split between no fewer than two i.p. exposures over the course of 24h	i.p.	at least twice sum up to 20mg/kg	1d		24, 48, 72h after the second dose--> RT PCR showed increased expression of BCL-XL in WT cortical astrocytes.
7	F344	M	200-220g	10mg/kg DNB in DMSO (10mg DNB / ml DMSO)	i.p.	0, 4, 24h	1d		4h after the final dose, before the lesion developes --> homogenate-->glucose level the same everywhere compared to ctrl, lactate level increases in inferior colliculi, vestibular nuclei and cortex.

[a]F=female, M=male.

[b](3/12) indicates 3 out of 12 animals exhibited the lesions described in the next column.

[c]+/- indicates the severity of lesions.

1. (Xu et al., 1999b)

2. (Philbert et al., 1987)

3. (Romero et al., 1991)

4. (Hu et al., 1999)

5. (Mavroudis et al., 2006a)

6. (Phelka et al., 2006)

7. (Phelka et al., 2003)

Table 1-3. The Comparison of Two Reductive Pathways of Nitro Compounds.

Reductive Pathway	Enzymes Involved	Oxygen Sensitivity	Tissue Specificity	Reaction	Contributions to Pathology	References
Microflora	Type I Nitroreductase (EC 1.6.99.1, also known as NADPH dehydrogenase)	Insensitive	Small intestinal > Liver > Heart > Brain	Fast: 3 steps with 2-electron transfer in each step	Methemoglobinemia	(Reddy et al., 1976, Facchini and Griffiths, 1981, Levin and Dent, 1982, Ask et al., 2004)
Erythrocyte and Somatic Microsomes	Type II Nitroreductase (EC 1.6.5.3, also known as NADH dehydrogenase)	Sensitive	Small intestinal > Brain > Lung > Heart	Slow: 6 steps with 1-electron transfer in each step		(Levin and Dent, 1982, Ask et al., 2004)

1.11 REFERENCES

Allaman I, Belanger M, Magistretti PJ (2011) Astrocyte-neuron metabolic relationships: for better and for worse. Trends Neurosci 34:76-87.

Aoyama K, Watabe M, Nakaki T (2008) Regulation of neuronal glutathione synthesis. J Pharmacol Sci 108:227-238.

Aschner M, Costa LG (2005) The role of glia in neurotoxicity. Boca Raton, FL: CRC Press.

Ask K, Decologne N, Asare N, Holme JA, Artur Y, Pelczar H, Camus P (2004) Distribution of nitroreductive activity toward nilutamide in rat. Toxicology and applied pharmacology 201:1-9.

Ault JG, Lawrence DA (2003) Glutathione distribution in normal and oxidatively stressed cells. Exp Cell Res 285:9-14.

Beauchamp RO, Irons RD, Rickert DE, Couch DB, Hamm TE (1982) A Critical-Review of the Literature on Nitrobenzene Toxicity. Crc Critical Reviews in Toxicology 11:33-84.

Belanger M, Allaman I, Magistretti PJ (2011) Brain energy metabolism: focus on astrocyte-neuron metabolic cooperation. Cell Metab 14:724-738.

Betz AL (1985) Identification of hypoxanthine transport and xanthine oxidase activity in brain capillaries. Journal of neurochemistry 44:574-579.

Biaglow JE, Jacobson B, Varnes M (1978) The oxidation of ascorbate by electron affinic drugs and carcinogens. Photochem Photobiol 28:869-876.

Blackburn DM, Gray AJ, Lloyd SC, Sheard CM, Foster PM (1988) A comparison of the effects of the three isomers of dinitrobenzene on the testis in the rat. Toxicology and applied pharmacology 92:54-64.

Bradley WG (2008) Neurology in clinical practice. Philadelphia: Butterworth-Heinemann/Elsevier.

Brown GK, Squier MV (1996) Neuropathology and pathogenesis of mitochondrial diseases. Journal of inherited metabolic disease 19:553-572.

Butterworth RF, Kril JJ, Harper CG (1993) Thiamine-dependent enzyme changes in the brains of alcoholics: relationship to the Wernicke-Korsakoff syndrome. Alcohol Clin Exp Res 17:1084-1088.

Cavanagh JB (1992) Methyl bromide intoxication and acute energy deprivation syndromes. Neuropathology and applied neurobiology 18:575-578.

Cavanagh JB (1993) Selective vulnerability in acute energy deprivation syndromes. Neuropathology and applied neurobiology 19:461-470.

Cavanagh JB, Harding BN (1994) Pathogenic factors underlying the lesions in Leigh's disease. Tissue responses to cellular energy deprivation and their clinico-pathological consequences. Brain : a journal of neurology 117 (Pt 6):1357-1376.

Cavanagh JB, Nolan CC (1993) The neurotoxicity of alpha-chlorohydrin in rats and mice: II. Lesion topography and factors in selective vulnerability in acute energy deprivation syndromes. Neuropathology and applied neurobiology 19:471-479.

Chandra AM, Qualls CW, Jr., Reddy G (1995) 1,3,5-Trinitrobenzene-induced encephalopathy in male Fischer-344 rats. Toxicol Pathol 23:527-532.

Cody TE, Witherup S, Hastings L, Stemmer K, Christian RT (1981) 1,3-dinitrobenzene: toxic effects in vivo and in vitro. Journal of toxicology and environmental health 7:829-847.

Cossum PA, Rickert DE (1987) Metabolism and toxicity of dinitrobenzene isomers in erythrocytes from Fischer-344 rats, rhesus monkeys and humans. Toxicology letters 37:157-163.

Dahl HH (1998) Getting to the nucleus of mitochondrial disorders: identification of respiratory chain-enzyme genes causing Leigh syndrome. American journal of human genetics 63:1594-1597.

de Mendonca A, Sebastiao AM, Ribeiro JA (2000) Adenosine: does it have a neuroprotective role after all? Brain Res Brain Res Rev 33:258-274.

Facchini V, Griffiths LA (1981) The involvement of the gastro-intestinal microflora in nitro-compound-induced methaemoglobinaemia in rats and its relationship to nitrogroup reduction. Biochemical pharmacology 30:931-935.

Foster PM (1989) M-dinitrobenzene: studies on its toxicity to the testicular Sertoli cell. Archives of toxicology Supplement = Archiv fur Toxikologie Supplement 13:3-17.

Harada N, Omura T (1980) Participation of cytochrome P-450 in the reduction of nitro compounds by rat liver microsomes. J Biochem 87:1539-1554.

Hengartner MO (2000) The biochemistry of apoptosis. Nature 407:770-776.

Hockenbery DM, Oltvai ZN, Yin XM, Milliman CL, Korsmeyer SJ (1993) Bcl-2 functions in an antioxidant pathway to prevent apoptosis. Cell 75:241-251.

Holder JW (1999) Nitrobenzene carcinogenicity in animals and human hazard evaluation. Toxicol Ind Health 15:445-457.

Holton JL, Nolan CC, Burr SA, Ray DE, Cavanagh JB (1997) Increasing or decreasing nervous activity modulates the severity of the glio-vascular lesions of 1,3-dinitrobenzene in the rat: effects of the tremorgenic pyrethroid, Bifenthrin, and of anaesthesia. Acta Neuropathol 93:159-165.

Hsu CH, Stedeford T, Okochi-Takada E, Ushijima T, Noguchi H, Muro-Cacho C, Holder JW, Banasik M (2007) Framework analysis for the carcinogenic mode of action of nitrobenzene. Journal of Environmental Science and Health Part C-Environmental Carcinogenesis & Ecotoxicology Reviews 25:155-184.

Hu HL, Bennett N, Holton JL, Nolan CC, Lister T, Cavanagh JB, Ray DE (1999) Glutathione depletion increases brain susceptibility to m-dinitrobenzene neurotoxicity. Neurotoxicology 20:83-90.

Hu HL, Bennett N, Lamb JH, Ghersi-Egea JF, Schlosshauer B, Ray DE (1997) Capacity of rat brain to metabolize m-dinitrobenzene: an in vitro study. Neurotoxicology 18:363-370.

Ikeda M, Kita A (1964) Excretion of P-Nitrophenol and P-Aminophenol in the Urine of a Patient Exposed to Nitrobenzene. British journal of industrial medicine 21:210-213.

Kauffman FC, Johnson EC (1974) Cerebral energy reserves and glycolysis in neural tissue of 6-aminonicotinamide-treated mice. J Neurobiol 5:379-392.

Kumar A, Chawla R, Ahuja S, Girdhar KK, Bhattacharya A (1990) Nitrobenzene poisoning and spurious pulse oximetry. Anaesthesia 45:949-951.

Levin AA, Dent JG (1982) Comparison of the metabolism of nitrobenzene by hepatic microsomes and cecal microflora from Fischer-344 rats in vitro and the relative importance of each in vivo. Drug metabolism and disposition: the biological fate of chemicals 10:450-454.

Li H, Wang H, Sun H, Liu Y, Liu K, Peng S (2003) Binding of nitrobenzene to hepatic DNA and hemoglobin at low doses in mice. Toxicol Lett 139:25-32.

Logan M, Sweeney MI (1997) Adenosine A1 receptor activation preferentially protects cultured cerebellar neurons versus astrocytes against hypoxia-induced death. Mol Chem Neuropathol 31:119-133.

Martin PR, Singleton CK, Hiller-Sturmhofel S (2003) The role of thiamine deficiency in alcoholic brain disease. Alcohol research & health : the journal of the National Institute on Alcohol Abuse and Alcoholism 27:134-142.

Marzo I, Brenner C, Zamzami N, Jurgensmeier JM, Susin SA, Vieira HL, Prevost MC, Xie Z, Matsuyama S, Reed JC, Kroemer G (1998) Bax and adenine nucleotide translocator cooperate in the mitochondrial control of apoptosis. Science 281:2027-2031.

Mason RP, Holtzman JL (1975) The mechanism of microsomal and mitochondrial nitroreductase. Electron spin resonance evidence for nitroaromatic free radical intermediates. Biochemistry 14:1626-1632.

Mavroudis G, Prior MJ, Lister T, Nolan CC, Ray DE (2006) Neurochemical and oedematous changes in 1,3-dinitrobenzene-induced astroglial injury in rat brain from a 1H-nuclear magnetic resonance perspective. J Neural Transm 113:1263-1278.

Meyer-Estorf G, Schulze PE, Herken H (1973) Distribution of 3 H-labelled 6-aminonicotinamide and accumulation of 6-phosphogluconate in the spinal cord. Naunyn-Schmiedeberg's archives of pharmacology 276:235-241.

Miller JA, Runkle SA, Tjalkens RB, Philbert MA (2011) 1,3-Dinitrobenzene-induced metabolic impairment through selective inactivation of the pyruvate dehydrogenase complex. Toxicological sciences : an official journal of the Society of Toxicology 122:502-511.

Morgan KT, Gross EA, Lyght O, Bond JA (1985) Morphologic and biochemical studies of a nitrobenzene-induced encephalopathy in rats. Neurotoxicology 6:105-116.

Mott JL, Zhang D, Freeman JC, Mikolajczak P, Chang SW, Zassenhaus HP (2004) Cardiac disease due to random mitochondrial DNA mutations is prevented by cyclosporin A. Biochem Biophys Res Commun 319:1210-1215.

O'Shaughnessy PJ, Morris ID, Huhtaniemi I, Baker PJ, Abel MH (2009) Role of androgen and gonadotrophins in the development and function of the Sertoli cells and Leydig cells: data from mutant and genetically modified mice. Mol Cell Endocrinol 306:2-8.

Parke DV (1961) Studies in detoxication. 85. The metabolism of m-dinitro[C]benzene in the rabbit. Biochem J 78:262-271.

Perez-Reyes E, Kalyanaraman B, Mason RP (1980) The reductive metabolism of metronidazole and ronidazole by aerobic liver microsomes. Mol Pharmacol 17:239-244.

Phelka AD, Beck MJ, Philbert MA (2003) 1,3-Dinitrobenzene inhibits mitochondrial complex II in rat and mouse brainstem and cortical astrocytes. Neurotoxicology 24:403-415.

Phelka AD, Sadoff MM, Martin BP, Philbert MA (2006) BCL-XL expression levels influence differential regional astrocytic susceptibility to 1,3-dinitrobenzene. Neurotoxicology 27:192-200.

Philbert MA, Billingsley ML, Reuhl KR (2000) Mechanisms of injury in the central nervous system. Toxicol Pathol 28:43-53.

Philbert MA, Nolan CC, Cremer JE, Tucker D, Brown AW (1987) 1,3-Dinitrobenzene-induced encephalopathy in rats. Neuropathology and applied neurobiology 13:371-389.

Ray DE, Brown AW, Cavanagh JB, Nolan CC, Richards HK, Wylie SP (1992) Functional/metabolic modulation of the brain stem lesions caused by 1,3-dinitrobenzene in the rat. Neurotoxicology 13:379-388.

Reader SC, Shingles C, Stonard MD (1991) Acute testicular toxicity of 1,3-dinitrobenzene and ethylene glycol monomethyl ether in the rat: evaluation of biochemical effect markers and hormonal responses. Fundam Appl Toxicol 16:61-70.

Reddy BG, Pohl LR, Krishna G (1976) The requirement of the gut flora in nitrobenzene-induced methemoglobinemia in rats. Biochemical pharmacology 25:1119-1122.

Reeve IT, Miller MG (2002) 1,3-Dinitrobenzene metabolism and protein binding. Chemical research in toxicology 15:352-360.

Rickert DE (1985) Toxicity of nitroaromatic compounds. Washington [D.C.]: Hemisphere Pub. Corp.

Rickert DE (1987) Metabolism of nitroaromatic compounds. Drug Metab Rev 18:23-53.

Rickert DE, Bond JA, Long RM, Chism JP (1983) Metabolism and excretion of nitrobenzene by rats and mice. Toxicology and applied pharmacology 67:206-214.

Romero I, Brown AW, Cavanagh JB, Nolan CC, Ray DE, Seville MP (1991) Vascular factors in the neurotoxic damage caused by 1,3-dinitrobenzene in the rat. Neuropathology and applied neurobiology 17:495-508.

Romero IA, Lister T, Richards HK, Seville MP, Wylie SP, Ray DE (1995) Early metabolic changes during m-Dinitrobenzene neurotoxicity and the possible role of oxidative stress. Free Radic Biol Med 18:311-319.

Romero IA, Ray DE, Chan MW, Abbott NJ (1996) An in vitro study of m-dinitrobenzene toxicity on the cellular components of the blood-brain barrier, astrocytes and endothelial cells. Toxicology and applied pharmacology 139:94-101.

Salmowa J, Piotrowski J, Neuhorn U (1963) Evaluation of exposure to nitrobenzene. Absorption of nitrobenzene vapour through lungs and excretion of p-nitrophenol in urine. Br J Ind Med 20:41-46.

Schneider H, Cervos-Navarro J (1974) Acute gliopathy in spinal cord and brain stem induced by 6-aminonicotinamide. Acta Neuropathol 27:11-23.

Sealy RC, Swartz HM, Olive PL (1978) Electron spin resonance-spin trapping. Detection of superoxide formation during aerobic microsomal reduction of nitro-compounds. Biochem Biophys Res Commun 82:680-684.

Sedel F, Challe G, Mayer JM, Boutron A, Fontaine B, Saudubray JM, Brivet M (2008) Thiamine responsive pyruvate dehydrogenase deficiency in an adult with peripheral neuropathy and optic neuropathy. Journal of neurology, neurosurgery, and psychiatry 79:846-847.

Silver J, Miller JH (2004) Regeneration beyond the glial scar. Nat Rev Neurosci 5:146-156.

Sperlagh B, Vizi ES (2011) The role of extracellular adenosine in chemical neurotransmission in the hippocampus and Basal Ganglia: pharmacological and clinical aspects. Current topics in medicinal chemistry 11:1034-1046.

Squier MV, Thompson J, Rajgopalan B (1992) Case report: neuropathology of methyl bromide intoxication. Neuropathology and applied neurobiology 18:579-584.

Steiner SR, Philbert MA (2011) Proteomic identification of carbonylated proteins in 1,3-dinitrobenzene neurotoxicity. Neurotoxicology 32:362-373.

Stevenson D, Jones AR (1985) Production of (S)-3-chlorolactaldehyde from (S)-alpha-chlorohydrin by boar spermatozoa and the inhibition of glyceraldehyde 3-phosphate dehydrogenase in vitro. Journal of reproduction and fertility 74:157-165.

Sweeney MI (1997) Neuroprotective effects of adenosine in cerebral ischemia: window of opportunity. Neurosci Biobehav Rev 21:207-217.

Tjalkens RB, Ewing MM, Philbert MA (2000) Differential cellular regulation of the mitochondrial permeability transition in an in vitro model of 1,3-dinitrobenzene-induced encephalopathy. Brain research 874:165-177.

Tjalkens RB, Phelka AD, Philbert MA (2003) Regional variation in the activation threshold for 1,3-DNB-induced mitochondrial permeability transition in brainstem and cortical astrocytes. Neurotoxicology 24:391-401.

U.S. Department of Health and Human Services (1995) Toxicological profile for 1,3-dinitrobenzene and 1,3,5-trinitrobenzene.

U.S. Environmental Protection Agency (1997) 1,3,5-Trinitrobenzene support documents.

U.S. Environmental Protection Agency (2009) Toxicological review of nitrobenzene.

Wang YP, Liu X, Schneider B, Zverina EA, Russ K, Wijeyesakere SJ, Fierke CA, Richardson RJ, Philbert MA (2012) Mixed Inhibition of Adenosine Deaminase

Activity by 1,3-Dinitrobenzene: A Model for Understanding Cell-Selective Neurotoxicity in Chemically-Induced Energy Deprivation Syndromes in Brain. Toxicological Sciences 125:509-521.

Xu J, Nolan CC, Lister T, Purcell WM, Ray DE (1999) Pharmacokinetic factors and concentration-time threshold in m-dinitrobenzene-induced neurotoxicity. Toxicology and applied pharmacology 161:267-273.

Zamzami N, Susin SA, Marchetti P, Hirsch T, Gomez-Monterrey I, Castedo M, Kroemer G (1996) Mitochondrial control of nuclear apoptosis. The Journal of experimental medicine 183:1533-1544.

CHAPTER 2

MIXED INHIBITION OF ADENOSINE DEAMINASE ACTIVITY BY 1,3-DINITROBENZENE: A MODEL FOR UNDERSTANDING CELL-SELECTIVE NEUROTOXICITY IN CHEMICALLY INDUCED ENERGY DEPRIVATION SYNDROMES IN BRAIN

2.1 ABSTRACT

Astrocytes are acutely sensitive to 1,3-dinitrobenzene (1,3-DNB) while adjacent neurons are relatively unaffected, consistent with other chemically induced energy deprivation syndromes. Previous studies have investigated the role of astrocytes in protecting neurons from hypoxia and chemical injury via adenosine release. Adenosine is considered neuroprotective, but it is rapidly removed by extracellular deaminases such as adenosine deaminase (ADA). The present study tested the hypothesis that ADA is inhibited by 1,3-DNB as a substrate mimic, thereby preventing adenosine catabolism. ADA was inhibited by 1,3-DNB with an IC_{50} of 284 µM; Hill-slope, n = 4.8 ± 0.4. Native-gel electrophoresis showed that 1,3-DNB did not denature ADA. Furthermore, adding Triton X-100 (0.01 – 0.05%, w/v), Nonidet P-40 (0.0015 – 0.0036%, w/v), or BSA (0.05 mg/ml, or changing [ADA] (0.2 nM and 2 nM) did not substantially alter the 1,3-DNB IC_{50} value. Likewise, dynamic light scattering showed no particle formation over a [1,3-DNB] range of 149 – 1043 µM. Kinetics revealed mixed inhibition with 1,3-DNB binding to ADA (K_I = 520 ± 100 µM, n = 1 ± 0.6) and the ADA-adenosine complex (K_{IS} = 262 ± 7 µM, n = 6 ± 0.6, indicating positive cooperativity). In

accord with the kinetics, docking predicted binding of 1,3-DNB to the active site and 3 peripheral sites. In addition, exposure of DI TNC-1 astrocytes to 10-500 µM 1,3-DNB produced concentration-dependent increases in extracellular adenosine at 24 h. Overall, the results demonstrate that 1,3-DNB is a mixed inhibitor of ADA and may thus lead to increases in extracellular adenosine. The finding may provide insights to guide future work on chemically induced energy deprivation.

2.2 INTRODUCTION

Used as an industrial synthetic intermediate, 1,3-DNB has been shown to elicit profound histopathological changes in the male reproductive system, liver, and central nervous system (Bond et al., 1981, Philbert et al., 1987, Blackburn et al., 1988b). The clinical manifestations of neurotoxicity include nausea, vomiting, hearing loss, and cognitive deficits, depending on the dose and duration of exposure (Cody et al., 1981b). Histopathological evaluation of brains from exposed rats reveals focal, bilateral edematous lesions in the vestibular and auditory pathways of the brainstem. Astrocytes are the primary targets of 1,3-DNB, and severe neuronal damage is absent during the acute phase of intoxication (Philbert et al., 1987). Neuropathological changes are associated with regional increases in glucose consumption and lactic acid formation as well as decreased ATP concentrations in affected areas of the brain (Brown and Miller, 1991a, Romero et al., 1995). Recently, our laboratory demonstrated that 1,3-DNB inhibits the pyruvate dehydrogenase complex in rat C6 glioma cells

(Miller et al., 2011b). Nevertheless, the precise molecular mechanisms of 1,3-DNB-linked differential cell-selective neurotoxicity have remained largely elusive.

ATP and its metabolites, e.g., ADP, AMP, and adenosine, are critical modulators of cellular sensitivity to a variety of endogenous and exogenous challenges (Burnstock, 2006, North and Verkhratsky, 2006, Ribeiro and Sebastiao, 2010). In particular, adenosine binds to adenosine receptors and modulates adenylyl cyclase activity, leading to a variety of subsequent biological responses under both physiological and pathological conditions (Fredholm, 2007b). Briefly, binding of adenosine to the four types of adenosine receptors either inhibits (A_1R and A_3R) or stimulates ($A_{2A}R$ and $A_{2B}R$) adenylyl cyclase activity, thereby modulating downstream events through adenosine signaling pathways. Experiments conducted in A_1R-knockout mice indicate that adenosine is important mainly in pathophysiological conditions (Johansson et al., 2001). For example, the binding of adenosine to adenosine A_1 receptors during hypoxia reduces the release of excitatory neurotransmitters. This inhibitory action has been demonstrated to contribute to neuroprotection mainly during hypoxia and seizures (Latini and Pedata, 2001).

Adenosine homeostasis is maintained by its formation, metabolism, and transport pathways. The primary pathway for the formation of adenosine is via hydrolysis of intracellular and extracellular AMP. The enzymes that aid in the catalysis of these processes are 5’-nucleotidase and ecto-5’-nucleotidase, with rate constants (K_M) in the millimolar and micromolar range, respectively (Latini and Pedata, 2001). It has been proposed that in neurons, production of adenosine

proceeds primarily via the intracellular pathway, while in astrocytes, extracellular production is dominant (Parkinson et al., 2005). Intracellular S-adenosylhomocysteine hydrolysis also contributes to formation of adenosine, but this source is not significant in the brain (Pak et al., 1994). Most adenosine metabolism depends on two pathways: phosphorylation to AMP by adenosine kinase (AK. EC 2.7.1.20), or deamination to inosine by adenosine deaminase (ADA. EC 3.5.4.4). In human whole brain, the K_M value of AK was reported to be 2 µM, whereas the K_M value of ADA was approximately 20 µM (Phillips and Newsholme, 1979). With a lower K_M value, AK also exhibits substrate inhibition at a relative low level of adenosine (> 0.5 µM). Adenosine influx and efflux is mediated by the equilibrative nucleoside transporters (ENT), which allow purine and pyrimidine nucleosides to traffic across the membrane in a concentration-driven mode (Latini and Pedata, 2001). The conversion of adenosine to inosine, which is meditated intracellularly and extracellularly by cytosolic and ecto-ADA, respectively, is crucial, as adenosine is the active neurotransmitter, whereas inosine is inactive. Thus, modification of ADA activity results in changes in adenosine levels, potentially leading to altered synaptic transmission. With the most obvious role reported to be degradation of endogenous adenosine, ecto-ADA also has been shown to be essential for the effectiveness of A_1R and G protein interactions (Cristalli et al., 2001).

Found ubiquitously in living organisms, ADA is a 41 kDa zinc metalloprotein with a wide distribution in most human tissues (Cristalli et al., 2001). As a key enzyme in purine metabolism, the active site of ADA is highly conserved within the three

mammalian species: murine, bovine, and human (Cristalli et al., 2001). ADA exists as two isoforms. The first isoform, ADA1, is localized in the cytosol and cell surface of most tissues, and thus is termed cytosolic ADA and ecto-ADA, respectively. On the other hand, the second isoform, ADA2, is produced by macrophages and found in blood plasma (Cristalli et al., 2001). The present study focuses on the ADA1 isoform, which will be referred to simply as ADA in this paper.

Inhibitors of ADA have been categorized as ground-state or transition-state substrate analogues and as ground-state inhibitors that do not closely mimic substrates. Binding of substrate analogues triggers a conformational change from the open state to the closed state of the enzyme, whereas other inhibitors bind to the open conformation (Cristalli et al., 2001, Kinoshita et al., 2005, Kinoshita et al., 2008).

We hypothesized that 1,3-DNB would bind to the closed form of ADA as a substrate-mimic inhibitor due to the fact that the substrate-mimic adenine inhibits ADA (Alunni et al., 2008), and the benzene ring of 1,3-DNB can be mapped onto the adenine component of adenosine, with its nitrogens superimposed on adenine's amino and N9 nitrogens as shown in Figure 2.1. The similarity in the shape of 1,3-DNB and adenine can be quantified by the degree of overlap of molecular volumes, yielding a Tanimoto coefficient of 0.827, where a perfect match would be exactly 1.000 (Butina, 1999). In addition, given that the nitro group of an inhibitor of carboxypeptidase A coordinates with the zinc atom of that

metalloenzyme (Wang et al., 2008), we postulated that a nitro group of 1,3-DNB could bind to the zinc atom in the active site of ADA.

The present study explored the mechanism of ADA inhibition by 1,3-DNB. In this paper, we report that 1,3-DNB inhibits ADA with an apparent IC_{50} of 284 µM. Furthermore, our kinetics studies found that the rate of inhibition depended upon substrate concentration, indicating that 1,3-DNB is a mixed inhibitor of ADA, in agreement with our modeling studies, which predict binding of 1,3-DNB to the active site as well as peripheral sites.

2.3 MATERIALS AND METHODS

2.3.1 Chemicals.

Dimethyl sulfoxide (DMSO), 1,3-dinitrobenzene (1,3-DNB), adenosine, potassium phosphate monobasic (KH_2PO_4), bovine serum albumin (BSA), bromphenol blue, Coomassie blue, and guanidine hydrochloride were obtained from Sigma (St. Louis, MO). Potassium hydroxide (KOH), toluene, acetone, glycerol, Tris base, Tris HCl, and glycine were obtained from Fisher Scientific (Pittsburgh, PA). Bovine intestinal adenosine deaminase (ADA, EC 3.5.4.4.) was purchased from Calbiochem (San Diego, CA). Triton X-100, Precision Plus Protein Dual Color Standards, Immuno-Blot PVDF membranes, 12% Ready Gel Tris-HCl Gel and 4-15% Ready Gel Tris-HCl Gel were purchased from Bio-Rad Laboratory (Hercules, CA). Nonidet P-40 was from USB Corporation (now Affymetrix, Santa Clara, CA). Novex Sharp Standard, Dulbecco modified Eagle's medium (DMEM); penicillin, streptomycin, glutamate (PSG); Dulbecco's phosphate buffered saline (D-PBS);

and fetal bovine serum (FBS) were obtained from Invitrogen (Carlsbad, CA). Adenosine and inosine sensors were purchased from Sarissa Biosensor (Coventry, UK). BCA protein assay kits and Subcellular Protein Fractionation kits were obtained from Thermo Scientific (Rockford, IL). Rabbit anti rat ADA and rabbit anti rat A_1R were purchased from Abcam (Cambridge, MA).

2.3.2 Purity of purchased adenosine deaminase (ADA).

To determine the purity and molecular weight of the purchased ADA, four different amounts of ADA (6, 1.8, 0.9, 0.45 µg) were loaded onto SDS-PAGE gel. SDS denatured protein standards were loaded at the same time with the samples. The gel was run for 90 min in Tri-Glycine buffer with 0.1% SDS (v/v) at a constant voltage of 200 V. When the front of ladder reached the bottom of the gel, the gel was stained with Coomassie blue and imaged using a FOTO/Analyst Investigator (Fotodyne, Hartland, WI).

2.3.3 Extinction coefficients of adenosine and inosine.

The extinction coefficients of adenosine and inosine were measured in the quartz cuvettes on Cary 100 Bio spectrophotometer (Varian, Santa Clara, CA). Adenosine and inosine was weighted and dissolved in Milli-Q water to prepare 10 mM stock solution. Different adenosine and inosine solutions ranging from 10 to 300 µM were prepared by mixing stock solutions with 100 mM potassium phosphate buffer (pH 7.5 at room temperature). Solutions of each concentration were prepared and read for at least three times.

2.3.4 Adenosine deaminase (ADA) assay.

ADA activity was assayed following the method described by Kaplan (Kaplan, 1955), using a Cary 100 Bio spectrophotometer (Varian, Santa Clara, CA). The purchased enzyme (ADA) was > 95% pure as determined by SDS gel-electrophoresis. The assay was performed at a final volume of 1.00 ml containing 100 mM potassium phosphate buffer (pH 7.5 at room temperature), 0.50 nM ADA, a fixed percentage of DMSO (5%, v/v), and various concentrations of adenosine (ranging from 4 µM to 200 µM) and 1,3-DNB (ranging from 140 µM to 2 mM). Under these conditions, the observed absorbance at 265 nm decreased due to the conversion of adenosine to inosine with a net negative change of 9800 $M^{-1}cm^{-1}$. The ADA activity was measured from the initial linear decrease in absorbance at 25˚C, and activities were calculated relative to contemporaneous DMSO-containing controls. The absorbance from the first seven minutes was recorded, and the absorbance from the first minute, comprising 7-9 data points, was used to calculate the initial velocity.

2.3.5 DI TNC-1 Cell Culture.

Immortalized astrocytes DI TNC-1 derived from diencephalon of Sprague-Dawley rats were obtained from American Type Culture Collection (ATCC). DI TNC-1 cells were kept in an incubator at constant temperature (37˚C) with 5% CO_2 / 95% air (v/v) supply. Dulbecco's Modified Eagle Medium supplemented with 10% (w/v) FBS and 1.0% PSG (v/v) was used for cell culture. Following 48 h of initial subculture plating, cells were rinsed with 5 ml D-PBS and treated by 1 ml 0.25% (w/v) trypsin. DI TNC-1 were exposed to 10 ml serum-free media

containing either 0.5% DMSO, 10 μM, 100 μM or 500 μM 1,3-DNB. One hour after the exposure, serum (1.00 ml) was added into each plate containing conditioned media, and then DI TNC-1 cells were continued incubating for 23 h. Four independent experiments were conducted for each exposure with DI TNC-1 passage 4 to 10.

2.3.6 Measurement of adenosine and inosine from DI TNC-1 conditioned media.

Adenosine, inosine, and null sensors were linked to a Multi-Channel Potentiostat (Pinnacle Technology, Lawrence, KS). Standard solutions of adenosine and inosine (1 μM to 50 μM) were used for calibration. Toluene (1.0 ml) was added to 11 ml of collected conditioned media to extract 1,3-DNB. Extraction was performed twice for each DMSO or 1,3-DNB exposure. Ado and Ino levels were measured and calibrated to protein concentration obtained by BCA protein assay.

2.3.7 Aggregation based inhibition.

All reactions were performed at 25 ºC using 100 mM potassium phosphate buffer (pH 7.50 at room temperature), 0.50 nM ADA, and 5% (v/v) DMSO. Adenosine concentration was held at 50 μM while 1,3-DNB concentrations were varied from 275 - 1000 μM. The IC_{50} was determined under four conditions: 1) addition of Triton X-100 at 0.01%, 0.02% and 0.05% (w/v); 2) addition of Nonidet-P-40 (NP-40) at 0.0015%, 0.0024%, and 0.003%; 3) addition of BSA (0.1 mg/ml); and 4) increasing the concentration of ADA to 1.49 nM. The ADA activity was measured from the initial linear decrease in absorbance at 25˚C. All reactions were initiated by the addition of adenosine into the cuvette.

2.3.8 Time dependence.

5 nM bovine ADA in 0.1M potassium phosphate buffer (pH 7.5) was treated with 5.5 mM 1,3-DNB or 5% (v/v) DMSO. The protein and ligand were mixed gently in a conical tube and incubated at 25 ºC. At the specified time-points (0, 15, 30, 45 and 60 min), the protein-ligand solution was added to pre-warmed cuvettes at 25 ºC containing 10 µl adenosine at 5 mM. ADA activity was measured at 25˚C for seven minutes and the absorbance from the first minute, comprising 7-9 data points, was used to calculate the initial velocity.

2.3.9 Native gel electrophoresis.

ADA (3.6 µg) was loaded into each lane of a 12%Tris-Cl polyacrylamide gel following preincubation for 30 min on ice with either DMSO or 1,3-DNB (0.35 -1 mM). Positive controls for denatured proteins were prepared by either heating ADA at 95˚C for 5 min in a dry bath incubator or via denaturation using 3M guanidine hydrochloride for 30min on ice, before loading onto the gel. Sample buffer contained 0.125 M Tris HCl at pH 6.8, 20% (v/v) glycerol and 1% (w/v) bromphenol blue in Milli-Q water. The gel was run as detailed earlier (Coligan, 1996). Briefly, the gel was pre-run for 60 min on ice with voltage held constant at 200 V. After samples were loaded, the gel was continuously run on ice for 3 h at constant current of 0.04 A in a Tris-glycine buffer. The gel was then stained with Coomassie blue and imaged using a FOTO/Analyst Investigator (Fotodyne, Hartland, WI).

2.3.10 Measurement of particle size using dynamic light scattering (DLS).

Particle size measurements were undertaken at 10˚C, 25˚C, and 37˚C using a DelsaNano C Particle Analyzer (Beckman Coulter, Brea, CA) with 1,3-DNB ranging from 149 μM to 1043 μM in 0.1 potassium phosphate (pH 7.5 at room temperature) with a DMSO concentration of 14.9% (v/v). In a separate experiment, the DMSO concentration was varied from 0.1% to 20% (v/v) while the concentration of 1,3-DNB was maintained at 1 mM.

2.3.11 Kinetics studies of 1,3-DNB inhibition of adenosine deaminase.

The inhibition of ADA activity was first measured at a fixed concentration of adenosine (50 μM) and varying concentrations of 1,3-DNB (0 – 2 mM). A value for an apparent IC50 was calculated by fitting Equation 1 to the data, where X = [1,3-DNB] and n = Hill slope. The Hill slope allows fitting for cooperative inhibition. To further analyze inhibition, ADA activity was measured with varying adenosine concentrations (4 μM to 200 μM) at several fixed 1,3-DNB concentrations (200 – 350 μM), from the initial linear decrease in absorbance at 25˚C. The inhibition mechanism was analyzed using the global fitting function of GraphPad Prism 5.03. Four possible inhibition mechanisms, including cooperative, competitive, uncompetitive, and noncompetitive-mixed inhibition, were fitted to the dependence of the ADA activity on adenosine and 1,3-DNB concentrations. The global fitting function analyzes multiple data sets simultaneously to generate one (global) best-fit value of parameters for all of the data sets. Global fitting was performed using equations derived from Figure 2.1 showing mixed inhibition. Equation 2 describes the mixed inhibition mechanism, while Equation 3

describes the noncompetitive mechanism, whereby 1,3-DNB binds only to the ES complex.

2.3.12 Molecular modeling.

To gain insight into the structural basis of the interactions of 1,3-DNB with ADA, *in silico* docking studies were performed using the structures of murine (PDB ID 3mvi), bovine (PDB ID 1krm) and human ADA (PDB ID 3iar). The human crystal structure was solved with Ni^{2+}in the active site, which was replaced by Zn^{2+}using YASARA Structure 11.3.22 (YASARA Biosciences, Vienna, Austria) (Krieger et al., 2004), so that the zinc metalloprotein was used for docking studies of all three species of ADA. Although the protein is monomeric, in crystal structures where two protein molecules were visible in the asymmetric unit, the A chain was selected for docking studies. The crystal structure of bovine ADA was found to contain 7 cis-peptide bonds in its peptide backbone. Cis-peptide bonds are usually not favored except at proline residues (Pal and Chakrabarti, 1999), and as such, all cis-peptide binds were corrected in YASARA. However, analysis of the human ADA structure revealed a cis-peptide bond between E113 and P114 (corresponding to E110 and P11 in bovine ADA). As a result, a cis-bond was added *in silico* to the peptide backbone of the energy-minimized structure of bovine ADA between E110 and P111. The resulting structure was refined via local annealing and subjected to a second round of energy minimization as described below. The two cis-peptide bonds in the murine ADA structure were confirmed via examination of the electron density map and were left uncorrected, in contrast to the 7 cis-peptide bonds in the bovine ADA structure that could not

be confirmed. Moreover, using Clustal Omega 1.0.3, alignments of the primary amino acid sequences of murine, human, and bovine ADA revealed these proteins to share 85.8% pairwise sequence identity (Figure 2.4 D). Furthermore, all ADA structures used in the present study represent the closed form of the enzyme, which is expected to be optimal for binding substrate analogues (Kinoshita et al., 2005).

The structures of 1,3-DNB and the adenine ring of adenosine were generated in ChemBioDraw Ultra12.02 (CambridgeSoft, Cambridge, MA) and optimized in MarvinSketch 5.4.1.1 (ChemAxon, http://www.chemaxon.com). The resulting structures were further refined via the energy minimization protocol in YASARA using the AMBER03 force field (Duan et al., 2003) prior to their use in docking or molecular alignments. The structure of adenosine for docking was obtained from the 2'-deoxyadenosine ligand in the crystal structure of human ADA (PDB ID 3iar); the 2'-hydroxyl group was inserted using YASARA. Molecular alignments of 1,3-DNB and the adenine ring of adenosine were carried out in YASARA and vROCS, version 3.1.2 (OEChem, version 1.7.2, OpenEye Scientific Software, Inc., Santa Fe, NM, www.eyesopen.com, 2011. Prior to their use in docking, the ADA structures were "cleaned" and energy-minimized using the corresponding protocols in YASARA and the AMBER03 force field. Twenty-five sequential global docking runs of the ligands (1,3-DNB or adenosine) onto the prepared receptors (murine, bovine, or human ADA structures) were undertaken within a cubic simulation cell ($a = b = c = 46$ Å) centered on the protein molecule. All docking runs were performed using the modified version of AutoDock 4.2.3

(http://autodock.scripps.edu) (Morris et al., 1998) distributed with YASARA. The AMBER03 force field and the Lamarckian Genetic Algorithm were used for docking. All atoms in the receptors were held rigid during docking, but flexibility was allowed in the amino and hydroxyl groups of adenosine and the nitro groups of 1,3-DNB. The final docked ligand poses were analyzed in YASARA and PyMOL ver 1.4 (Schrödinger, Cambridge, MA) using a root mean square deviation (RMSD) cut-off of 5.0 Å to define a cluster of ligand conformations.

2.3.13 Cell fractionation.

Immortalized astrocytes (DI TNC-1) were harvested and subcellular protein from cytoplasmic extract and membrane extract were prepared using instructions provided by the supplier (Thermo Scientific). Briefly, 1×10^6 trypsinized DI TNC-1 cells were collected in tubes and pelleted via centrifugation at 500 × g for 5 min. The cells were rinsed with ice-cold PBS and pelleted by centrifugation at 500 × g for 3 min. After the supernatant was discarded, 100 µl ice-cold Cytoplasmic Extraction Buffer (CEB) was added to the pellet. Next the cells were incubated with CEB for 10 min with rocking at 4ºC. Following centrifugation at 500 × g for 5 min, the supernatant was collected as cytoplasmic extract. 100 µl ice-cold Membrane Extraction Buffer (MEB) was added to the pellets. The pellets were suspended in MEB, and incubated for 10 min with gentle rocking at 4ºC following which, the samples were centrifuged at 3000 × g for 5 min and the supernatant was collected as membrane extract.

2.3.14 Western blot analysis.

Protein samples for A_1R detection were isolated by boiling DI TNC-1 cells in RIPA buffer (0.1% SDS (w/v), 1% Triton X-100 (v/v), 150 mM NaCl, 50mM Tris-HCl pH 7.8, 0.5 % sodium deoxycholate (w/v) and 0.1% Protease Inhibitor Cocktail (v/v, Roche Diagnostics, Indianapolis, IN)) for 5 min. Protein samples for ADA detection were prepared as described in the previous section (Cell Fractionation). Equal amounts of protein (30 µg), were loaded into each well. The gels were run for 90 min in Tri-Glycine buffer with 0.1% SDS (v/v) at a constant voltage of 200 V. The separated protein mixtures were then transferred onto PVDF membranes (Bio-Rad) at a constant voltage of 120 V for 40 min. The membranes were blocked in 0.5% (w/v) nonfat dry milk using SNAP ID (Millipore, Billerica, MA) and incubated with primary antibodies against A_1R (1:1000, Abcam) or ADA (1:2500, Abcam). The bands were visualized via phosphorimaging using a Fujifilm FLA-5000 (Tokyo, Japan) following development using the ECF Western Blotting Reagent Pack (GE Healthcare, Piscataway, NJ).

2.3.15 Statistical analysis.

Statistical differences between groups were determined by one-way ANOVA followed by multiple comparisons undertaken using a Tukey post-hoc test. All statistical analyses were undertaken in GraphPad Prism 5.03 (GraphPad Software Inc., La Jolla, CA). A *p*-value cutoff of 0.05 was used to determine statistical significance.

2.4 RESULTS

2.4.1 The purity and molecular weight of purchased ADA

Of all four lanes loaded with different amount of samples, only one band of each lane revealed on SDS PAGE, suggesting that the purchased ADA was pure. The position of band (between 30 and 40 kDa) indicated that it was monomer of ADA 1 (molecular weight 33 kDa).

2.4.2 Extinction coefficient of adenosine and inosine

Due to nonlinearity observed when the concentration of adenosine exceeded 200 μM, only the absorbance from 0-200 μM was used to calculate extinction coefficients (Figure 2.3). Within this range, both adenosine and inosine solution showed good linearity with R^2 being 0.9923 and 0.994, respectively. Under these conditions, the observed absorbance at 265 nm decreased due to the conversion of adenosine to inosine with a net negative change of 9800 $M^{-1}cm^{-1}$.

2.4.3 1,3-DNB inhibits ADA activity

Figure 2.5 shows that the activity of ADA decreased upon addition of 1,3-DNB, indicating that this compound inhibits ADA. The inhibitory activity shows a sharp dependence on 1,3-DNB concentration, suggesting a cooperative inhibition mechanism. Therefore, to obtain a value for the IC_{50}, a sigmoid curve model that allows for cooperative inhibition (Equation 2-1) was fit to the data (R^2 = 0.953). This analysis gave an apparent IC_{50} value for 1,3-DNB of 284 μM, with a Hill slope (n) of 4.80 ± 0.44. This corresponds to an apparent IC_{50} (95% CI) of 273 (263 – 283) μM.

2.4.4 Effect of 1,3-DNB on the extracellular adenosine and inosine level in conditioned media

Cells that were unexposed to solvent or 1,3-DNB had extracellular adenosine levels below the limit of detection (50 nM) (data not shown). In the vehicle control group (DMSO 0.50%, v/v), the adenosine level was also below 50 nM during the 24 h exposure period. The highest 1,3-DNB concentration (500 µM) produced a significant elevation in the concentration of inosine + hypoxanthine, whereas all three 1,3-DNB concentrations (10, 100, 500 µM) produced elevated adenosine levels compared to the control group ($p < 0.05$) in the 24 h exposure (Figure 2.6).

2.4.5 Aggregation based inhibition test

To examine whether 1,3-DNB inhibition is caused by aggregation, four common characteristics of aggregators were investigated. These are as follows: 1. inhibition is markedly sensitive to nonionic detergents e.g., decreasing in potency by a factor of 2 or more; 2. inhibition occurs by nonspecific binding to protein; 3. inhibition is sensitive to the enzyme concentration; and 4. the inhibitor forms particles that are detectable by dynamic light scattering (DLS) in the absence of the enzyme (Seidler et al., 2003). First, two different nonionic detergents Triton X-100 and Nonidet P-40 (Figure 2.7 A and B) were used to test whether 1,3-DNB inhibition of ADA is highly sensitive to detergents. There was no significant change in the IC_{50} value produced by Nonidet P-40, and although the change in the IC_{50} from Triton X-100 was only -26%, it is in the wrong direction (increased rather than decreased potency) and smaller in magnitude than the factor of 2 or more deemed necessary for an aggregating inhibitor. Next, the specificity of

inhibition was tested via the addition of BSA at a final concentration of 0.05 mg/ml (data not shown). Under this condition, the IC_{50}, 284 µM, was not significantly different from the value in the absence of BSA, 301 µM ($p > 0.1$). Then, we demonstrated that the IC_{50} value of 1,3-DNB was unaffected ($p > 0.50$) by increasing the concentration of ADA from 0.2 nM to 2.0 nM (data not shown), with measured IC_{50} (µM) values of 275 µM and 279 µM, respectively. Finally, no particles were detectable by DLS over a 1,3-DNB concentration range from 149 µM to 1043 µM (data not shown). Taken together, these results demonstrate that 1,3-DNB does not exhibit the common properties of an aggregation-based inhibitor.

2.4.6 Time dependence

To determine whether the inhibition of ADA by 1,3-DNB is time dependent, ADA was pre-incubated with DMSO or 1,3-DNB and the activity as a function of pre-incubation time was measured. Relative ADA activity was obtained by comparing the ADA activity in DMSO or 1,3-DNB pre-incubated ADA with buffer pre-incubated ADA. A constant decrease in enzyme activity corresponding to 20% in the presence of DMSO and 50% in the presence of DMSO + 1,3-DNB was observed over the 60-min time-course groups (Figure 2.8). This finding suggests that the inhibition of ADA by 1,3-DNB is not dependent upon the time of incubation.

2.4.7 Denaturation experiment

To further examine the inhibitory mechanism of 1,3-DNB, native gel electrophoresis was employed to examine the possibility that this compound decreases ADA activity by denaturing the protein. In the gel, the band for ADA in the lanes pre-incubated with DMSO and 1,3-DNB (lanes 2 – 4) ran at the same position as native ADA (lane 1) (Figure 2.9). The position of denatured ADA was significantly altered, as observed for the lanes loaded with ADA denatured with either heat (lane 6) or guanidine hydrochloride (lane 7). These data demonstrate that incubation of ADA with 1,3-DNB does not lead to irreversible denaturation. Although it might seem theoretically possible to extend these results using fluorescence spectroscopy and circular dichroism, it was not possible to carry out these experiments in practice, owing to the inner filter effect and high absorbance of 1,3-DNB (data not shown).

2.4.8 Kinetics and curve fitting

The values determined for the steady state kinetic parameters of ADA-catalyzed deamination of adenosine assayed at pH 7.5 and 25°C were k_{cat} = 23100 ± 960 min $^{-1}$ and K_M = 43 ± 3 μM (Table 2-1). Addition of 1,3-DNB led to decreased values for k_{cat}, k_{cat}/K_M, and K_M, indicating either mixed or noncompetitive inhibition (Table 2-1). Mixed inhibition was chosen over noncompetitive, because of its somewhat higher R^2 value and lower error in global fitting (Table 2-2). This agrees with the double reciprocal Lineweaver-Burk plot of ADA activity under different concentrations of 1,3-DNB, which exhibited changes in all three kinetic parameters, consistent with mixed inhibition (Figure 2.10 D). Therefore, these

data reveal that 1,3-DNB inhibits ADA using the mixed mechanism shown in Figure 2.1 with inhibition constants of K_I =520 ± 100 μM and K_{IS} = 262 ± 7 μM.

2.4.9 ADA has multiple potential 1,3-DNB binding sites: the active site and peripheral sites

Analysis of the docking results revealed the presence of four distinct clusters of 1,3-DNB poses on murine ADA (Figure 2.11 A) with estimated free energies of binding ΔG_b ranging from -6.31 to -6.99 kcal/mol and corresponding estimated binding constants (K_i) ranging from 7.5 μM to 25.6 μM. The cluster with the most favorable ΔG_b (-6.99 kcal/mol) was centered in the active site of murine ADA with the active site zinc located 2.9 Å from the O2 atom of 1,3-DNB (Figure 2.11 B), and the ND1 atom of His17 positioned 3.1 Å from the O4 atom of 1,3-DNB. The three additional energetically favorable clusters of 1,3-DNB poses were identified as centered on Arg156, Try240 and Val96, with predicted binding energies of -6.56, -6.47, and -6.31 kcal/mol, respectively. The murine ADA residues that contact 1,3-DNB are detailed in Table 2-3. Similar results were obtained in docking experiments with 1,3-DNB against the bovine (PDB ID 1krm) and human (PDB ID 3iar) protein, with energetically favorable ligand poses evident in the active site, together with a putative peripheral binding site centered on Tyr240 (Table 2-3). Docking 1,3-DNB onto bovine ADA revealed the most energetically favored site (ΔG_b = -7.68 kcal/mol) to be extraneous to the active site (ΔG_b for 1,3-DNB docked into the active site = -6.76 kcal/mol). However, this apparent anomaly could be an artifact due to the extensive pre-docking manipulations that were undertaken to clean and refine the bovine ADA structure, given its relatively

low resolution (2.40 Å compared with 1.60 Å for murine ADA and 1.52 Å for human ADA) and its multiple cis-peptide bonds.

Similar results were obtained with docking adenosine into ADA, wherein the highest-scoring clusters were within the active site (ΔG_b = -9.19, -8.53, and -8.25 kcal/mol for human, murine, and bovine ADA, respectively). Among peripheral binding sites, one held in common among the 3 species of ADA was defined by Tyr240 (ΔG_b = -6.12, -5.83, and -6.01 kcal/mol for human, murine, and bovine ADA, respectively). The binding constants, K_i, derived from these binding energies were in the range 0.19-0.89 μM for the active site and 33-53 μM for the Tyr240 peripheral site.

2.4.10 A_1R and ADA both exist on DI TNC-1 cells

As seen in Figure 2.12, western blotting analysis shows the presence of A_1R and ADA in both cytoplasmic and membrane extracts in all groups of DI TNC-1 cells (nontreated, 0.5% DMSO (v/v) and 500 μM 1,3-DNB for 24 h).

2.5 DISCUSSION

In this paper, we present evidence for a mixed mode of inhibition of ADA by 1,3-DNB. Following confirmation of the inhibition of ADA by 1,3-DNB at the biochemical level and cellular levels (Figure 2.5 and Figure 2.6), the chemical basis of the mechanism of inhibition was further investigated. The Hill slope (n; steepness of the log IC_{50} curve) of 1,3-DNB inhibition on ADA was approximately 5, suggesting possible aggregation, denaturation or cooperative inhibition of adenosine deaminase by 1,3-DNB (Prinz, 2009). After the possibilities of

aggregation (Figure 2.7) and denaturation (Figure 2.9) were eliminated, the kinetics of 1,3-DNB inhibition were examined. Substrate inhibition was also observed in steady-state turnover catalyzed by ADA when the adenosine concentration exceeded 150 µM (data not shown). For our analysis, activity measurements were determined at adenosine concentrations in the range 4 – 75 µM, where substrate inhibition was minimal. Then the steady-state kinetics parameters were determined by fitting the Michaelis-Menton equation to the data. As summarized in Table 2-1, addition of 1,3-DNB led to a decrease in the values of k_{cat}, $k_{cat}/K_{M,}$ and K_M. The substantial decrease in the value of k_{cat} indicates that 1,3-DNB inhibits ADA by binding to the ES complex, consistent with either mixed (binds to E and ES, Figure 2.1) or noncompetitive (binds to ES complex) inhibition. The decrease in the values of k_{cat}/K_M and K_M are also consistent with a mixed inhibition mechanism. In addition, fitting k_{cat} and k_{cat}/K_M values to Equation 4 revealed that 1,3-DNB binds to the ES complex, but not E, with positive cooperativity (Figure 2.10 A and B, n = 5 ± 2 for k_{cat}, while n = 1 ± 0.6 for k_{cat}/K_M). This cooperativity is consistent with the high Hill slope observed in IC_{50} experiments.

In the present study, the potential inhibitory effect of 1,3-DNB was examined at two levels of complexity: in a cell culture system and in a cell-free environment. Two higher 1,3-DNB concentrations (100 and 500 µM) used in the former system were very close to the kinetic parameters calculated from the latter (IC_{50} = 283 µM, K_I = 520 µM and K_{IS} = 262 µM). Thus, it is reasonable to infer that the elevated adenosine level seen in the cell culture experiment was due at least in

part to ADA inhibition. However, the IC_{50} value obtained through the biochemical experiment should not be assumed to be the concentration that inhibited half of the ADA in the conditioned media, as in the more complex cellular system, 1,3-DNB can be metabolized, and ADA can turn over (Scheme 2). Metabolically active DI TNC-1 cells should be able to synthesize more ADA to replenish inhibited enzyme, given the fact that the viability of DI TNC-1 cells did not decrease significantly even with the highest 1,3-DNB concentration. In addition, ADA activity could be modified by more than one mechanism. For example, after metabolic activation, 1,3-DNB could covalently bind to proteins or cause protein carbonylation (Reeve and Miller, 2002a, Steiner and Philbert, 2011). Because brain tissue has the capacity to metabolize 1,3-DNB to its major metabolite, 1,3-nitroaniline, in 2 h (Hu et al., 1997b), it is possible that ADA could be inhibited in multiple ways by 1,3-DNB and its metabolites during the 24 h exposure. Yet this theory needs to be further validated.

The mechanism by which 1,3-DNB could increase extracellular adenosine concentrations has been summarized in Scheme 2. From cell and animal experiments, it is known that 1,3-DNB exposure causes a rapid disruption of mitochondrial function by inhibiting mitochondrial complex II in rat brainstem and cortical astrocytes (Phelka et al., 2003). This disruption of mitochondrial bioenergetics would likely result in reduced ATP production. A 44% decrease in cellular ATP level was observed in the susceptible neuroblastoma cell line SY5Y (Tjalkens et al., 2000b). The formation of the mitochondrial permeability transition pore (mtPTP) disrupts mitochondrial integrity and leads to rapid hydrolysis of

ATP to adenosine via the reverse action of F_1F_0 ATPase (Williams et al., 2005). Because of ATP hydrolysis, which could happen both intra- and extracellularly, metabolites such as adenosine and inosine are expected to increase. This theory is consistent with our observation of elevated extracellular adenosine level in the 1,3-DNB-treated groups. From the biochemical experiment in this study, we have also learned that 1,3-DNB could inhibit ADA within seconds, and this inhibition would be expected to further increase adenosine levels.

Once the adenosine concentration is elevated due to these primary events (labeled with I in Figure 2.13), it would in turn cause substrate inhibition of adenosine kinase, the enzyme that phosphorylates adenosine to AMP. This mechanism would further increase the adenosine level as a secondary effect of 1,3-DNB toxicity (labeled with II in Figure 2.13).

In 1,3-DNB toxicity, astrocytes appear to be the primary target followed by secondary neuronal damage (Philbert et al., 1987). As a universal neuromodulator with known neuroprotective effects (Stone et al., 2009), adenosine is hypothesized to be a key player in 1,3-DNB neurotoxicity by binding to adenosine 1 receptors (A_1R). A_1R has been identified as one of the two anchoring proteins for ecto-ADA in a variety of tissues, including brain (Cristalli et al., 2001). One study, conducted using human brain tissue, suggested that ecto-ADA has dual functions, both reducing the extracellular adenosine concentration and binding to A_1R as an allosteric effector to increase receptor functionality (Gracia et al., 2008). As a mixed inhibitor of ADA, 1,3-DNB could influence the A_1R signaling pathway by interfering with the dual functions of ADA. By inhibiting

ADA, the local adenosine concentration around neurons would be elevated, allowing more adenosine molecules to bind to A_1R, leading to decreased rates of firing (Fredholm et al., 2005, Fredholm, 2007b), and presumably, reduced ATP consumption and improved neuronal survival rate.

In our study, the DI TNC-1 cells were exposed for 24 h to three concentrations of 1,3-DNB (10, 100 and 500 µM), which were within the range of 1,3-DNB concentrations that have been used previously on both DI TNC-1 cells and primary astrocytes to test viability. Although compared to the control group, the mitochondrial reductase activity of 500 µM 1,3-DNB-treated DI TNC-1 cells exhibited an apparent decrease of 30% at the end of 24 h exposure. Statistical analysis showed that this reduction was not significant ($p > 0.05$) (Steiner and Philbert, 2011). The other study done on primary astrocytes presented an unchanged LDH release compared to the control group ($p > 0.05$) (Romero et al., 1995). Thus DI TNC-1 cell viability would not be expected to vary significantly in our experiment.

Besides cellular-level research, 1,3-DNB toxicity has also been studied extensively on animals. One of the commonly used dosages on rats by i.p. is 10 mg/kg/day in DMSO.

compiles several studies that use this same dosage but on rats with different genders and body weights. If we calculate the blood volume of the rats using the equation below (Lee and Blaufox, 1985),

Blood Vol (BV, ml) = Body Weight (BW) × 0.06 + 0.77;

then by c = n/BV, we can estimate the blood concentration of 1,3-DNB upon treatment as approximately 900 μM. Because the brain and other tissues have the ability to metabolize 1,3-DNB (Hu et al., 1997b, Reeve and Miller, 2002a), the real-time 1,3-DNB concentration would be expected to decrease gradually from this estimate. Thus, the highest 1,3-DNB concentration (500 μM) used in our study falls below the blood concentrations estimated from in vivo studies.

Previously reported values for the K_M of adenosine as a substrate for ADA encompass a span of 13 to 53 μM, depending upon temperature, pH, and ionic composition of the buffer (Xu and Venton, 2010b); thus, our value of 43 ± 3 μM determined at pH 7.5 and 25°C falls within this range. The k_{cat} is expected to increase with increasing temperature with a Q10 between 2 and 4 (Wolfenden and Snider, 2001). At pH 7.5 and 20°C, the k_{cat} was reported to be 11940 min^{-1} (Kurz et al., 1992); our value of 23100 min^{-1} determined at pH 7.5 and 25°C yields a Q10 of 3.7 and therefore lies within the scope of expected values.

The extracellular adenosine level in the DI TNC-1 cells upon exposure to 1,3-DNB at 500 μM was about 0.33 pmol/μg protein, which is comparable to 1.5 pmol/mg wet tissue, the reported adenosine levels in hypoxic conditions (Takahashi et al., 2010b). Given that 1,3-DNB induces methemoglobinemia

(Cody et al., 1981b), resulting in reduced capacity of oxygen transport, it is expected that hypoxia-like pathology would be seen in 1,3-DNB neurotoxicity. In another study using enzyme-based sensors, adenosine concentration was reported to be about 20 μM from rat hippocampal slices after hypoxia (Frenguelli et al., 2003), which is similar in magnitude to our data (about 30 μM) in conditioned media before normalization against total protein). Taken together, these results indicate that our investigation provides an accurate and convenient way to quantify extracellular adenosine levels in studies of 1,3-DNB neurotoxicity and other similar pathological conditions in vitro.

Our *in silico* findings with the murine and human forms of ADA show the most energetically favorable 1,3-DNB conformations to be within the active site of the enzyme (Figure 2.11 and Table 2-3). Binding to the active site would be expected to occur when extracellular adenosine concentrations are low (k_{cat}/K_M condition), because the affinity of adenosine to ADA is much higher than that of 1,3-DNB, both as predicted by our docking results and as determined experimentally (Frick et al., 1986). This low concentration of adenosine suggests low occupancy of the ADA catalytic center, and very likely binding of 1,3-DNB to the active site. Additionally the high concentration of 1,3-DNB used in this study (500 μM) leads to the possibility that several peripheral sites were occupied with predicted lowest energy conformations ranging from -6.02 to -6.84 kcal/mol for all 3 species of ADA (Table 2-3). In particular, the site defined by Try240 presents a putative allosteric binding site and a target for future investigations into the interaction between ADA and its inhibitors.

Whereas theoretical ΔG_b and K_I values can often be used to rank the relative potencies of ligands for a binding site, or in this case to rank the relative favorability of binding sites for a given ligand, it is considered problematic to use these values to predict absolute values of experimental binding constants (Ferrara et al., 2004). For example, our experimental results demonstrate that the absolute inhibitory potency of 1,3-DNB for ADA is up to 70 times less than that predicted by docking. Nevertheless, the relative similarities in ΔG_b values among the identified ligand clusters indicate likely binding to the active site accompanied by probable interactions with potential allosteric sites defined by Arg156, Try240, and Val96. Thus, our docking studies are in accord with our kinetics results, together predicting additional allosteric sites of interaction between 1,3-DNB and ADA, thereby presenting avenues for future research.

Taken together, this work presents biochemical evidence that 1,3-DNB inhibits the activity of ADA, which could contribute to the observed elevated extracellular adenosine level of approximately 0.33 pmol/µg protein. However, given that our studies have been conducted *in vitro* and *in silico*, further investigations into the *in vivo* interactions between 1,3-DNB and ADA are needed to gain a more complete understanding of this interaction in a physiological context.

2.6 ACKNOWLEDGEMENTS

This work was supported by National Institute of Health grant 1RO1 ES08846 (MAP). I appreciate the help from members of the Philbert laboratory (Jennifer Fernandez, Laura Maurer, Sonja Capracotta, Angela Dixon) for their technical

assistance with various portions of the reported studies, and Xiaomu Guan and Andrea Stoddard from Professor Fierke's laboratory for their advice and assistance.

This research has been previously published: Wang YP, Liu X, Schneider B, Zverina EA, Russ K, Wijeyesakere SJ, Fierke CA, Richardson RJ, Philbert MA (2012) Mixed Inhibition of Adenosine Deaminase Activity by 1,3-Dinitrobenzene: A Model for Understanding Cell-Selective Neurotoxicity in Chemically-Induced Energy Deprivation Syndromes in Brain. Toxicological Sciences 125:509-521.

2.7 EQUATIONS

Equation 2-1.Calculate IC_{50} in cooperative inhibition.

$$Y = \frac{100}{1 + 10^{(\mathrm{Log\ IC50} - X)n}}$$

Equation 2-2. Global fitting for mixed inhibition mechanism.

$$\frac{v_0}{[E]} = \frac{\dfrac{k_{cat}}{\left(1 + \dfrac{[I]^n}{K_{IS}^n}\right)}[S]}{\dfrac{\left(1 + \dfrac{[I]}{K_I}\right)}{\left(1 + \dfrac{[I]^n}{K_{IS}^n}\right)}K_M + [S]}$$

Equation 2-3. Global fitting for noncompetitive inhibition mechanism.

$$\frac{v_0}{[E]} = \frac{\dfrac{k_{cat}}{\left(1 + \dfrac{[I]^n}{K_{IS}^n}\right)}[S]}{K_M + [S]}$$

Equation 2-4. Calculate positive cooperativity in k_{cat} and k_{cat} / K_M conditions

$$k_{app} = \frac{k}{1 + \frac{[I]^n}{K^n}}\ ;\ \text{where } k = k_{cat} \text{ or } \frac{k_{cat}}{K_M}\ ,\ K = K_I \text{ or } K_{IS}$$

2.8 FIGURES

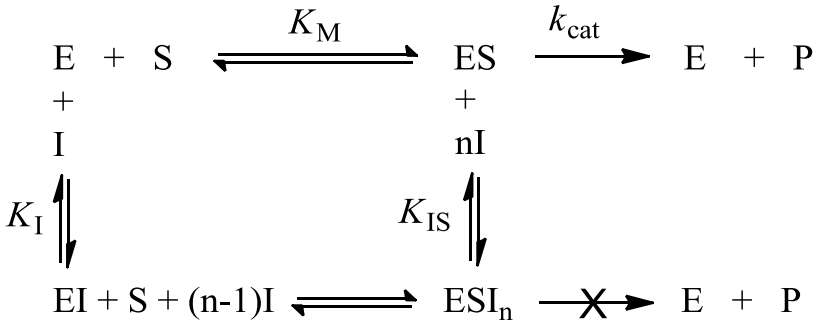

Figure 2.1. Model describing inhibition of adenosine deaminase (E, ADA) catalyzed deamination of adenosine (S) to form inosine (P) by 1,3-dinitrobenzene (I, 1,3-DNB).

The mixed inhibition observed for DNB indicates that the inhibitor both competes with adenosine for binding to E, as described by the inhibition constant, K_I, and binds to the ES complex, as described by the inhibition constant K_{IS}.

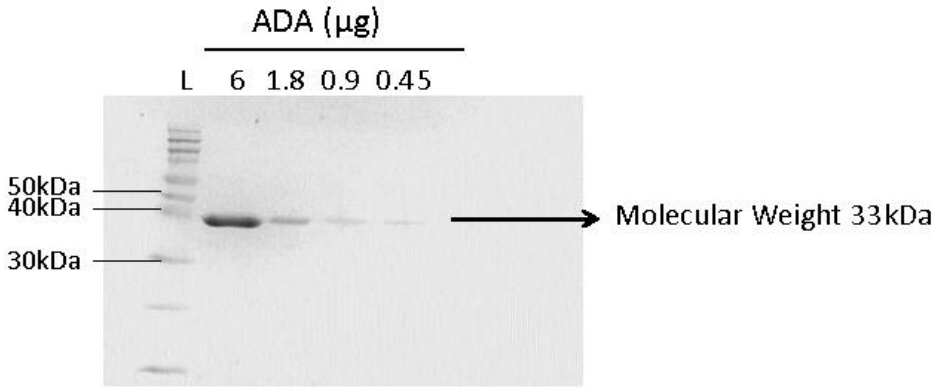

Figure 2.2. Characterization of purchased ADA.

Lane L contained SDS-denatured protein standards with apparent MW in kDa shown to the left. Lanes 1-4 were loaded with the different amount of ADA protein. The loading volume of lanes was made even by RIPA buffer (0.1% SDS (w/v), 1% Triton X-100 (v/v), 150 mM NaCl, 50mM Tris-HCl pH 7.8, 0.5 % sodium deoxycholate (w/v) and 0.1% Protease Inhibitor Cocktail (v/v, Roche Diagnostics, Indianapolis, IN).

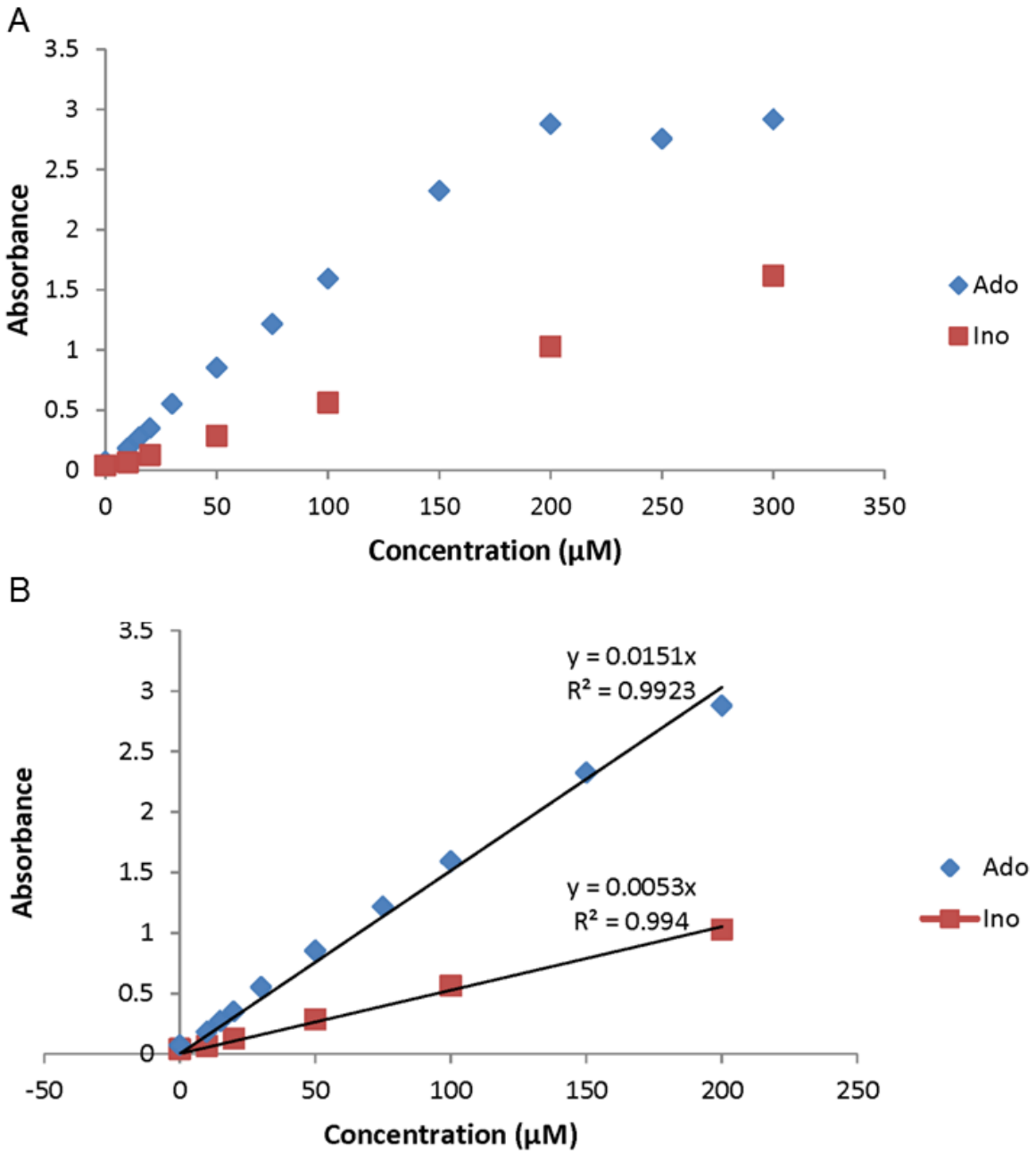

Figure 2.3. Extinction coefficients of adenosine and inosine.

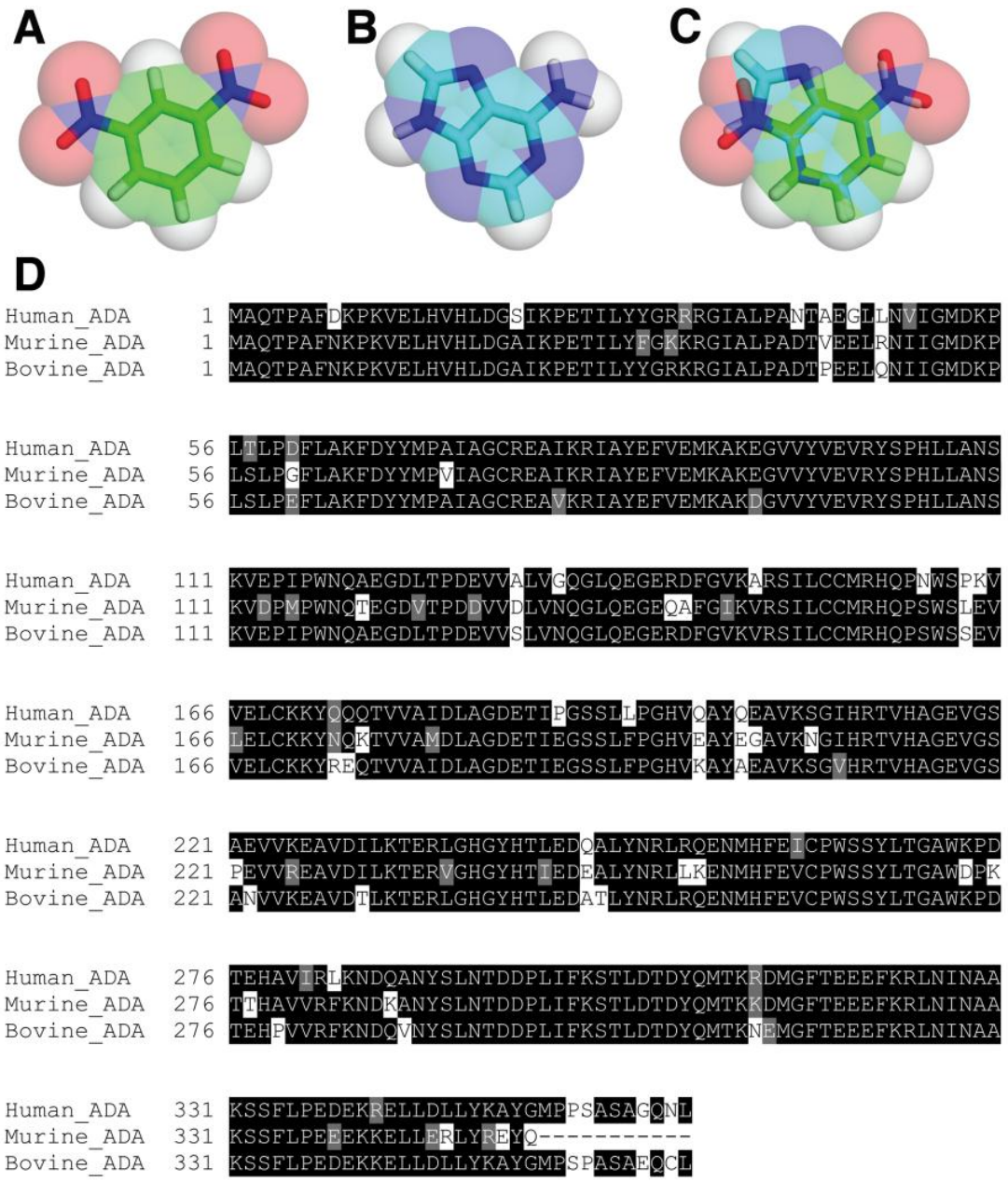

Figure 2.4. Structural and sequence alignments of 1,3-DNB and ADA.

(A) – (C). Models of (A) 1,3-DNB, (B) Adenine ring of adenosine, and (C) 1,3-DNB superimposed on the adenine ring of adenosine. Small molecule alignment was carried out in YASARA and depicted using PyMOL. For quantification, molecular alignment was done with vROCS 3.1.2, yielding a shape Tanimoto coefficient of 0.827 between 1,3-DNB and the adenine ring of adenosine (a perfect shape match would yield a Tanimoto coefficient of exactly 1.000). Molecules are shown as capped sticks within semi-transparent space-filling spheres. Atom colors: carbon = green (1,3-DNB) or cyan (adenine); nitrogen =

dark blue; oxygen = red; hydrogen = white. (D). Sequence alignments of the human, murine, and bovine forms of ADA. Conserved residues are shaded in either black (identical residues) and gray (similar residues); overall pairwise sequence identity is 85.8% across the 3 species.

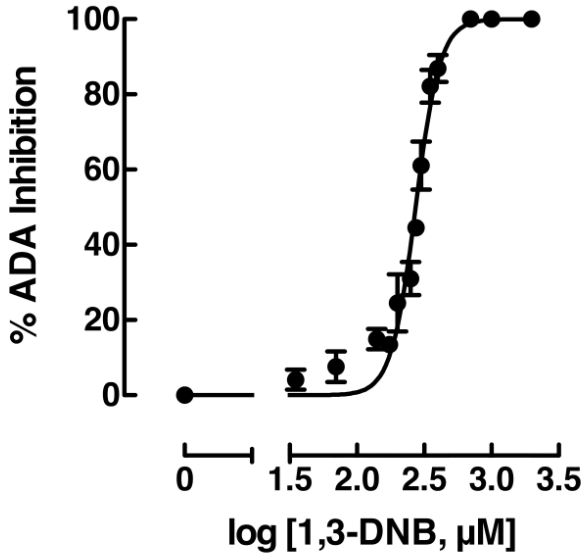

Figure 2.5. 1,3-DNB inhibits the activity of ADA.

The activity of ADA was measured at 50 μM adenosine and varied 1,3-DNB concentrations (35, 70, 140, 175, 200, 250, 275, 300, 350, 400, 700, 1000 and 2000 μM). Symbols represent mean ± SEM (n ≥ 3) from different experiments. The solid line is the fit of Equation 1 to the data.

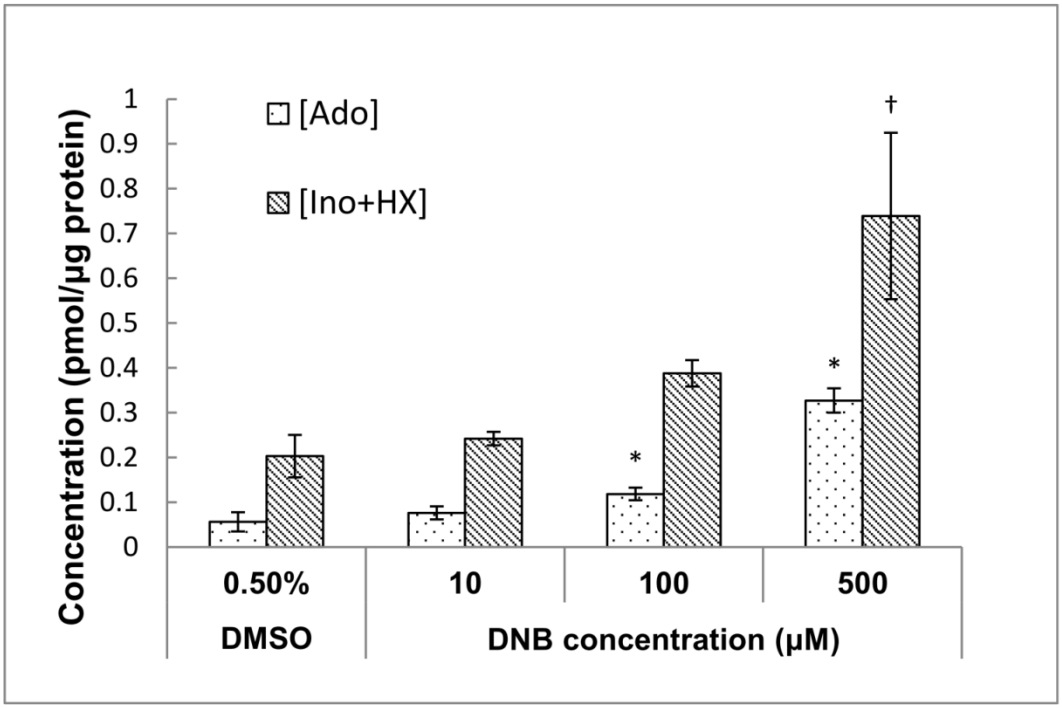

Figure 2.6. Extracellular adenosine (Ado) level, and extracellular inosine (Ino) plus hypoxanthine (HX) level in DMSO- and 1,3-DNB-treated DI TNC cells.

1,3-DNB was extracted with toluene from the conditioned media before measurement. DMSO, as the vehicle control, was tested at 0.5%, 1,3-DNB concentrations were 10, 100 and 500µM . The exposure time was 24 h for all groups. Adenosine level was below detection limit for the DMSO-treated group. Four independent experiment results were collected and normalized against protein concentrations of each sample. Bars represent mean ± SEM.

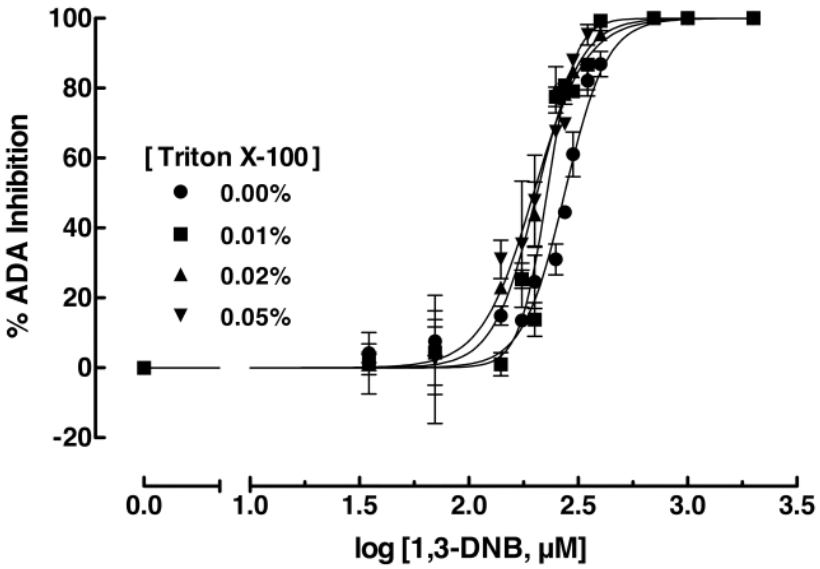

Figure 2.7. Evaluation of 1,3-DNB as an aggregation-based inhibitor.

Triton X-100 was mixed with potassium phosphate buffer (100 mM, pH 7.5) containing adenosine (50 μM) and 1,3-DNB (35, 70, 140, 175, 200, 250, 275, 300, 350, 400, 700, 1000 and 2000 μM) to final concentrations of 0.01%, 0.02% and 0.05% (w/v), then ADA (0.5 nM) was added to initiate the reaction. Symbols represent mean ± SEM from at least three independent experiments for each point.

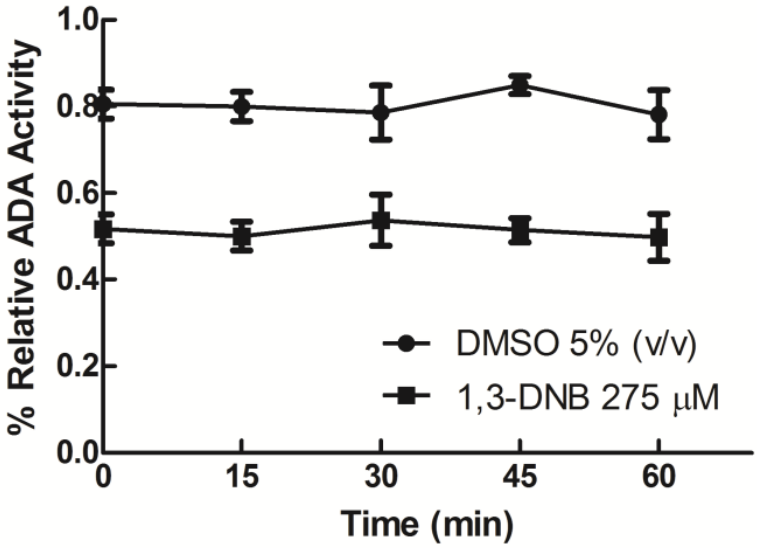

Figure 2.8. Time-dependence of inhibition.

5 % DMSO (v/v) or 5.5 mM 1,3-DNB with 5% DMSO (v/v) was preincubated with ADA (5 nM) in potassium phosphate buffer at 25 ˚C in water bath. At various times of incubation (15, 30, 45, 60 min), 990 µl mixture was added into pre-warmed cuvette containing 10 µl of 5 mM adenosine. The initial rate of reaction was measured. Bars represent mean ± SEM of three separate tests for each time point.

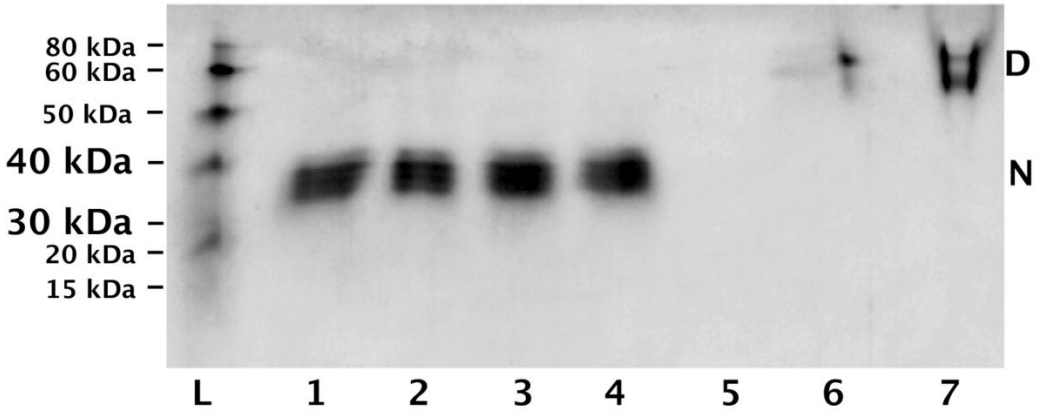

Figure 2.9. Native electrophoretic gel stained by Coomassie blue and rendered in grayscale.

Lane L contained SDS-denatured protein standards with apparent MW in kDa shown to the left. Lanes 1-4 and 6-7 were loaded with the same amount of ADA protein (3.6 µg) preincubated as follows: lane 1, buffer only; lane 2 DMSO (1.0 mM); lane 3, DMSO + 0.35 mM 1,3-DNB; lane 4, 1 mM 1,3-DNB; lane 5, 1 mM 1,3-DNB only; lane 6, heated at 95 °C for 5 min; lane 7, 3M guanidine hydrochloride. N = nondenatured ADA band at approximately 35 kDa; D = denatured ADA at approximately 60-80 kDa. All ADA samples except heat denaturation (lane 6) were preincubated on ice 30 min.

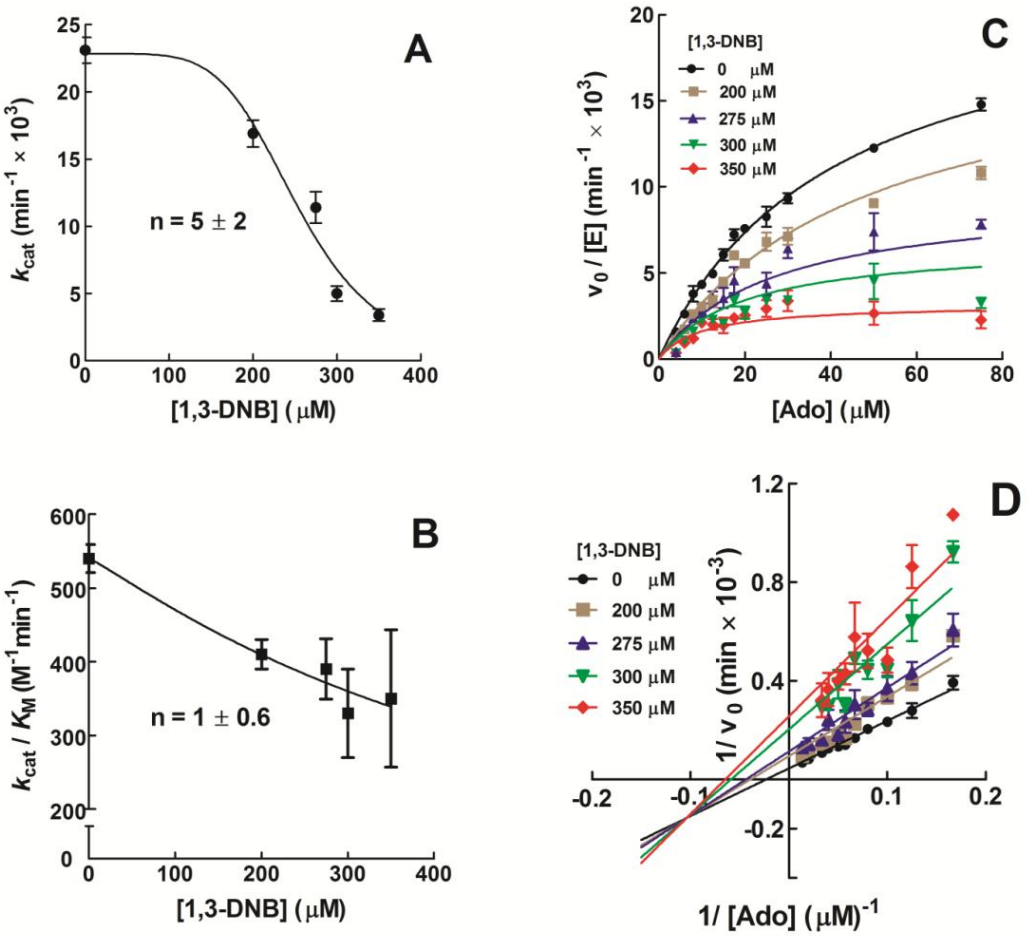

Figure 2.10. Kinetics of inhibition of ADA by 1,3-DNB.

All experiments were conducted at pH 7.5 and t = 25°C. (A) and (B). Fit of k_{cat} and k_{cat}/K_M values (Table 2-1) to Equation 4; (C). Best global fit for the kinetics of ADA in the presence of varying concentrations of 1,3-DNB and adenosine concentrations (4 - 75 μM). Equation 1 derived for cooperative, mixed inhibition (Figure 2.1) is fitted to the data; (D). Lineweaver-Burk plot for the dependence of ADA activity on 1,3-DNB and adenosine concentrations. Symbols represent means ± SEM of at least 4 independent experiments at each concentration for all panels.

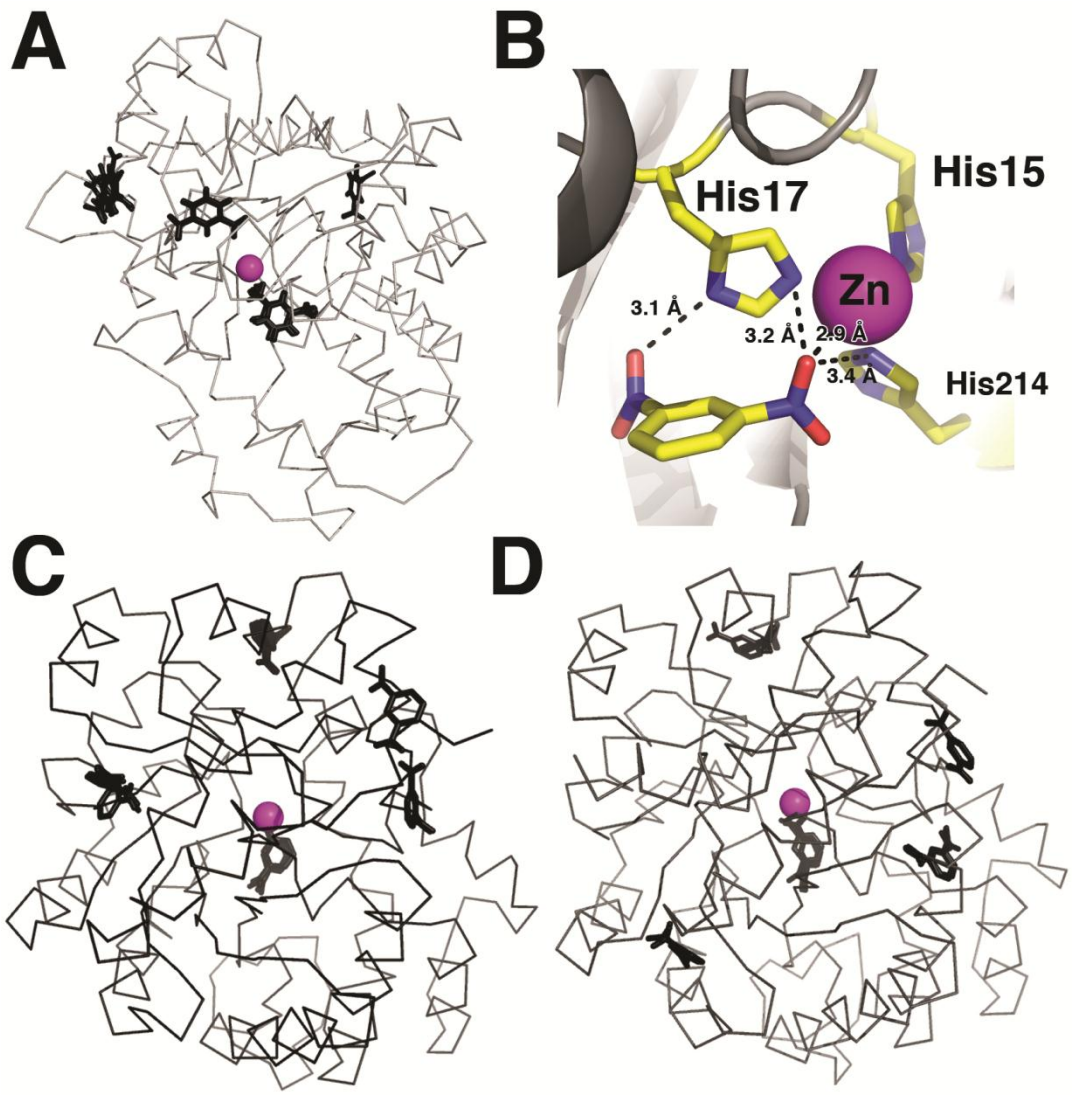

Figure 2.11. Docking studies reveal multiple energetically favorable binding sites in ADA.

(A). Final results from docking 1,3-DNB onto murine ADA (PDB ID 3mvi) showing the presence of four distinct clusters of 1,3-DNB poses on the protein molecule. (B). Interaction between 1,3-DNB and the active site of murine ADA showing polar contact between the active site residues of murine ADA and 1,3-DNB. (C). and (D). Like (A) except showing final docking results for 1,3-DNB against (C) bovine and (D) human ADA. Diagrams were rendered in PyMOL with carbon atoms colored yellow, oxygen in red, and nitrogen in blue with the catalytic zinc shown as a magenta sphere. Hydrogen atoms are omitted for clarity. Calculated free energies of binding for 1,3-DNB against murine, bovine and human ADA, together with residues involved in contacting each ligand conformation are detailed in Table 2-3.

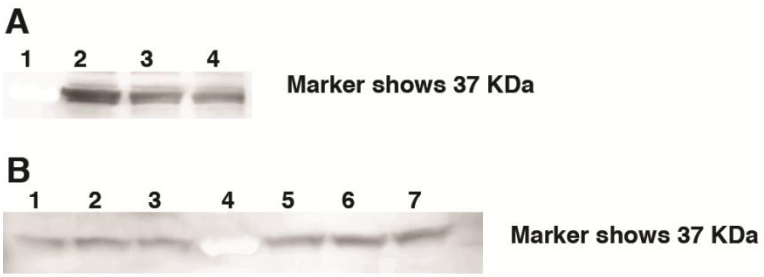

Figure 2.12. Expression of ADA by western blot.

(A) A_1R exists on DI TNC-1 cells in 24 h exposure to culture media, 0.5% DMSO and 500 µM DNB in 24 h (lane 2-4, respectively). Precision Plus Protein Dual Color Standards were loaded into lane 1. (B) Cytoplasmic ADA (lane 1, nontreated; lane 2, 0.5% DMSO; and lane 3, 500 µM DNB) and membrane ADA (lane 5, nontreated; lane 6, 0.5% DMSO; and lane 7, 500 µM DNB) exist on DI TNC-1 cells in 24 h exposure to culture media, 0.5% DMSO and 500 µM DNB in 24 h. Precision Plus Protein Dual Color Standards were loaded into 4.

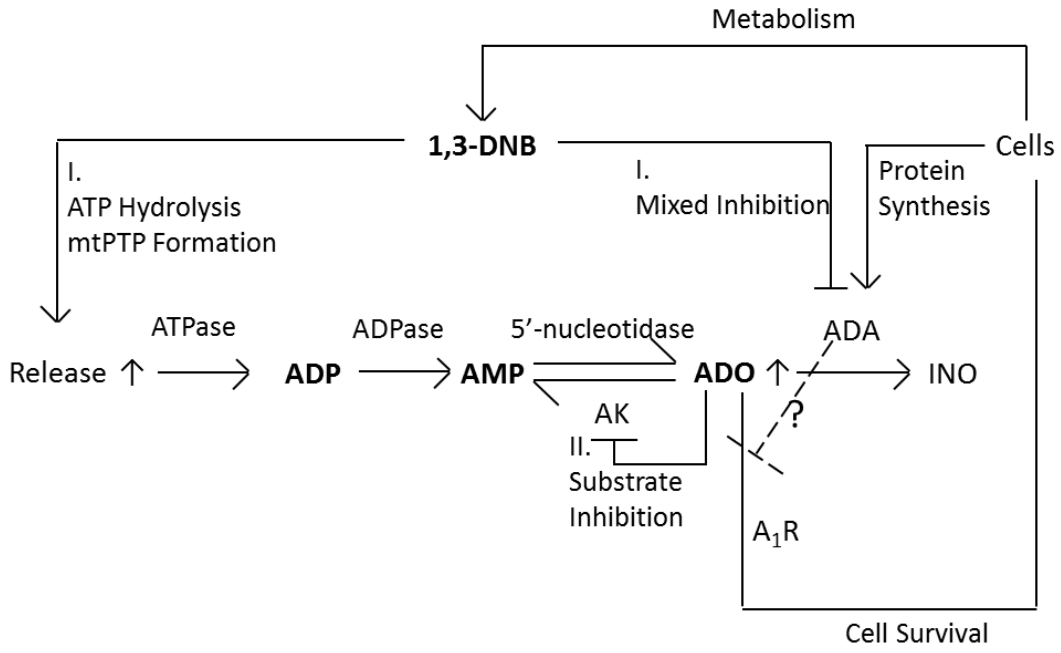

Figure 2.13. The proposed mechanism of increased adenosine level in 1,3-DNB toxicity.

The primary effects of 1,3-DNB include mitochondrial malfunction, which results in increased ATP hydrolysis and leakage, and inhibition of adenosine deaminase (ADA) (Roman number I, solid line). These events lead to increased extracellular adenosine level in a 1,3-DNB concentration dependent manner. The elevated adenosine level, in return, inhibits the activity of adenosine kinase (AK) (Roman number II, solid line). This is a secondary event that happens only when the adenosine level is above 0.5 μM. Whether the inhibition of ADA would affect the binding of adenosine to A_1R has remained untested in this study, and thus is marked by a dashed line with a question mark. Cells also have the ability to metabolize 1,3-DNB and synthesize new ADA, adding more complexity to the system. Although not tested in this study, it has been reported that by binding to A_1R, adenosine has been observed to have neuroprotective effects.

2.9 TABLES

Table 2-1. Steady-state Parameters of Adenosine Deaminase in the Presence of 1,3-Dinitrobenzene [a]

1,3-DNB	k_{cat} (min^{-1})	K_M (μM)	k_{cat}/K_M (min^{-1} μM^{-1})
0 μM 1,3-DNB	23100 ± 960	43 ± 3	540 ± 19
200 μM 1,3-DNB	16900 ± 990	42 ± 4	410 ± 20
275 μM 1,3-DNB	11400 ± 1150	30 ± 6	390 ± 41
300 μM 1,3-DNB	5000 ± 560	15 ± 4	330 ± 60
350 μM 1,3-DNB	3400 ± 440	10 ± 4	350 ± 93

[a] Parameters were best-fitted values obtained from the Michaelis-Menton equations ($v_0/[E]=k_{cat}[S]/(K_M+[S])$ for fitting k_{cat} and K_M values, and $v_0/[E]=(k_{cat}/K_M)[S]/(1+[S]/K_M)$ for fitting k_{cat}/K_M values). Since k_{cat}/K_M values were determined independently from the k_{cat} and K_M values, the k_{cat}/K_M values differ slightly from the ratio of mean values of k_{cat} and K_M.

Table 2-2. List of Steady-State Parameters and Goodness of Fit from the Global Fit of Adenosine Deaminase Activity [a]

3D (Global) Fit		
Best-fit values	**Noncompetitive**	**Mixed**
k_{cat} **(min^{-1})**	21000 ± 830	22459 ± 1025
K_M **(μM)**	36 ± 3	41 ± 3
N	4.1 ± 0.24	6 ± 0.6
K_I **(μM)**	= K_{IS}	519 ± 101
K_{IS} **(μM)**	276 ± 4	262 ± 7
Goodness of Fit		
R^2	0.9251	0.9372
Absolute Sum of Squares	1.63E+08	1.37E+08
Sy.x	894.4	820.8

[a] The experiment was done at pH 7.5 and T = 25°C. Adenosine concentration ranged from 4 to 75 μM; 1,3-DNB concentrations varied from 200 μM to 350 μM. Results represent best-fit values from at least 4 independent trials per concentration of 1,3-DNB and adenosine.

Table 2-3. Analysis of Docked 1,3-Dinitrobenzene Clusters

Receptor	Cluster	ΔG_b (kcal/mol)[a]	K_i (μM)[b]	Contacting residues[c]
Murine ADA	1	-6.99	7.5	**HIS17** ASP19 PHE61 LEU62 PHE65 ARG101 TYR102 SER103 LEU106 CYS153 MET155 ALA183 GLY184 **HIS214** ASP296 **ZN**
	2	-6.56	15.4	ARG156 GLU186 THR187 ILE188 GLU189 GLY190 SER191 SER192 GLY219 SER220 GLU222 VAL223 GLU226
	3	-6.47	18.1	TYR240 HIS241 ILE243 GLU244 SER266 ALA271 TRP272 ASP273 THR277 HIS278 ALA279
	4	-6.31	23.6	VAL96 TYR97 GLY145 ILE146 LYS147 LEU335 GLU339 GLU342 LEU343 ARG346
Bovine ADA	1	-7.68	2.3	TYR240 HIS241 SER266 ALA271 TRP272 LYS273 THR276 GLU277 HIS278 ALA279 VAL281
	2	-6.76	11.16	PRO5 ALA5 PHE7 ASP8 LYS11 LYS92 ASP93 GLY94 THR303 LEU304 ASP305 TYR307
	3	-6.76	11.1	**HIS17** ASP19 PHE61 LEU62 PHE65 TYR102 SER103 LEU106 CYS153 MET 155 ALA 183 GLY 184 **HIS 214** ASP 295 ASP 296 **ZN**
	4	-6.65	13.3	PRO5 ALA6 PHE7 ASP8 LYS9 LYS312 THR318 GLU319 PHE321
	5	-6.02	38.7	GLU234 ARG235 LEU236 GLU255 ASN258 MET257 HIS258 ASN289 LYS331 SER332
Human ADA	1	-6.91	8.65	**HIS17** ASP19 PHE61 LEU62 PHE65 ARG101 TYR102 SER103 LEU106 CYS153 MET155 ALA183 GLY184 **HIS214** ASP296 **ZN**
	2	-6.84	9.76	TYR240 HIS241 GLY270 ALA271

			TRP272 LYS273 THR276 GLU277 HIS278 ALA279
3	-6.79	10.48	PRO5 ALA6 PHE7 ASP8 LYS9 LYS11 LYS92 GLU93 THR303 LEU304 ASP305 TYR308
4	-6.46	18.43	CYS169 GLN173 VAL177 VAL178 ALA179 GLY208 ILE209 HIS210 PHE334 LEU335 PRO336
5	-6.23	27.23	VAL16 SER21 ILE22 LYS23 PRO24 GLU85 PHE86 MET89 LYS90 PRO297 LEU298

[a] Estimated free energy of binding; more negative values correspond to increasing favorability of binding
[b] Estimated binding constant; smaller values correspond to more favorable binding.
[c] Contacting residues within the active site including the catalytic zinc and involved in coordination with the catalytic zinc are shown in bold face.

Table 2-4. Estimated 1,3-DNB Concentration upon Administration to Rats in Previous Studies.

Year of Publication	Rat	G	Dosage	Boday Weight (BW)	Median Weight (g)	Blood Vol (BV, ml) = BW x 0.06 + 0.77	[DNB, (in Molar)] = dosage x weight / M / BV
2006	F344	M	10mg/kg	220-270g	245	15.47	0.94
2003	F344	M	DNB	200-220g	210	13.37	0.93
1999	F344	F	in DMSO	250-300g	275	17.27	0.95

[a] (Mavroudis et al., 2006b)
[b] (Phelka et al., 2003)
[c] (Xu et al., 1999a)
[d] G-gender. M-Male, F-Female

2.10 REFERENCES

Alunni, S., Orru, M., and Ottavi, L. (2008). A study on the inhibition of adenosine deaminase. *J Enzyme Inhib Med Chem*. **23**, 182-189.

Blackburn, D. M., Gray, A. J., Lloyd, S. C., Sheard, C. M., and Foster, P. M. (1988). A comparison of the effects of the three isomers of dinitrobenzene on the testis in the rat. *Toxicol Appl Pharmacol*. **92**, 54-64.

Bond, J. A., Chism, J. P., Rickert, D. E., and Popp, J. A. (1981). Induction of hepatic and testicular lesions in Fischer-344 rats by single oral doses of nitrobenzene. *Fundam Appl Toxicol*. **1**, 389-394.

Brown, C. D., and Miller, M. G. (1991). Effect of Culture Age on 1,3-Dinitrobenzene Metabolism and Indicators of Cellular Toxicity in Rat Testicular Cells. *Toxicology in Vitro*. **5**, 269-275.

Burnstock, G. (2006). Historical review: ATP as a neurotransmitter. *Trends Pharmacol Sci*. **27**, 166-176.

Butina, D. (1999). Unsupervised data base clustering based on Daylight's fingerprint and Tanimoto similarity: A fast and automated way to cluster small and large data sets. *Journal of Chemical Information and Computer Sciences*. **39**, 747-750.

Cody, T. E., Witherup, S., Hastings, L., Stemmer, K., and Christian, R. T. (1981). 1,3-dinitrobenzene: toxic effects in vivo and in vitro. *J Toxicol Environ Health*. **7**, 829-847.

Coligan, J. E. (1996). Current protocols in protein science, edited, pp. pp. 10.3.1–10.3.11, John Wiley and Sons, New York.

Cristalli, G., Costanzi, S., Lambertucci, C., Lupidi, G., Vittori, S., Volpini, R., and Camaioni, E. (2001). Adenosine deaminase: functional implications and different classes of inhibitors. *Med Res Rev*. **21**, 105-128.

Duan, Y., Wu, C., Chowdhury, S., Lee, M. C., Xiong, G., Zhang, W., Yang, R., Cieplak, P., Luo, R., Lee, T. *et al*. (2003). A point-charge force field for molecular mechanics simulations of proteins based on condensed-phase quantum mechanical calculations. *J Comput Chem*. **24**, 1999-2012.

Ferrara, P., Gohlke, H., Price, D. J., Klebe, G., and Brooks, C. L. (2004). Assessing scoring functions for protein-ligand interactions. *Journal of Medicinal Chemistry*. **47**, 3032-3047.

Fredholm, B. B. (2007). Adenosine, an endogenous distress signal, modulates tissue damage and repair. *Cell Death Differ*. **14**, 1315-1323.

Fredholm, B. B., Chen, J. F., Masino, S. A., and Vaugeois, J. M. (2005). Actions of adenosine at its receptors in the CNS: insights from knockouts and drugs. *Annu Rev Pharmacol Toxicol*. **45**, 385-412.

Frenguelli, B. G., Llaudet, E., and Dale, N. (2003). High-resolution real-time recording with microelectrode biosensors reveals novel aspects of adenosine release during hypoxia in rat hippocampal slices. *J Neurochem*. **86**, 1506-1515.

Frick, L., Wolfenden, R., Smal, E., and Baker, D. C. (1986). Transition-state stabilization by adenosine deaminase: structural studies of its inhibitory complex with deoxycoformycin. *Biochemistry*. **25**, 1616-1621.

Gracia, E., Cortes, A., Meana, J. J., Garcia-Sevilla, J., Herhsfield, M. S., Canela, E. I., Mallol, J., Lluis, C., Franco, R., and Casado, V. (2008). Human adenosine deaminase as an allosteric modulator of human A(1) adenosine receptor: abolishment of negative cooperativity for [H-3](R)-pia binding to the caudate nucleus. *Journal of Neurochemistry*. **107**, 161-170.

Hu, H. L., Bennett, N., Lamb, J. H., GhersiEgea, J. F., Schlosshauer, B., and Ray, D. E. (1997). Capacity of rat brain to metabolize m-dinitrobenzene: an in vitro study. *Neurotoxicology*. **18**, 363-370.

Johansson, B., Halldner, L., Dunwiddie, T. V., Masino, S. A., Poelchen, W., Gimenez-Llort, L., Escorihuela, R. M., Fernandez-Teruel, A., Wiesenfeld-Hallin, Z., Xu, X. J. et al. (2001). Hyperalgesia, anxiety, and decreased hypoxic neuroprotection in mice lacking the adenosine A1 receptor. *Proc Natl Acad Sci U S A*. **98**, 9407-9412.

Kaplan, N. O. (1955). Specific Adenosine Deaminase from Intestine. *Methods in Enzymology*. **2**, 473-475.

Nakanishi, I., Terasaka, T., Kuno, M., Seki, N., Warizaya, M., Matsumura, H., Inoue, T., Takano, K., Adachi, H., Mori, Y. and Fujii, T. (2005). Structural basis of compound recognition by adenosine deaminase. *Biochemistry*. **44**, 10562-10569.

Kinoshita, T., Tada, T., and Nakanishi, I. (2008). Conformational change of adenosine deaminase during ligand-exchange in a crystal. *Biochem Biophys Res Commun*. **373**, 53-57.

Krieger, E., Darden, T., Nabuurs, S. B., Finkelstein, A., and Vriend, G. (2004). Making optimal use of empirical energy functions: Force-field parameterization in crystal space. *Proteins-Structure Function and Bioinformatics*. **57**, 678-683.

Kurz, L. C., Moix, L., Riley, M. C., and Frieden, C. (1992). The rate of formation of transition-state analogues in the active site of adenosine deaminase is encounter-controlled: implications for the mechanism. *Biochemistry*. **31**, 39-48.

Latini, S., and Pedata, F. (2001). Adenosine in the central nervous system: release mechanisms and extracellular concentrations. *Journal of Neurochemistry*. **79**, 463-484.

Lee, H. B., and Blaufox, M. D. (1985). Blood volume in the rat. *J Nucl Med*. **26**, 72-76.

Mavroudis, G., Prior, M. J., Lister, T., Nolan, C. C., and Ray, D. E. (2006). Neurochemical and oedematous changes in 1,3-dinitrobenzene-induced astroglial injury in rat brain from a 1H-nuclear magnetic resonance perspective. *J Neural Transm*. **113**, 1263-1278.

Miller, J. A., Runkle, S. A., Tjalkens, R. B., and Philbert, M. A. (2011). 1,3-Dinitrobenzene Induced Metabolic Impairment Through Selective Inactivation of the Pyruvate Dehydrogenase Complex. *Toxicol Sci*. **122**, 502-511.

Morris, G. M., Goodsell, D. S., Halliday, R. S., Huey, R., Hart, W. E., Belew, R. K., and Olson, A. J. (1998). Automated docking using a Lamarckian genetic algorithm and an empirical binding free energy function. *Journal of Computational Chemistry*. **19**, 1639-1662.

North, R. A., and Verkhratsky, A. (2006). Purinergic transmission in the central nervous system. *Pflugers Arch*. **452**, 479-485.

Pak, M. A., Haas, H. L., Decking, U. K., and Schrader, J. (1994). Inhibition of adenosine kinase increases endogenous adenosine and depresses neuronal activity in hippocampal slices. *Neuropharmacology*. **33**, 1049-1053.

Pal, D., and Chakrabarti, P. (1999). Cis peptide bonds in proteins: residues involved, their conformations, interactions and locations. *J Mol Biol*. **294**, 271-288.

Parkinson, F. E., Xiong, W., and Zamzow, C. R. (2005). Astrocytes and neurons: different roles in regulating adenosine levels. *Neurol Res*. **27**, 153-160.

Phelka, A. D., Beck, M. J., and Philbert, M. A. (2003). 1,3-Dinitrobenzene inhibits mitochondrial complex II in rat and mouse brainstem and cortical astrocytes. *Neurotoxicology*. **24**, 403-415.

Philbert, M. A., Nolan, C. C., Cremer, J. E., Tucker, D., and Brown, A. W. (1987). 1,3-Dinitrobenzene-Induced Encephalopathy in Rats. *Neuropathology and Applied Neurobiology*. **13**, 371-389.

Phillips, E., and Newsholme, E. A. (1979). Maximum activities, properties and distribution of 5' nucleotidase, adenosine kinase and adenosine deaminase in rat and human brain. *J Neurochem*. **33**, 553-558.

Prinz, H. (2009). Hill coefficients, dose-response curves and allosteric mechanisms. *J Chem Biol*. **3**, 37-44.

Reeve, I. T., and Miller, M. G. (2002). 1,3-Dinitrobenzene metabolism and protein binding. *Chem Res Toxicol*. **15**, 352-360.

Ribeiro, J. A., and Sebastiao, A. M. (2010). Modulation and metamodulation of synapses by adenosine. *Acta Physiol (Oxf)*. **199**, 161-169.

Romero, I. A., Lister, T., Richards, H. K., Seville, M. P., Wylie, S. P., and Ray, D. E. (1995). Early metabolic changes during m-Dinitrobenzene neurotoxicity and the possible role of oxidative stress. *Free Radic Biol Med*. **18**, 311-319.

Seidler, J., McGovern, S. L., Doman, T. N., and Shoichet, B. K. (2003). Identification and prediction of promiscuous aggregating inhibitors among known drugs. *Journal of Medicinal Chemistry*. **46**, 4477-4486.

Steiner, S. R., and Philbert, M. A. (2011). Proteomic identification of carbonylated proteins in 1,3-dinitrobenzene neurotoxicity. *Neurotoxicology*. **32**, 362-373.

Stone, T. W., Ceruti, S., and Abbracchio, M. P. (2009). Adenosine receptors and neurological disease: neuroprotection and neurodegeneration. *Handb Exp Pharmacol*, **193**, 535-587.

Takahashi, T., Otsuguro, K., Ohta, T., and Ito, S. (2010). Adenosine and inosine release during hypoxia in the isolated spinal cord of neonatal rats. *Br J Pharmacol*. **161**, 1806-1816.

Tjalkens, R. B., Ewing, M. M., and Philbert, M. A. (2000). Differential cellular regulation of the mitochondrial permeability transition in an in vitro model of 1,3-dinitrobenzene-induced encephalopathy. *Brain Res*. **874**, 165-177.

Wang, S. H., Wang, S. F., Xuan, W., Zeng, Z. H., Jin, J. Y., Ma, J., and Tian, G. R. (2008). Nitro as a novel zinc-binding group in the inhibition of carboxypeptidase A. *Bioorg Med Chem*. **16**, 3596-3601.

Williams, E. S., Phelka, A., Ray, D. E., and Philbert, M. A. (2005). Astrocytes in Acute Energy Deprivation Syndromes. Second Edition ed., 237-250 pp., CRC Press, Boca Raton, FL.

Wolfenden, R., and Snider, M. J. (2001). The depth of chemical time and the power of enzymes as catalysts. *Acc Chem Res*. **34**, 938-945.

Xu, J., Nolan, C. C., Lister, T., Purcell, W. M., and Ray, D. E. (1999). Pharmacokinetic factors and concentration-time threshold in m-dinitrobenzene-induced neurotoxicity. *Toxicol Appl Pharmacol*. **161**, 267-273.

Xu, Y. D., and Venton, B. J. (2010). Rapid determination of adenosine deaminase kinetics using fast-scan cyclic voltammetry. *Physical Chemistry Chemical Physics*. **12**, 10027-10032.

CHAPTER 3

THE NEUROPROTECTIVE EFFECTS OF ADENOSINE IN 1,3-DINITROBENZENE TOXICITY IN RAT PRIMARY NEURONS

3.1 ABSTRACT

1,3-Dinitrobenzene (1,3-DNB) produces neuropathic changes with characteristic injury to astrocytes and attendant sparing of neurons in the brainstem of rats. 1,3-Dinitrobenzene is also a mixed inhibitor of the extracellular enzyme, adenosine deaminase (ADA). Inhibition of ADA leads to increased levels of adenosine: a neuromodulator that has demonstrated neuroprotective effects in a variety of neuropathic states including hypoxia and stroke. This study examines the relationship among astrocyte-dependent release of adenosine, subsequent activation of neuronal adenosine receptor A (A_1R) and suppression of neuronal excitability. Studies in rats show that silencing of neuronal activity through tympanic rupture lessens dependence upon glucose metabolism and spares neurons from 1,3-DNB-induced neuropathy. It is, therefore, hypothesized that the release of adenosine from astrocytes enhances neuronal survival. First, extracellular adenosine was measured in 1,3-DNB exposed primary astrocytes by enzyme based sensors. We found that compared to vehicle control groups, extracellular adenosine elevated by 11 folds to 6 µM following 12 h exposure of 500 µM 1,3-DNB. Next, we assessed if exogenous adenosine improves neuronal viability by adding low to medium micro molar of adenosine to 1,3-DNB exposed

primary neurons, Our results show that neurons co-exposed of exogenous adenosine (10 and 100 µM) and 1,3-DNB had significantly higher ATP levels by 25% and 50% respectively, compared with 1,3-DNB exposure alone. Furthermore, adding A_1R agonist CPA increased membrane integrity of 1,3-DNB exposed neurons by approximately 100%. The effect of increasing membrane integrity was diminished by potent A_1R antagonist DPCPX. These results support the idea that astrocyte injury and release of adenosine into the extracellular space may be a neuroprotective process that is mediated through A_1R on neurons. Neuronal potassium dependent cytoplasmic Ca^{2+} increase was visualized by the fluorescent dye Fluo-4 AM. The time to onset and the magnitude of cytoplasmic Ca^{2+} increases following stimulation with 25 mM KCl in the extracellular buffer were delayed and reduced by 5 µM adenosine in 10 µM DNB exposed neurons. To pinpoint which AR signaling pathway(s) mediates inhibited excitability, A_1R agonist CPA, A_1R antagonist DPCPX and $A_{2a}R$ agonist CGS 21680 were used. Results show that CPA had stronger inhibitory effects than adenosine in reducing cytoplasmic Ca^{2+} increase. DPCPX itself did not significantly alter neuronal excitability, but it diminished the inhibitory effects from adenosine. No significant change in time to onset or the magnitude of intracellular Ca^{2+} increase was observed in CGS 21680 treated neurons. This study advances our knowledge in the molecular mechanism of neuroprotection observed in the early stage of 1,3-DNB neurotoxicity.

3.2 INTRODUCTION

1,3-Dinitrobenzene is highly lipophilic and has been used widely as an industrial intermediate (1989). Both human and animal intoxication have been reported following exposure to1,3-DNB. Affected systems include circulatory, male reproductive and nervous. Symptoms include vomiting, loss of hearing, headache, nausea and loss of cognition (Cody et al., 1981a, Blackburn et al., 1988a, Vasquez et al., 1995). Histopathological evaluation of brains from exposed rats reveals focal bilateral edematous lesions in the vestibular nuclei, deep cerebellar roof nuclei, and ventral cochlear nucleus (part of auditory pathways) of the brainstem (Philbert et al., 1987). Lesions resemble in regional distribution of lesions and cell-selectivity the symmetrical spongiform brain stem lesions observed in Acute Energy Deprivation Syndromes [AEDS; (Cavanagh, 1988, 1993)]. Acute Energy Deprivation Syndromes have been observed in other diseases of nutritional deficiency or toxicity due to ingestion of antimetabolites such as thiamine deficiency and (S)-α-chlorohydrin toxicity (Cavanagh and Nolan, 1993). One important neuropathological feature of AEDS is the observed differential cellular sensitivity of astrocytes as the primary target, while neurons, endothelial cells and oligodendrocytes are spared in the early stage of toxicity. 1,3-DNB toxicity causes astrocyte end foot processes to swell and necrosis appeared 12 h after the final dose of the 3 x 10 mg/kg dose schedule of 1,3-DNB (Figure 3.1). Neurons remain intact and regain function if the 1,3-DNB challenge is removed within 36 h (Philbert et al., 1987, Romero et al., 1991). Up to this

point, the molecular mechanisms of the selective cell injury produced by exposure to 1,3-DNB have remained largely elusive.

Research from our laboratory has shown that 1,3-DNB induces depolarization of astrocytic mitochondria in a dose dependent manner (Tjalkens et al., 2000a, Phelka et al., 2006). Exposure of C6 glioma cells to 1 mM 1,3-DNB for 36 h significantly diminished intracellular ATP levels by 60% compared to the vehicle control group (Miller et al., 2011a). 1,3-Dinitrobenzene also induced oxidative stress in immortalized type I astrocytes DI TNC-1 cells that eventually led to carboxylation of specific proteins, such as F_1-ATP synthase subunit beta in 1 mM and 1 μM 1,3-DNB conditions (Steiner and Philbert, 2011). Using 2-deoxyglucose, Bagley and colleagues showed that the most susceptible regions of the brainstem, i.e., the auditory and vestibular systems, had the highest requirements for glucose (Bagley et al., 1989). The higher basal requirement for energy equivalents in neurons would lead one, therefore, to the logical conclusion that neurons would be more sensitive to the deleterious effects of neurotoxicants and antimetabolites that induce AEDS than their astrocytic counterparts. (Attwell and Laughlin, 2001, Pellerin and Magistretti, 2004). This histopathological paradox provides the foundation for the studies included in this manuscript.

Reduced energy demand or consumption has been demonstrate to associate with less severe lesions in 1,3-DNB neurotoxicity. Bifenthrin, a chemical that causes hyperexcitability, causes ataxia with 3 x 9 mg/kg 1,3-DNB, a dosage that did not cause ataxia by itself. On the other hand, anaesthesia such as isoflurane

and urethane ameliorate lesions (Holton et al., 1997). Another study showed that in rats with one side tympanic membrane rupture, reduced auditory function coincided with reduced metabolism and attenuated lesion in rats (Ray et al., 1992). These *in vivo* studies suggest that reduced energy consumption decreases the severity of lesion in 1,3-DNB toxicity.

Of the large amounts of energy neurons require to maintain normal function, electrical activity accounts for at least 50% in the entire brain (Lutz et al., 2003). The excitability of neurons is a balance of inhibitory and excitatory receptor activation by regulatory molecules and status of ion channels (Davis, 2006, O'Leary and Wyllie, 2011). One of these regulatory molecules is adenosine, the hydrolysis product of ATP (Sperlagh and Vizi, 2011). Adenosine binds to adenosine receptors (AR) and causes a variety of subsequent biological responses by modulating the activity of adenylyl cyclase (AC, EC 4.6.1.1) (Fredholm, 2007a). In short, binding to the four types of ARs will generate either inhibitory (A_1R or A_3R) or stimulatory ($A_{2a}R$ and $A_{2b}R$) effects on AC. Adenosine in the extracellular space is inactivated by adenosine deaminase (ADA, EC 3.5.4.4) to inosine or by adenosine kinase (AK, EC 2.7.1.20) in the cytoplasm to adenosine monophosphate. During hypoxia-induced death, activation of A_1R by agonist CPA reduces the release of lactate dehydrogenase (LDH, EC 1.1.1.27) from neuron mono-culture and consequently protected cerebellar neurons (Logan and Sweeney, 1997).

1,3-DNB induces methemoglobinemia (Cody et al., 1981a), resulting in reduced capacity of oxygen transport, it is expected that hypoxia-like pathology would

also be observed in 1,3-DNB neurotoxicity. In addition, 1,3-Dinitrobenzene inhibits the activity of ADA, leading to significantly increased adenosine levels in DI-TNC cells (Wang et al., 2012).Therefore, we hypothesize that extracellular adenosine levels increase in 1,3-DNB exposed astrocytes. Adenosine binding to A_1R suppresses neuronal excitability, leading to reduced energy consumption and improved neuronal survival.

In this paper, we report that astrocytic release of adenosine increases ATP levels and membrane integrity of 1,3-DNB exposed neurons. Exogenous adenosine also delays and reduces the time to onset and magnitude of cytoplasmic Ca^{2+} increase following KCl stimulation.

The present study explored the mechanism of ADA inhibition by 1,3-DNB. In this paper, we report that 1,3-DNB inhibits ADA with an apparent IC_{50} of 284 µM. Furthermore, our kinetics studies found that the rate of inhibition depended upon substrate concentration, indicating that 1,3-DNB is a mixed inhibitor of ADA, in agreement with our modeling studies, which predict binding of 1,3-DNB to the active site as well as peripheral sites. These studies lend further support to the idea that astrocytes provide acute protection against neurotoxicants and antimetabolites by paracrine control of neuronal function.

3.3 MATERIALS AND METHODS

3.3.1 Chemicals and Supplies

Dimethyl sulfoxide (DMSO), 1,3-dinitrobenzene (1,3-DNB), potassium chloride (KCl), adenosine, Poly-L-lysine (PLL) solution, potassium phosphate monobasic

(KH_2PO_4), N6-cyclopentyladenosine (CPA), 8-Cyclopentyl-1,3-dipropylxanthine (DPCPX), CGS-21680 hydrochloride hydrate (CGS-21680), BrightMax white sealing films and bovine serum albumin (BSA) were obtained from Sigma (St. Louis, MO). Potassium hydroxide (KOH) and toluene were obtained from Fisher Scientific (Pittsburgh, PA). Triton X-100 was purchased from Bio-Rad Laboratory (Hercules, CA). Fluo-4 AM (Cell Permeant, Special Packaging), Pluronic F-127 (20% solution in DMSO), HEPES Buffer Solution (1 M), Hank's Balanced Salt Solution (HBSS, no calcium, no magnesium, no phenol red), Neurobasal Medium Minus Phenol Red, Neurobasal Medium, Horse Serum (heat-inactivated), normal goat serum (NGS), B-27 Serum-Free Supplement (50X), 0.25% Trypsin-EDTA, GlutaMAX, Antibiotic-Antimycotic (Anti-Anti) and Dulbecco's phosphate buffered saline (D-PBS) were obtained from Invitrogen (Carlsbad, CA). Adenosine and inosine sensors were purchased from Sarissa Biosensor (Coventry, UK). BCA protein assay kits and Lab-Tek Chamber Slide System were obtained from Thermo Scientific (Rockford, IL). Cortex tissue and Hibernate A without Calcium were purchased from Brainbits (Springfield, IL). Papain was bought from Worthington Biochemical (Lakewook, NJ). CellTiter-Glo® Luminescent Cell Viability Assay Kits and MultiTox-Fluor Multiplex Cytotoxicity Assay Kits were obtained from Promega (Madison, WI). Coverslips (22 X 22 mm^2) were purchased from Corning (Corning, NY). Poly-D-lysine (PDL) coated 96 well white/clear plates were purchased from BD Bioscience (Franklin Lakes, NJ).

3.3.2 Single Device Fabrication

The custom single well chamber slip is comprised of a polydimethylsiloxane (PDMS) block with a circular core that is sealed to a cover slip. To prepare the wall of the well, a degassed PDMS mixture, comprised of a 1:10 (w/w) ratio of elastomer to curing agent, was poured into a Petri dish to a height of 11mm and fully cured at 60°C for 3 hours (resulting PDMS substrate height ~10 mm). A scalpel was used to cut (18 x 18 x 10) mm^3 blocks from the PDMS slab, and a biopsy punch (8 mm diameter) was used to bore a hole from the center of each PDMS block. PDMS substrates were soaked in 70% ethanol (EtOH) for 2 hours. In a sterile laminar flow hood, PDMS substrates were rinsed thoroughly with sterile distilled water (di$H_2$0). PDMS substrates were left to dry overnight, or until all ethanol has evaporated (aspiration can be applied to remove residual EtOH). Square cover glasses (22 X 22 mm^2) were sonicated in diH_2O for 30 minutes. In a laminar flow hood, the cover glasses placed in an EtOH (70%) and bathed overnight. Cover glasses were rinsed with sterile diH20 and dried overnight. To assembly the chamber, a pair of EtOH sterilized tweezers were used to center the cored region of a PDMS substrate over a square cover glass and apply gentle over all regions of the top face of the PDMS well, ensuring complete sealing. Fully constructed chambers were housed in Petri-dishes, were they were exposed to ultraviolet (UV) light, a germicidal, for 1 hour. In preparation for cell loading, 150µL of PLL was added to each well. Petri-dishes were wrapped in parafilm (to curb evaporation) and PLL was allowed to adhere overnight. The following day, PLL was aspirated and the wells were twice filled and rinsed with

sterile diH20. Prior to loading cells, the wells were dried, under UV light, for 30 minutes.

3.3.3 Primary cortical neuron and primary astrocyte isolation

Rat cortex brain tissue was purchased from BrainBits (Springfield, IL). Primary cell isolation was performed according to the manufacturer's instruction with some modifications. Briefly, embryonic day 18 rat cortices were stored in 4°C until use. The media in the tissues storage vial was removed and saved for later use. Then the tissues were incubated in 2 mg/ml papain solution in Hibernate-Ca in 37°C bead bath for 30 min. After replacing the papain solution with the original vial media, the tissues were dissociated by 15 repeated triturations. The dissociated cells were collected by centrifugation at 200x g for 1 min. To obtain primary neurons, the pellet was resuspended by 1 ml neurobasal media with 2% (v/v) B27 supplement, 0.25% (v/v) 10x GlutaMax and 1% (v/v) Anti-Anti. Plating concentrations are demonstrated as follows, $1x10^5$ cells/ml per chamber onto PLL coated 8 well chamber slide for neuron purity test, $3x10^5$ cells/ml per device for Ca2+ wave visualization, $3x10^5$ cells/ml per well onto PDL coated 96 well plates for biochemical assays, $5x10^5$ cells/ml per well onto PDL coated 6 well plates for mRNA extraction. For all the experiments, primary neurons were used between day 6 and day 8. To obtain primary astrocytes, the pellet was resuspended by 1 ml neurobasal media with 10% (v/v) heat-inactivated horse serum, 1% (v/v) Antibiotic-Antimycotic, and 0.25% (v/v) 10x GlutaMax. Initial plating concentration upon isolation was 8×10^4 cells/ml per plate. After cells reached 80% confluence, they were detached by 0.25% trypsin and reseeded as

passage 2 at various densities: $2x10^4$ cells/ml onto tissue culture treated 48 well plates for primary astrocyte purity test, $3x10^4$ cells/ml per plate for extracellular Ado measurement and for biochemical assays. Only primary astrocytes of passage 2 and 3 were used in all the experiments.

3.3.4 Purity test for primary neurons and primary astrocytes by immunocytochemistry of MAP-2 and GFAP

Manually remove the culture media in the chamber of neuronal culture, and rinse the cells with D-PBS. Cold methanol stored in -20°C was added to fix the cells for 30 min. Then after rinse with D-PBS twice, the cells were permeabilized with 0.3% Triton®-X diluted in D-PBS for 30min at room temperature followed by three rinses with D-PBS. Next the cells were blocked by 5% goat serum in D-PBS for 30 min at room temperature on a rocker plate. To stain neurons, conjugated microtubule-associated protein-2 (MAP-2) was diluted in D-PBS at 1:1000 and neurons were incubated at 4°C overnight. To stain astrocytes, rabbit anti-rat glial fibrillary acidic protein (GFAP) was used at the dilution 1:1000 and astrocytes were incubated at 4°C overnight. Then astrocytes were rinsed twice with D-PBS followed by secondary antibody incubation with Alexa Fluor® 488 Goat Anti-Rabbit IgG (H+L) for 1 hr at room temperature on a rocker plate. DAPI dilactate 327 nM was used to visualize the nuclei. Stained sample were visualized under 20x on EVOS fl (Advanced Microscopy Group Bothell, WA). Cell numbers were counted from five separate non-overlapping fields using the × 20 objective.

3.3.5 Adenosine level measurement in primary astrocytes

Astrocytes were seeded on PDL coated 10 cm dishes at initial concentration of $3x10^4$ cells/ml. After 4-6 days when cells reached confluence, they were treated and conditioned media was collected for measurement as described previously (Wang et al., 2012). In brief, adenosine, inosine, and null sensors were linked to a Multi-Channel Potentiostat (Pinnacle Technology, Lawrence, KS). Fresh solutions of adenosine and inosine (1, 5, 10, 20 and 50 µM) were prepared for calibration. Toluene (1.0 ml) was added to 10 ml of conditioned media to extract 1,3-DNB. Extraction was performed twice for each DMSO or 1,3-DNB exposure. Adenosine and inosine levels were measured and calibrated against protein concentrations obtained by BCA protein assay.

3.3.6 ATP level of primary neurons

A luminescent assay was used to assess the viability of 1,3-DNB treated neurons by measuring the ATP level. $3x10^4$ primary neurons in 100 µl phenol free neurobasal media were seeded onto PDL coated white/clear 96 well plates and allowed to grow for 6-8 days to mature. When axons were fully developed, neurons were treated with various chemicals for 12 or 24 h. At the end of the exposure, 100 µl mixed CellTiter-Glo reagents was added to the wells and incubated in room temperature for 10 min after the plate was gently shaken by microplate shaker SARSTEDT (Nümbrecht, Germany). The intensity of luminescence was read by GloMax®-Multi Detection System (Promega). All experiments were repeated with at least three biologically different samples with

media backgrounds subtracted from readings, each sample with three replicate wells.

3.3.7 Membrane integrity of primary neurons

The membrane integrity was also examined as it correlates with cell viability. Primary neurons of the same density were plated onto the same plate as described in 3.3.6. After 6-8 days of culture, 100 µM 1,3-DNB was added with adenosine (1, 10 and 100 µM). In some experiments, potent ADA inhibitor pentostatin was mixed in the dosing solution to prevent exogenous adenosine being metabolized by ADA. Live cell fluorescence was measured by the cell-permeant substrate GF-AFC, which was cleaved by live-cell proteases to fluorescent molecule AFC in cytoplasm. Dead cells that had lost membrane integrity released proteases to extracellular environment, in which the cell-impermeable molecule bis-AAF-R110 was cleaved to fluorescent R110. The intensity of fluorescence was measured by GloMax®-Multi Detection System (Promega). The background of media and/or exogenous chemicals reacting with reagents was subtracted from the final reading. All experiments were repeated with four biologically different samples, each sample with three replicate wells.

3.3.8 Measurement of Fluo4-AM fluorescence in single well device

Intracellular Ca2+ concentration was visualized by Fluo-4 AM on DSU microscope. After receiving different treatments, neurons were loaded with 1 µM Fluo-4 AM in buffer that contained 2% (v/v) 1M HEPES buffer and 98% (v/v) 1xHBSS. After incubated in 37°C for 30 min, the dye was carefully removed by pipette. Then neurons were rinsed with buffer twice and then incubated in buffer

for another 30 min to allow intracellular dyes to be cleaved by esterases. The pictures of cytoplasmic calcium were taken on Olympus IX81. The parameters of settings have been listed as follows: Neutral Density value was 4, the oil objective was 40 x, the filter was GFP-WF, the interval of each picture was 1 sec, the total time was 600 sec. 50 mM KCl was added to the equal volume of buffer at 300 sec to reach a final KCl concentration of 25 mM.

3.3.9 Quantification of cytoplasmic Ca2+ concentration

Studies have found that the change in fluorescence intensity is directly related to the calcium increases from action potentials (Berridge et al., 1998, Kwan, 2008).

The average fluorescence intensity of soma was used to quantify Ca^{2+} concentration. A region of interest (ROI) with 20x20 pixel was selected within each soma, while a ROI with 50x50 pixel was chosen from the background of each image. Average fluorescence intensities of soma and background were calculated from the ROIs. Time lapse change of fluorescence was quantified as the following equation,

$$\text{Fluorescence}(t) = \frac{FL_{soma}(t) - FL_{BG}(t)}{FL_{soma}(t=0) - FL_{BG}(t=0)},$$

Where FL_{soma} and FL_{BG} are average fluorescence of soma and background at time t, respectively.

From each fluorescence plot, (1) peak fluorescence intensity and (2) time to reach peak fluorescence after adding KCl were determined. First, the Hodrick-Prescott (HP) filter was used to smooth the fluorescence plot. Second, the local

maxima values were identified from the plot. Third, among these values, the first local maximum with fluorescence intensity greater than 1.5 (equivalent to 50% increase) was defined as the peak point. Finally, at this peak point, the fluorescence intensity and time to reach the peak fluorescence after adding KCl were calculated. If there is no peak point that satisfies the above criteria (i.e., local maximum was not found or local maximum value was less than 1.5), for the purpose of statistical analysis, the peak time was manually set as the final observation time. Then the peak fluorescence intensity was calculated at the manually set peak time. All analyses were conducted using MATLAB R2010a.

3.3.10 Statistical analysis

For biochemical experiments in sessions 3.3.6, 3.3.7, and 1.3.9, average values of each biological sample were calculated. Then the average values of the same exposure were compared with other exposures using one-way ANOVA to determine significance. We consider $p < 0.05$ as a significant difference in this study.

3.4 RESULTS

3.4.1 Primary cortical neuron and astrocytes purity

Primary astrocytes were flat and polygonal (Figure 3.2 A) indicating proliferation (Ramakers and Moolenaar, 1998). Axon development was obvious indicating neuron maturity (Figure 3.2 D). Primary astrocyte and neuron purity was 90-95% and 85-90% after day 6 of culture. Purities of neurons and astrocyte are both are

comparable to previous studies (Morrison and de Vellis, 1983, Lin et al., 2011, Shao et al., 2011).

3.4.2 Extracellular adenosine increased in 1,3-DNB-exposed-astrocytes

Under normal conditions, extracellular adenosine was below the sensor's limit of detection (50 nM) (data not shown). In the vehicle control group (DMSO 0.1%, v/v), the extracellular adenosine level did not increase significantly at any time point. 100 μM 1,3-DNB exposure for 6 h significantly elevated extracellular adenosine to 4 μM (#, $p < 0.05$). 500 μM 1,3-DNB exposure for 6 h and 12 h caused extracellular adenosine increase to 4 and 6 μM, respectively (*, $p < 0.05$) (Figure 3.3).

3.4.3 ATP level in primary astrocytes

During a 12 h exposure course, only the highest 1,3-DNB concentration (1000 μM) produced significant ATP level decrease in primary astrocytes ($p < 0.05$) (Figure 3.4). Due to the constraints of the experimental process (cells were lysed by directly adding lysis buffer to the wells without media removal), ATP levels obtained were from both intracellular and extracellular sources.

3.4.4 ATP level in primary neuron

Cellular ATP levels were decreased by 1,3-DNB exposure in both dose- and time- dependent manners. At 12 h, 1,3-DNB concentrations of 100 μM or more caused greater than 36% ATP loss ($p<0.05$). At 24 h, 1,3-DNB concentrations of 20 μM or more caused greater than 34% ATP loss ($p<0.05$) (Figure 3.5 A). Since 100 μM 1,3-DNB was the minimum concentration to cause ATP loss in 12 h, this

concentration was used in further experiments. To select the window for neuroprotective effect study, we tested effects of 100 μM 1,3-DNB on cellular ATP level on different time points. At this concentration, 3 h exposure caused significant ATP reduction in primary neurons (*, $p < 0.05$). No difference in ATP loss was observed among 3 h, 6 h and 12 h exposure groups. However ATP levels of these three groups were all higher than the 24 h exposure (#, $p < 0.05$), indicating 12 h window is important for neuroprotection evaluation (Figure 3.5 B). 100 μM 1,3-DNB exposure for 12 h, with 100 μM CPA significantly increased ATP level in primary neurons (*, $p < 0.05$). With prolonged exposure time to 24 h, 10 μM and 100 μM CPA both showed significant effects in preserving ATP (#, $p < 0.05$) (Figure 3.5 C).

3.4.5 Membrane integrity of primary neurons

No adenosine concentration had any effect in improving membrane integrity in 1,3-DNB exposure. However, in the presence of pentostatin, a potent ADA inhibitor, 10 and 100 μM adenosine significantly increased membrane integrity, compared to the adenosine free group (*, $p<0.05$) (Figure 3.6 A). And this protective effect was blocked by A1R antagonist DPCPX, regardless the presence of pentostatin (Figure 3.6 B).

3.4.6 Potassium induced cytoplasmic Ca^{2+} increased was suppressed by A1R agonist

DMSO 0.1% or 1,3-DNB 10 μM exposure for 12 h did not significantly alter the excitability of primary neurons ($p = 0.37$) (Figure 3.7and Figure 3.8 C and D). Ado 5 μM and co-exposure of DNB and Ado 5 μM took significantly longer time to

reach the peak fluorescence than NT or DMSO or DNB ($p < 0.05$). The difference between Ado 5 µM and co-exposure of DNB and Ado 5 µM is statistically significant ($p < 0.05$) (Figure 3.7 and Figure 3.8 E and F). $A_{2a}R$ agonist CGS 21680 1 µM or A_1R agonist DPCPX 1 µM did not significantly change neuronal excitability ($p = 0.19$) (Figure 3.7 and Figure 3.8 G and H).

3.5 DISCUSSION

In this paper, we report three major findings, 1). Extracellular adenosine concentration was increased to approximately 5 µM in 1,3-DNB exposed primary cortical astrocytes (Figure 3.3); 2). Excitability of primary neurons were suppressed by exogenous adenosine, and this inhibition was mediated through A_1R (Figure 3.7 and Figure 3.8); 3). Exogenous adenosine and A_1R agonist, CPA, significantly increased the ATP levels and membrane integrity of 1,3-DNB exposed primary neurons (Figure 3.5 and Figure 3.6). This protection was also mediated through A_1R signaling pathway. Together, these results indicate a neuroprotective role of adenosine in 1,3-DNB toxicity.

We hypothesized that adenosine is responsible for differential cellular sensitivity, primarily the delayed neuronal death, which occurs secondarily after astrocyte swelling and necrosis (Philbert et al., 1987). To test this hypothesis, we first measured the extracellular adenosine level in primary astrocytes within the temporal window that neuronal damage has not taken place *in vivo*. Our results show that, extracellular adenosine level increased more than 11 folds in 6 h 500 µM 1,3-DNB exposure, and 6 and 9 folds in 12 h 100 µM and 500 µM 1,3-DNB in primary astrocytes (Figure 3.3). This result was obtained without causing

significant cell death, as suggested by ATP level (Figure 3.4) and the protein concentrations (data not shown) of these cells. In the absence of severe cell damage, the elevated adenosine level could be at least partially attributed to two mechanisms: the opening of mitochondrial permeability transition pore (mtPTP) and ADA inhibition. Firstly, it has been reported that 1,3-DNB induces mitochondrial depolarization by opening mtPTP in cortical astrocytes with an EC_{50} value of 289 µM (Tjalkens et al., 2003). 100 and 500 µM 1,3-DNB can at least partially induce the opening of mtPTP, leading to ATP leakage from mitochondrial matrix to cytoplasm. Cytoplasmic ATP enters extracellular environment by concentration-driven equilibrative nucleoside transporters (ENTs) (Chaudry, 1982, Parkinson et al., 2005). Both cytoplasmic and extracellular ATP is further metabolized to adenosine by a series of enzymes. Thus ATP leakage from mitochondria may have contributed to elevated adenosine level. Secondly, 1,3-DNB is a known inhibitor of ADA with an IC_{50} value of 284 µM (Wang et al., 2012), falling into the range of two higher 1,3-DNB concentrations (100 and 500 µM). Although it is inappropriate to assume that half of the enzyme activity was inhibited in 284 µM 1,3-DNB, inhibition of ADA is likely to occur in higher 1,3-DNB concentration exposed groups, leading to accumulation of adenosine.

ATP levels were also measured on primary neurons that were exposed to various concentrations of 1,3-DNB for 12 h (Figure 3.5 A). The comparison of ATP levels from primary astrocytes and neurons under the same exposure suggests that severity of ATP loss depends on cell type. In astrocytes, ATP levels did not significantly decrease until 1000 µM 1,3-DNB (Figure 3.4), whereas

in neurons, 100 µM 1,3-DNB caused ATP levels drop by 36% (Figure 3.5 A). The differential threshold to ATP loss reveals that neurons are more susceptible to 1,3-DNB toxicity in mono-culture. However, *in vivo* experiments have shown that neuronal damage occurs after astrocyte swelling and necrosis (Philbert et al., 1987, Romero et al., 1991). The discrepancy of *in vivo* and *in intro* mono-culture makes us curious about the potential explanations.

One possible explanation is that reduced energy consumption leads to milder lesions. Previous studies have shown that ataxia and lesions in the brain stem are more pronounced in rats dosed with bifenthrin (Holton et al., 1997), a drug that causes hyperexcitation in animals (Song and Narahashi, 1996). In another study, rats with one side ear drum rupture exhibited decreased glucose consumption as well as less severe lesions in the auditory pathway, a region that exhibits histopathological changes in 1,3-DNB toxicity (Ray et al., 1992). However, the actual mechanism of how energy consumption is reduced *in vivo* remains unknown. For the first time, we found that an important neuronal activity regulator, adenosine increased significantly from below 50 nM to approximately 5 µM in 12 h 1,3-DNB exposure (Figure 3.3). More importantly, our results have shown that at the same exposure time, adenosine 5 µM or A_1R agonist CPA significantly reduced cytoplasmic Ca^{2+} increase upon KCl stimulation in neurons (Figure 3.7and Figure 3.8 E and F). Together, these findings suggest that 1,3-DNB increases the level of extracellular adenosine, and adenosine binds in turn to the inhibitory A_1R to suppress the excitability of neurons, leading to reduced energy consumption.

Although significantly suppressed excitability was observed in 5 µM adenosine, 1 µM adenosine failed to produce such inhibitory effect (data not shown). This result points to the need to precisely quantify the extracellular adenosine level *in vivo*. Although the enzyme based sensors were a quick and convenient way to quantify extracellular adenosine level in conditioned media, data obtained from *in vitro* measurement cannot be used to infer the actual adenosine concentration *in vivo*. The reason lies on the fact that the ratio of cells to volume of conditioned media is different from the ratio of tissue to volume of cerebrospinal fluid (CSF). In addition, different cell types have different purine release profiles (Parkinson et al., 2005). Therefore, the investigation of extracellular adenosine levels in this study is only preliminary, more accurate and relevant adenosine concentrations should be measured by performing *in vivo* microdialysis.

Besides the necessity to obtain accurate adenosine level, to understand the relative quantification of adenosine to adenosine receptors is of equal importance, because the outcome of adenosine signaling pathway also depends on the expression level of adenosine receptors (Cunha, 2005). Due to the low abundance of $A_{2b}R$ and A_3R in brain, our discussion will only focus on the contributions of A_1R and $A_{2a}R$ signaling pathways. In basal physiological condition, both A_1R and $A_{2a}R$ are activated by adenosine (Fredholm, 2007a). Therefore, if we hypothesize that adenosine is responsible for the regional and / or cellular differential sensitivity in 1,3-DNB toxicity, the distribution of these two types of receptors becomes important.

Research has shown that in humans, A_1R has relatively low level of distribution in midbrain and brain stem (Fastbom et al., 1987b), lower than in sensorimotor cortex or temporal lobes (Bauer et al., 2003). Similar results have been observed in rats and other animal species. On the other hand, cerebral cortex in rat, mouse and guinea-pig had intermediate to high expression, shown by radioactive probe (Fastbom et al., 1987a). If 1,3-DNB exposure does not change the expression or the activity of the receptors, lower expression of inhibitory A_1R could explain the more susceptibility in brain stem. However, before making this assumption, further experiments must be conducted to explore if 1,3-DNB plays a role in changing the expression level or the activity of ARs.

Interestingly, our study found significant difference in excitability between cell co-exposed with 1,3-DNB and adenosine and with adenosine alone, even though 1,3-DNB alone did not significantly alter neuronal excitability (Figure 3.8 E and F). This difference suggests that 1,3-DNB plays a role in altering excitability. Structure alignment of adenosine and 1,3-DNB demonstrates that the adenine ring partially overlaps with the benzene ring of 1,3-DNB (Wang et al., 2012). Therefore, 1,3-DNB may be a weak agonist of $A_{2a}R$ or a weak antagonist of A_1R, but further investigation is still needed.

Another finding from the cytoplasmic Ca^{2+} increase measurement was that no significant effects were observed in CGS 21680 exposed neurons (Figure 3.8 G and H). This observation may be due to the poor selectivity of CGS 21680 to both A_1R and $A_{2a}R$ when the expression of A_1R is dominant (Halldner et al., 2004, Lopes et al., 2004). In our study, neurons from cortex were used, a region in

which A_1R is more abundant than $A_{2a}R$ (Fastbom et al., 1987a, Johansson et al., 1997). And since no procedure was performed to saturate A_1R before adding CGS 21680, therefore the final outcome is a mixed result from both A_1R and $A_{2a}R$ activation.

It has been widely accepted that the relationship between astrocytes and neurons is critical in maintaining homeostatic, regulating energy metabolism and modulating plasticity (Escartin et al., 2006, Vijayaraghavan, 2009, Allaman et al., 2011). Adenosine has been shown to play an important role in modulating neurotransmitter release and energy metabolism (Fredholm, 2007a, Jones, 2009). This work presents evidence that extracellular adenosine levels increases in 1,3-DNB toxicity, and that adenosine protects neurons by reducing excitability. These findings advance our knowledge of astrocyte-neuron interaction in neurological diseases, yet further investigation of adenosine level *in vivo* is still needed.

3.6 ACKNOWLEDGEMENTS

This work has been made possible by National Institutes of Health (1RO1 ES08846 to M.A.P.). We appreciate the input of our collaborator Dong Hoon Song. We also would like to thank members of the Philbert laboratory for their helpful discussions and technical support (Caitlin Parsons, Rebecca Gentner, Jennifer Fernandez, Laura Maurer, and Kristen Russ). We would like to acknowledge technical assistance from the laboratory staff in Professor Loch-Caruso's laboratory.

3.7 EUQATION

Equation 3-1. Calculate the fluorescence in neurons.

$$\text{Fluorescence}(t) = \frac{FL_{soma}(t) - FL_{BG}(t)}{FL_{soma}(t=0) - FL_{BG}(t=0)},$$

FL_{soma} and FL_{BG} are average fluorescence of soma and background at time t, respectively.

3.8 FIGURES

Time (h)	0	2	4	6	8	12	24
in vitro and *in vivo* Events	ADA / PDHc / SDH (in vitro) inhibition; F1-ATP synthase β-subunit carboxylation	GSH depletion; $\Delta\Psi_m$ decrease; Significant ROS increase	Peak ROS at 5 h	Significant $[Ado]_e$ increase		ATP decrease	Increased cumulative glucose consumption; SDH (in vivo) inhibition; ATP depletion
Reference	a-d	e, d, f	d	a		b	b, c, e
Clinical Manifests	Final dose	Increased met-Hg	Peak blood flow			Petechial hemorrhages; Astrocyte swelling	Hemorrhage; Mild - moderate ataxia
Reference		g	h			h	g, h, i

Figure 3.1. Time course of 1,3-DNB neurotoxicity

a. (Wang et al., 2012)
b. (Miller et al., 2011a)
c. (Phelka et al., 2003)
d. (Steiner and Philbert, 2011)
e. (Romero et al., 1995)
f. (Tjalkens et al., 2000a)
g. (Kumar et al., 1990)
h. (Romero et al., 1991)
i. (Cody et al., 1981a)

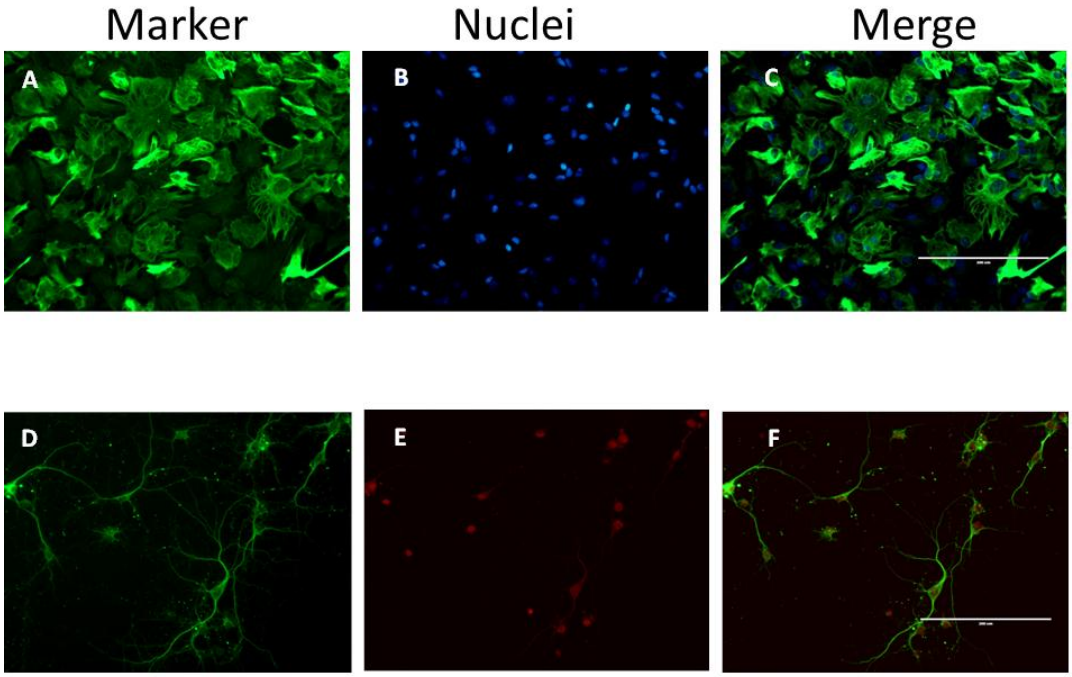

Figure 3.2. Purity of primary astrocytes (A, B, C) and primary neurons (D, E, F) isolated from cortex pair from embryonic day 18 rat.

(A) GFAP staining, (B) nuclei staining with DAPI, (C). overlay picture of (A) and (B). (D). MAP-2 staining, (E) nuclei staining with PI, (F) overlay picture of (D) and (E). Scale bars in (C) and (F) indicate 200 µm. Purity was calculated as the number of GFAP or MAP-2 positive cells divided by the number of nuclei positive cells in five random fields. Astrocyte purity (passage 2 and 3) is 90-95%. Neuron purity is 86-90%.

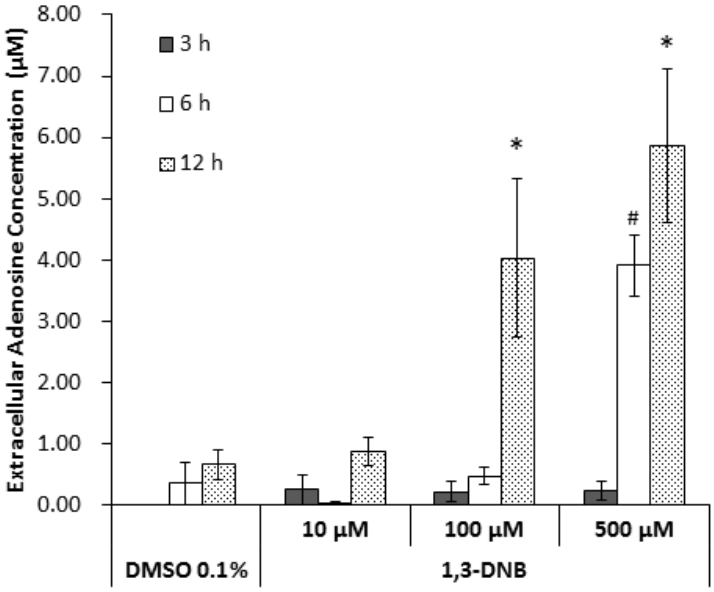

Figure 3.3. Extracellular adenosine level in DMSO and 1,3-DNB treated primary astrocytes.

1,3-DNB was extracted with toluene from the conditioned media before measurement. Adenosine level that was below the detective limit has been replaced with zero. At least four independent experiment results were collected and represented as mean ± SEM. Bar represent mean ± SEM.

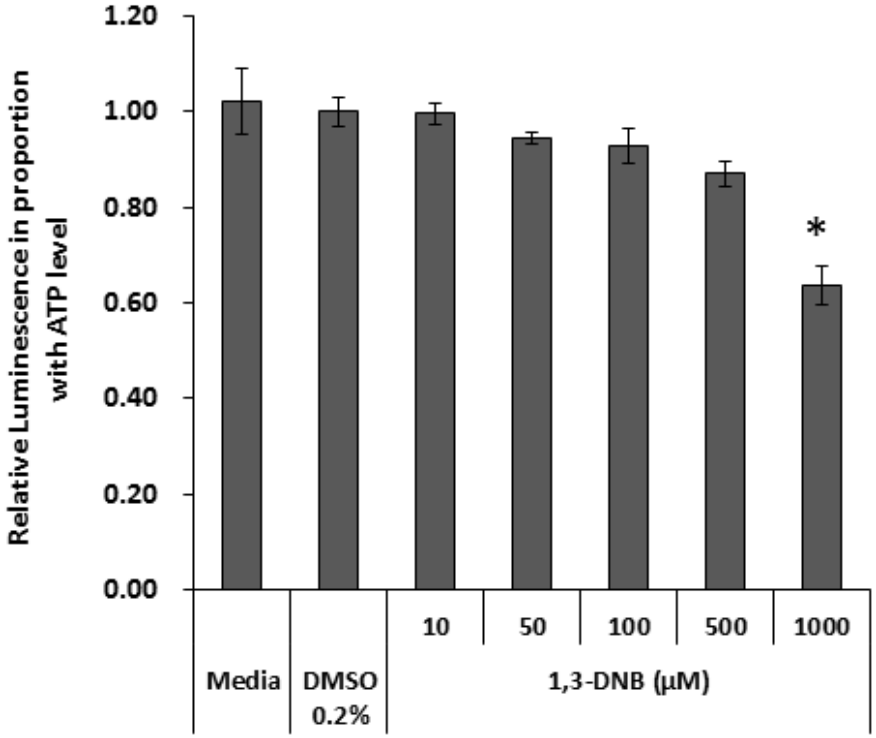

Figure 3.4. Relative ATP levels measured by luminescence in primary astrocytes exposed to 1,3-DNB for 12 h.

The absolute luminescence of each exposure was normalized against the luminescence of DMSO exposure. Results were collected from 3 biologically different samples with 3 replicate wells for each sample. All data was normalized against the luminescence values of vehicle group (DMSO 0.2%). Data represent mean ± SEM.

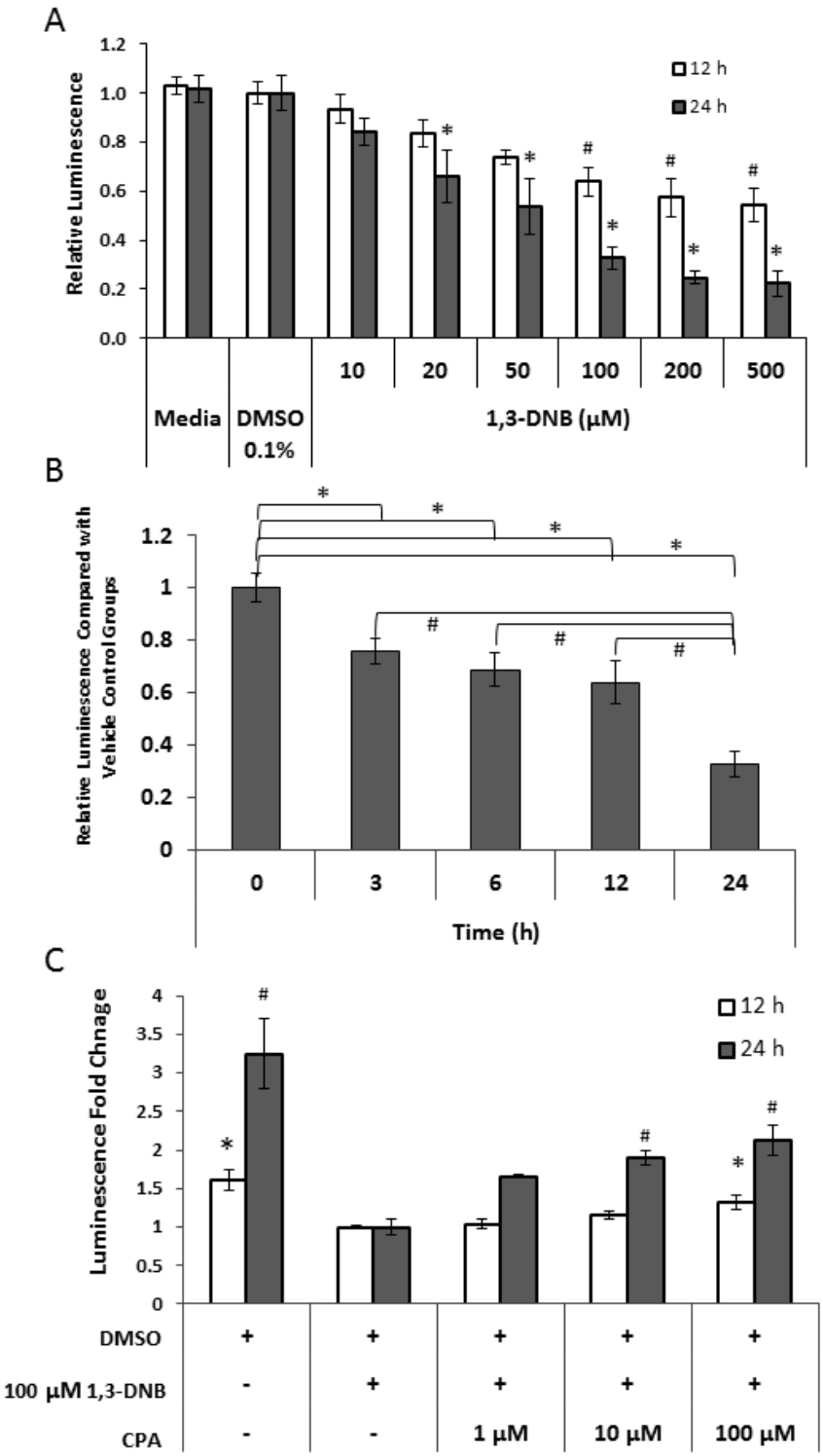

Figure 3.5. ATP levels of primary neurons.

(A) Neurons exposed to various 1,3-DNB concentrations for 12 h and 24 h. All data was normalized against vehicle control group (DMSO 0.1%, v/v). (B) Neurons exposed to 100 µM 1,3-DNB for various time. Values represent the percentage of luminescence compared to vehicle control groups (DMSO 0.1 %, v/v) at each time point. (C) Of each exposure course, values of luminescence were normalized against the values in 1,3-DNB along exposure to better visualize the effects of CPA. Results were collected from 3 biologically different samples with 3 replicate wells for each sample. Data represent mean ± SEM.

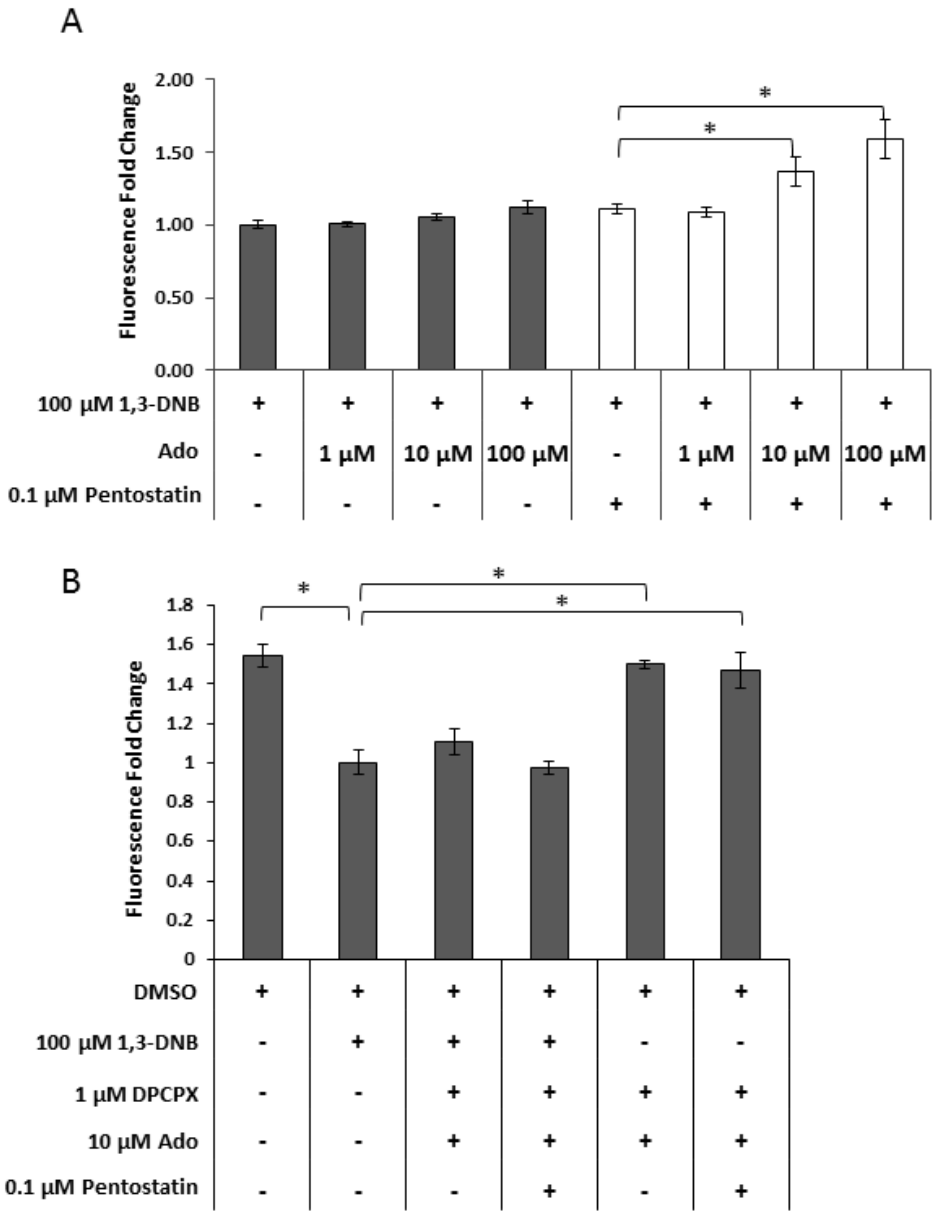

Figure 3.6. Ado and increased primary neuron membrane integrity measured by fluorescence in 1,3-DNB 12 h exposure.

All data was normalized against the fluorescent intensity of 100 µM 1,3-DNB exposed group. Results were collected from 3 biologically different samples with 3 replicate wells for each sample. Data represent mean ± SEM.

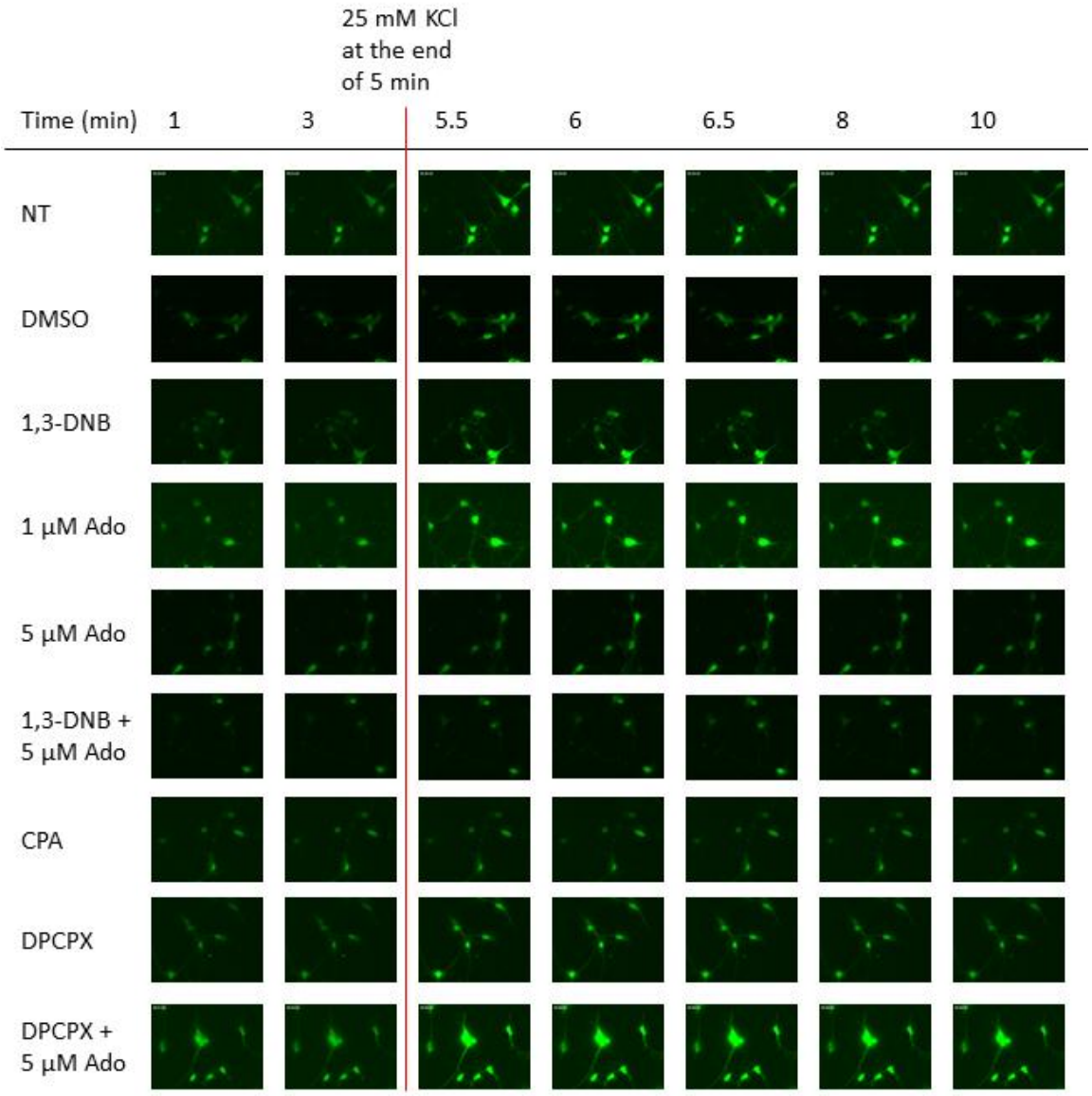

Figure 3.7. Potassium induced cytoplasmic Ca^{2+} increase in intact primary neurons exposed to different chemicals for 12 h.

[Ca^{2+}] was measured by 1 µM Fluo-4 AM. DMSO was 0.1%, 1,3-DNB was 10 µM, CPA was 1 µM, DPCPX was 1 µM. Figure shows representative results of at least 10 cells from 3 biologically different samples were analyzed.

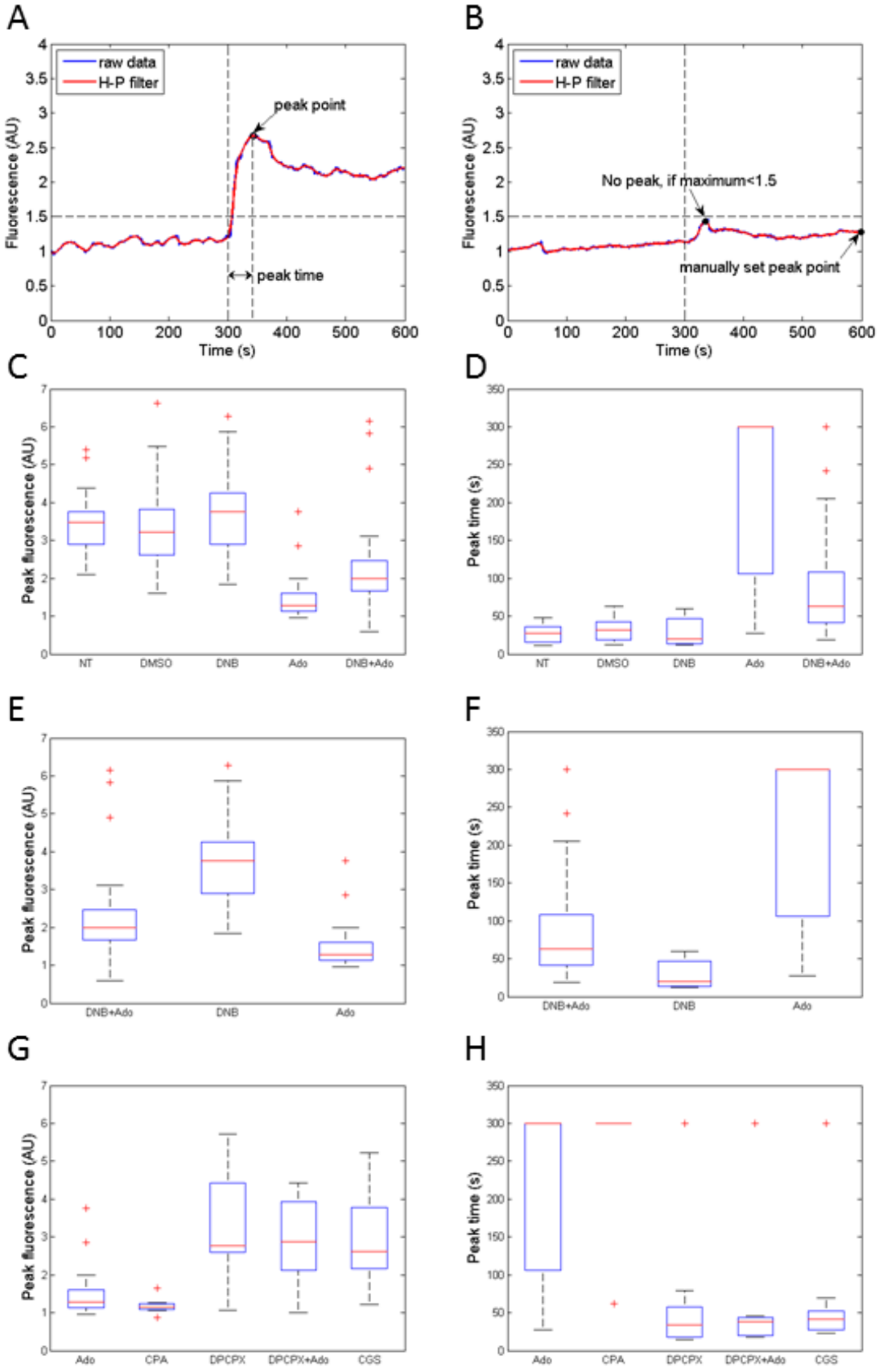
A
raw data
H-P filter
peak point
peak time
Fluorescence (AU)
Time (s)
B
raw data
H-P filter
No peak, if maximum<1.5
manually set peak point
Fluorescence (AU)
Time (s)
C
Peak fluorescence (AU)
NT
DMSO
DNB
Ado
DNB+Ado
D
Peak time (s)
NT
DMSO
DNB
Ado
DNB+Ado
E
Peak fluorescence (AU)
DNB+Ado
DNB
Ado
F
Peak time (s)
DNB+Ado
DNB
Ado
G
Peak fluorescence (AU)
Ado
CPA
DPCPX
DPCPX+Ado
CGS
H
Peak time (s)
Ado
CPA
DPCPX
DPCPX+Ado
CGS

Figure 3.8. Quantification of peak fluorescence and the time to reach peak fluorescence.

(A) Peak fluorescence, time and slope were calculated at each set of a time series data. To obtain a smoothed curve, Hodrick-Prescott (HP) filter was used. (B) If the local maximum of the fluorescence intensity is less than 1.5 (which is equivalent to 50% increase), it is assumed that there is no peak. If there was no peak, peak time was set as 300 sec and peak fluorescence was calculated as the fluorescence intensity at t=600 sec. (C-H) Number of cells used for analysis of each exposure group is as follows: No treatment (NT)=27, DMSO=24, 1,3-DNB=27, Ado=31, DNB+Ado=24, CPA=12, DPCPX=10, DPCPX+Ado=10. Outliers are marked as "+".Significance was determined by one-way ANOVA ($p < 0.05$).

3.9 REFERENCES

(1989) Toxicology update. Dinitrobenzene. Journal of applied toxicology : JAT 9:199-202.

Allaman I, Belanger M, Magistretti PJ (2011) Astrocyte-neuron metabolic relationships: for better and for worse. Trends Neurosci 34:76-87.

Ames A, 3rd, Li YY (1992) Energy requirements of glutamatergic pathways in rabbit retina. The Journal of neuroscience : the official journal of the Society for Neuroscience 12:4234-4242.

Attwell D, Laughlin SB (2001) An energy budget for signaling in the grey matter of the brain. Journal of cerebral blood flow and metabolism : official journal of the International Society of Cerebral Blood Flow and Metabolism 21:1133-1145.

Bauer A, Holschbach MH, Meyer PT, Boy C, Herzog H, Olsson RA, Coenen HH, Zilles K (2003) In vivo imaging of adenosine A1 receptors in the human brain with [18F]CPFPX and positron emission tomography. Neuroimage 19:1760-1769.

Berridge MJ, Bootman MD, Lipp P (1998) Calcium--a life and death signal. Nature 395:645-648.

Blackburn DM, Gray AJ, Lloyd SC, Sheard CM, Foster PM (1988) A comparison of the effects of the three isomers of dinitrobenzene on the testis in the rat. Toxicology and applied pharmacology 92:54-64.

Cavanagh JB (1988) Lesion localisation: implications for the study of functional effects and mechanisms of action. Toxicology 49:131-136.

Cavanagh JB (1993) Selective vulnerability in acute energy deprivation syndromes. Neuropathology and applied neurobiology 19:461-470.

Cavanagh JB, Nolan CC (1993) The neurotoxicity of alpha-chlorohydrin in rats and mice: II. Lesion topography and factors in selective vulnerability in acute energy deprivation syndromes. Neuropathology and applied neurobiology 19:471-479.

Chaudry IH (1982) Does ATP cross the cell plasma membrane. Yale J Biol Med 55:1-10.

Cody TE, Witherup S, Hastings L, Stemmer K, Christian RT (1981) 1,3-dinitrobenzene: toxic effects in vivo and in vitro. Journal of toxicology and environmental health 7:829-847.

Cunha RA (2005) Neuroprotection by adenosine in the brain: From A(1) receptor activation to A (2A) receptor blockade. Purinergic Signal 1:111-134.

Di Iorio P, Kleywegt S, Ciccarelli R, Traversa U, Andrew CM, Crocker CE, Werstiuk ES, Rathbone MP (2002) Mechanisms of apoptosis induced by purine nucleosides in astrocytes. Glia 38:179-190.

Escartin C, Valette J, Lebon V, Bonvento G (2006) Neuron-astrocyte interactions in the regulation of brain energy metabolism: a focus on NMR spectroscopy. J Neurochem 99:393-401.

Fastbom J, Pazos A, Palacios JM (1987a) The distribution of adenosine A1 receptors and 5'-nucleotidase in the brain of some commonly used experimental animals. Neuroscience 22:813-826.

Fastbom J, Pazos A, Probst A, Palacios JM (1987b) Adenosine A1 receptors in the human brain: a quantitative autoradiographic study. Neuroscience 22:827-839.

Fredholm BB (2007) Adenosine, an endogenous distress signal, modulates tissue damage and repair. Cell death and differentiation 14:1315-1323.

Ghezzi A, Atkinson NS (2011) Homeostatic control of neural activity: a Drosophila model for drug tolerance and dependence. International review of neurobiology 99:23-50.

Gomes CV, Kaster MP, Tome AR, Agostinho PM, Cunha RA (2011) Adenosine receptors and brain diseases: neuroprotection and neurodegeneration. Biochimica et biophysica acta 1808:1380-1399.

Halldner L, Lopes LV, Dare E, Lindstrom K, Johansson B, Ledent C, Cunha RA, Fredholm BB (2004) Binding of adenosine receptor ligands to brain of adenosine receptor knock-out mice: evidence that CGS 21680 binds to A1 receptors in hippocampus. Naunyn Schmiedebergs Arch Pharmacol 370:270-278.

Haun SE, Segeleon JE, Trapp VL, Clotz MA, Horrocks LA (1996) Inosine mediates the protective effect of adenosine in rat astrocyte cultures subjected to combined glucose-oxygen deprivation. J Neurochem 67:2051-2059.

Holton JL, Nolan CC, Burr SA, Ray DE, Cavanagh JB (1997) Increasing or decreasing nervous activity modulates the severity of the glio-vascular lesions of 1,3-dinitrobenzene in the rat: effects of the tremorgenic pyrethroid, Bifenthrin, and of anaesthesia. Acta Neuropathol 93:159-165.

Howarth C, Peppiatt-Wildman CM, Attwell D (2010) The energy use associated with neural computation in the cerebellum. Journal of cerebral blood flow and metabolism : official journal of the International Society of Cerebral Blood Flow and Metabolism 30:403-414.

Johansson B, Georgiev V, Fredholm BB (1997) Distribution and postnatal ontogeny of adenosine A2A receptors in rat brain: comparison with dopamine receptors. Neuroscience 80:1187-1207.

Johansson B, Halldner L, Dunwiddie TV, Masino SA, Poelchen W, Gimenez-Llort L, Escorihuela RM, Fernandez-Teruel A, Wiesenfeld-Hallin Z, Xu XJ, Hardemark A, Betsholtz C, Herlenius E, Fredholm BB (2001) Hyperalgesia, anxiety, and decreased hypoxic neuroprotection in mice lacking the adenosine A1 receptor. Proceedings of the National Academy of Sciences of the United States of America 98:9407-9412.

Jones BE (2009) Glia, adenosine, and sleep. Neuron 61:156-157.

Kwan AC (2008) What can population calcium imaging tell us about neural circuits? J Neurophysiol 100:2977-2980.

Lin MS, Hung KS, Chiu WT, Sun YY, Tsai SH, Lin JW, Lee YH (2011) Curcumin enhances neuronal survival in N-methyl-d-aspartic acid toxicity by inducing RANTES expression in astrocytes via PI-3K and MAPK signaling pathways. Prog Neuropsychopharmacol Biol Psychiatry 35:931-938.

Logan M, Sweeney MI (1997) Adenosine A1 receptor activation preferentially protects cultured cerebellar neurons versus astrocytes against hypoxia-induced death. Mol Chem Neuropathol 31:119-133.

Lopes LV, Halldner L, Rebola N, Johansson B, Ledent C, Chen JF, Fredholm BB, Cunha RA (2004) Binding of the prototypical adenosine A(2A) receptor agonist CGS 21680 to the cerebral cortex of adenosine A(1) and A(2A) receptor knockout mice. Br J Pharmacol 141:1006-1014.

Lopes LV, Sebastiao AM, Ribeiro JA (2011) Adenosine and related drugs in brain diseases: present and future in clinical trials. Current topics in medicinal chemistry 11:1087-1101.

Lutz PL, Nilsson GE, Prentice HM (2003) The brain without oxygen : causes of failure--physiological and molecular mechanisms for survival. Dordrecht ; Boston: Kluwer Academic Pub.

Miller JA, Runkle SA, Tjalkens RB, Philbert MA (2011) 1,3-Dinitrobenzene-induced metabolic impairment through selective inactivation of the pyruvate dehydrogenase complex. Toxicological sciences : an official journal of the Society of Toxicology 122:502-511.

Morrison RS, de Vellis J (1983) Differentiation of purified astrocytes in a chemically defined medium. Brain Res 285:337-345.

O'Leary T, Wyllie DJ (2011) Neuronal homeostasis: time for a change? The Journal of physiology 589:4811-4826.

Parkinson FE, Xiong W, Zamzow CR (2005) Astrocytes and neurons: different roles in regulating adenosine levels. Neurol Res 27:153-160.

Pellerin L, Magistretti PJ (2004) Neuroenergetics: calling upon astrocytes to satisfy hungry neurons. The Neuroscientist : a review journal bringing neurobiology, neurology and psychiatry 10:53-62.

Phelka AD, Sadoff MM, Martin BP, Philbert MA (2006) BCL-XL expression levels influence differential regional astrocytic susceptibility to 1,3-dinitrobenzene. Neurotoxicology 27:192-200.

Philbert MA, Nolan CC, Cremer JE, Tucker D, Brown AW (1987) 1,3-Dinitrobenzene-induced encephalopathy in rats. Neuropathology and applied neurobiology 13:371-389.

Ramakers GJ, Moolenaar WH (1998) Regulation of astrocyte morphology by RhoA and lysophosphatidic acid. Exp Cell Res 245:252-262.

Ray DE, Brown AW, Cavanagh JB, Nolan CC, Richards HK, Wylie SP (1992) Functional/metabolic modulation of the brain stem lesions caused by 1,3-dinitrobenzene in the rat. Neurotoxicology 13:379-388.

Romero I, Brown AW, Cavanagh JB, Nolan CC, Ray DE, Seville MP (1991) Vascular factors in the neurotoxic damage caused by 1,3-dinitrobenzene in the rat. Neuropathology and applied neurobiology 17:495-508.

Shao JL, Wan XH, Chen Y, Bi C, Chen HM, Zhong Y, Heng XH, Qian JQ (2011) H2S protects hippocampal neurons from anoxia-reoxygenation through cAMP-mediated PI3K/Akt/p70S6K cell-survival signaling pathways. J Mol Neurosci 43:453-460.

Song JH, Narahashi T (1996) Modulation of sodium channels of rat cerebellar Purkinje neurons by the pyrethroid tetramethrin. J Pharmacol Exp Ther 277:445-453.

Sperlagh B, Vizi ES (2011) The role of extracellular adenosine in chemical neurotransmission in the hippocampus and Basal Ganglia: pharmacological and clinical aspects. Current topics in medicinal chemistry 11:1034-1046.

Steiner SR, Philbert MA (2011) Proteomic identification of carbonylated proteins in 1,3-dinitrobenzene neurotoxicity. Neurotoxicology 32:362-373.

Tjalkens RB, Ewing MM, Philbert MA (2000) Differential cellular regulation of the mitochondrial permeability transition in an in vitro model of 1,3-dinitrobenzene-induced encephalopathy. Brain research 874:165-177.

Tjalkens RB, Phelka AD, Philbert MA (2003) Regional variation in the activation threshold for 1,3-DNB-induced mitochondrial permeability transition in brainstem and cortical astrocytes. Neurotoxicology 24:391-401.

Vasquez GB, Reddy G, Gilliland GL, Stevens WJ (1995) Dinitrobenzene induces methemoglobin formation from deoxyhemoglobin in vitro. Chemico-biological interactions 96:157-171.

Vijayaraghavan S (2009) Glial-neuronal interactions--implications for plasticity and drug addiction. AAPS J 11:123-132.

Wang YP, Liu X, Schneider B, Zverina EA, Russ K, Wijeyesakere SJ, Fierke CA, Richardson RJ, Philbert MA (2012) Mixed Inhibition of Adenosine Deaminase Activity by 1,3-Dinitrobenzene: A Model for Understanding Cell-Selective Neurotoxicity in Chemically-Induced Energy Deprivation Syndromes in Brain. Toxicological Sciences 125:509-521.

CHAPTER 4

CONCLUSION

4.1 OBJECTIVES

This dissertation aims to advance the understanding of mechanism of differential cellular sensitivities of astrocytes and neurons using 1,3-DNB as a model chemical to induce AEDS. In AEDS, lesions only occur in specific regions such as inferior colliculi, cerebellar roof, vestibular and superior olivary nuclei. And of the affected regions, astrocytes are the primary target and neuronal death occurs in later stage (Philbert et al., 1987, Romero et al., 1991). The molecular mechanisms of differential regional sensitivity and differential cellular sensitivity have remained elusive. Many studies have addressed the first observation in 1,3-DNB induced energy deprivation syndromes (Tjalkens et al., 2000a, Phelka et al., 2003, Tjalkens et al., 2003, Phelka et al., 2006). However, very few attempts, if any, have been made to understand differential cellular sensitivity.

In this research, we hypothesize that astrocytes, the glial cells that play a critical role in neurovascular and neurometabolic coupling (Allaman et al., 2011), have neuroprotective effects in 1,3-DNB toxicity. The neuroprotection effects are hypothesized to result from reduced energy consumption mediated by adenosine binding to inhibitory A_1R on neurons in 1,3-DNB toxicity. To test this hypothesis, extracellular adenosine levels were quantified in astrocyte conditioned media

using enzyme based sensors. Then using the obtained adenosine concentrations, we investigated the excitability of neurons by measuring cytoplasmic Ca^{2+} increase upon KCl stimulation. The viability of neurons under different exposures was assessed by measuring ATP levels and membrane integrity.

4.2 MAJOR RESULTS AND DISCUSSION

Figure 4.1 summarizes three major findings of two data chapters in this research.

In the first data chapter (chapter 2), we found that 1,3-DNB inhibits the activity of ADA in both cell-culture study and cell-free environment. The mechanism of inhibition was then further explored by enzyme kinetics and computational modeling. This finding is important for three reasons. Firstly, it adds a new target to the list of 1,3-DNB toxicity (Figure 4.2). Secondly, it shows adenosine concentration elevated as a result of ADA inhibition. Since adenosine has been reported to have neuroprotective effects, it provides the rationale to investigate the role of adenosine in 1,3-DNB toxicity in next stage of research. Finally, this study shows the importance and advantage of employing computational modeling as a tool in biological studies.

In the second data chapter (chapter 3), we found that extracellular adenosine levels increase in 1,3-DNB exposed primary astrocytes. Increased adenosine binds, in turn, to inhibitory A_1R, and suppresses neuronal excitability, leading to reduced energy consumption and increased viability of primary neurons in 1,3-DNB toxicity. This research advances our knowledge in mechanism of neuroprotection in chemical induced energy deprivation syndromes and lays the

foundation of therapy development for some neurological disorders with early stage of glio-vascular lesion and late stage of neuronal loss.

4.2.1 1,3-DNB is a mixed inhibitor of ADA

Our investigation includes three levels of complexity, cell-free environment, cell culture level and *in silico*. We first confirmed the hypothesis that 1,3-DNB inhibits the activity of ADA, then we further investigated the mechanism of inhibition by conducting kinetics and computational modeling studies.

Purified enzyme and 1,3-DNB were used to assess the activity of ADA under various 1,3-DNB concentrations. The activity of ADA decreased sharply with increased 1,3-DNB concentration, hence, a sigmoid curve model for cooperative inhibition was employed to obtain IC_{50}. From this equation, we obtained an IC_{50} value of 284 μM, with a Hill slope (n) of 4.80 ± 0.44. High Hill slopes indicate mechanisms other than classic inhibition, such as aggregator-based inhibition and denaturant. Therefore, in following experiments, we examined whether 1,3-DNB is an aggregator or a denaturant of ADA. Our results demonstrate that 1,3-DNB does not exhibit the common properties of an aggregation-based inhibitor or a denaturant. After ruling out the possibility of being aggregator or denaturant, we tested if the inhibition was time dependent by pre-incubating 1,3-DNB with ADA . We found that 1,3-DNB caused a consistent 20% decrease in ADA activity over the 60 min pre-incubation course. This result suggests that the inhibition is not time dependent, and can only be one of the four mechanisms of inhibition: competitive, uncompetitive, noncompetitive and mixed. Kinetics study of ADA activity over varying 1,3-DNB and adenosine concentrations showed decreased

k_{cat}, $k_{cat}/K_{M,}$ and K_M values, indicating either mixed or noncompetitive inhibition. Since mixed inhibition has a slightly higher R^2 value and lower error in global fitting, mixed inhibition mechanism was chosen as our conclusion from biochemical study.

Consistent with our results yielded from enzyme kinetics, computational modeling showed 1,3-DNB has multiple binding sites on ADA, including one on the active site and 3-4 peripheral sites (exact number depends on species). According to computational docking results, 1,3-DNB binding to each of these sites is energetically favorable with estimated free energies of binding ΔG_b ranging from -6.31 to -6.99 kcal/mol and corresponding estimated binding constants (K_i) ranging from 7.5 μM to 25.6 μM. The site defined by Try240 presents a putative allosteric binding site and a target for future investigations into the interaction between ADA and its inhibitors. Besides supportive evidence from computational modeling, extracellular adenosine measurement also showed dose dependent adenosine increase in 1,3-DNB exposed DI TNC cells.

The results (k_{cat}, $k_{cat}/K_{M,}$ and K_M values and extracellular adenosine levels) in other comparable conditions yielded from this study are comparable to other reported values (Kurz et al., 1992, Takahashi et al., 2010a, Xu and Venton, 2010a).

This study advances our current knowledge of 1,3-DNB toxicity. Previous studies have shown that 1,3-DNB has multiple adverse effects on cells, such as increased oxidative stress, decreased anti-oxidative defense, mitochondrial

disorder and enzyme inhibition (Romero et al., 1995, Tjalkens et al., 2000a, Phelka et al., 2003, Tjalkens et al., 2003, Miller et al., 2011a, Steiner and Philbert, 2011). This study identified another direct target in 1,3-DNB toxicity (Figure 4.1). The consequence of this direct inhibition is not limited to the affected cells, but can also regulate the activity of other cells, since adenosine is an universal neuromodulator.

One interesting finding is that our docking studies are in accord with our kinetics results, together predicting additional allosteric sites of interaction between 1,3-DNB and ADA, thereby presenting avenues for future research by employing computational modeling tools to compare the structural similarity between toxicants and known small molecules, especially substrates of enzymes and ligands of receptors. Once structural similarity has been identified, docking and cell culture studies can focus more on interactions between the small molecule and its natural enzyme / receptor. This way, researchers can avoid aimless search and only focus on potential targets narrowed down by computational modeling.

4.2.2 Extracellular adenosine levels increase in 1,3-DNB exposed primary astrocytes

After we found out that 1,3-DNB is a mixed inhibitor of ADA, we then examined if the extracellular adenosine levels increased in 1,3-DNB exposure. Adenosine is an important signal that is generated intracellularly or on the surface (Fredholm, 2007a). As a neuromodulator, adenosine has several CNS effects such as decreasing inflammation and neuroprotection in stroke and seizure (Latini and

Pedata, 2001, Parkinson et al., 2005). 10, 100 and 500 µM 1,3-DNB was added to primary astrocytes for 3, 6 or 12 h. At the end of exposure, extracellular adenosine was measured by enzyme based sensor. Results show that, 100 µM 1,3-DNB increased extracellular adenosine concentration by 6 fold to 4 µM; 500 µM 1,3-DNB increased extracellular adenosine concentrations by 11 and 9 fold to 4 and 6 µM occurring at 6 and 12 h compared to control groups ($p<0.05$) in conditioned media.

This result was measured from astrocytes that did not have significant ATP loss, as indicated by the luminescence intensity of the astrocytes that received different exposures. Thus, elevated adenosine levels in 1,3-DNB exposure (100 and 500 µM) can be attributed to two event, 1) ATP leakage from mitochondria to cytoplasm and then to extracellular environment through mtPTP (Tjalkens et al., 2003) and ENT(Chaudry, 1982, Parkinson et al., 2005), respectively; 2) inhibition of ADA by 1,3-DNB (Wang et al., 2012).

The limitation of this study is that, the concentration of adenosine obtained in cell culture should not be assumed to be the same as *in vivo* adenosine concentration in 1,3-DNB toxicity. There are two reasons for it. Firstly, the ratios of tissue volumes to extracellular liquid volume are different in *in vivo* scenario and in mono culture of primary culture. Secondly, different cell types release different kinds and concentration of purines. Due to these reasons, microdialysis should be performed for more accurate measure.

4.2.3 Adenosine suppresses neuroexcitability and increases neuronal survival in 1,3-DNB toxicity

After we obtained the adenosine concentration from astrocytes conditioned media, we used that concentration to test whether the viability was improved and whether the excitability was suppressed in 1,3-DNB exposed neurons. ATP levels and membrane integrity were chosen as two parameters to measure viability. Excitability was assessed by quantification of cytoplasmic Ca^{2+} increase upon KCl stimulation (Linden, 1991, Kwan, 2008).

Cellular ATP levels were decreased by 1,3-DNB exposure in both dose- and time- dependent manners. 100 µM 1,3-DNB was the minimum concentration to cause ATP loss in 12 h, hence this concentration was used in further experiments. Since no difference in ATP loss was observed among 3 h, 6 h and 12 h exposure groups, but a significant ATP loss in 24 h exposure ($p < 0.05$), we decided that 12 h window is important for neuroprotection evaluation.

At 12 h, co-exposure of 100 µM 1,3-DNB and 100 µM CPA had significantly higher ATP level than 1,3-DNB alone in primary neurons ($p < 0.05$). When exposure prolonged to 24 h, 10 µM and 100 µM CPA both showed significant effects in preserving ATP ($p < 0.05$). This result showed that A_1R agonist CPA helps ATP preserve in 1,3-DNB toxicity.

Membrane integrity was significantly decreased after 12 h 1,3-DNB exposure. And adenosine (1, 10 and 100 µM) did not have any effect in improving membrane integrity. However, when the activity of ADA was inhibited by

pentostatin, 10 and 100 µM adenosine significantly increased membrane integrity, compared to the adenosine free group ($p<0.05$). Since this protective effect was blocked by A_1R antagonist DPCPX, we believe that this effect is also mediated through A_1R.

Next, the excitability of neurons was examined under different exposures. DMSO 0.1%, 1,3-DNB 10 µM, $A_{2a}R$ agonist CGS 21680 1 µM or A_1R agonist DPCPX 1 µM exposure for 12 h did not significantly alter the excitability of primary neurons. Neurons exposed to 5 µM Ado or DNB and 5 µM Ado all had significantly lower excitability compared to DMSO exposed groups ($p < 0.05$). More interesting, neurons exposed to Ado 5 µM alone had statistically lower excitability than those expose to DNB and Ado 5 µM ($p < 0.05$). This difference suggests that 1,3-DNB plays a role in increasing excitability. Previous study has demonstrated that adenine ring of adenosine partially overlaps with the benzene ring of 1,3-DNB (Wang et al., 2012). Therefore, 1,3-DNB may be a weak agonist of $A_{2a}R$ or a weak antagonist of A_1R, but further investigation is still needed.

Previous studies have shown that severity of ataxia and lesions in the brain stem associates with energy consumption in rats (Ray et al., 1992, Song and Narahashi, 1996, Holton et al., 1997). However, the actual mechanism of how energy consumption is reduced *in vivo* remains unknown. For the first time, we show evidence that the molecular mechanism of neuroprotection in 1,3-DNB toxicity is mediated through adenosine binding to A_1R, which leads to reduced excitability.

Another significance of this study is that we suggested a possible mechanism of neuroprotection that relies on the interaction between astrocytes and neurons. Astrocytes have been known to derive various factors that are essential for neuronal function and viability, such as neurotrophic factors, cytokines and glutathione (green pathway) (Blondel et al., 2000, Dringen, 2000, Farina et al., 2007, Allaman et al., 2011). Based on known facts, possible mechanisms of neuroprotection in 1,3-DNB toxicity has been summarized in Figure 4.3. Firstly, astrocytes provide lactate for neurons to generate energy. Previous research has observed increased glucose consumption and lactate accumulation in culture media of 1,3-DNB exposed primary astrocytes (orange pathway) (Romero et al., 1995). In ischemia and glucose deprivation, this pathway is believed to have neuroprotective effects (Rouach et al., 2008, Berthet et al., 2009). In 1,3-DNB toxicity, it is possible that elevated lactate are transported into neurons as substrates to synthesis pyruvate. Secondly, astrocytes inhibit the release of excitatory neurotransmitters in presynaptic neurons and decrease excitability of postsynaptic neurons. Our results have shown that upon 1,3-DNB challenge, extracellular adenosine increases (blue pathway) (Wang et al., 2012). Elevated adenosine generates both presynaptic and postsynaptic actions by binding to inhibitory A_1R. In presynaptic terminals, A_1R signaling pathway depresses glutamate release (blue circles with blue dots) (Escartin et al., 2006). In postsynaptic terminals, A_1R signaling pathway increases K^+ conductance and decreases Ca^{2+} entry (blue arrows) (Linden, 1991, Haydon and Carmignoto,

2006). Thus, neuronal excitability is suppressed, leading to energy preservation in 1,3-DNB exposed neurons.

4.3 FUTURE DIRECTION

4.3.1 Metabolism and distribution of 1,3-DNB in brain

The capacity of metabolizing 1,3-DNB in different tissue or even different cell types should be further investigated. Previous studies have demonstrated that different tissues and cell types have different capacities to metabolize 1,3-DNB (Cossum and Rickert, 1987, Brown and Miller, 1991b, Hu et al., 1997a, Reeve and Miller, 2002b). Furthermore, 1,3-DNB metabolism has been shown to associate with radical generation, which is toxic to living bodies (Reeve and Miller, 2002b, Li et al., 2003, Hsu et al., 2007). Thus to investigate the capacity to metabolize 1,3-DNB may provide some insights to the differential regional and cellular sensitivity.

From Figure 4.2 we can see that most of the direct targets in 1,3-DNB toxicity locate in cytoplasm or even within mitochondria, indicating that 1,3-DNB has great permeability across membrane. This fits the chemical property of 1,3-DNB, which is hydrophobic and lipophilic. Thus further exploration of which organelle(s) has the highest 1,3-DNB distribution may help narrow down the potential targets for computational modeling study.

4.3.2 Docking 1,3-DNB onto other proteins

Computational modeling should be employed more extensively in the future study to avoid aimless hypothesis. The structural similarity between 1,3-DNB and adenosine has made 1,3-DNB an inhibitor for ADA (Wang et al., 2012) and a potential agonist/antagonist of ARs (Wijeyesakere, unpublished data). It is possible that 1,3-DNB also can bind to other enzymes, ion channels and receptors. Computational modeling saves time and materials, thus can be used as a tool to screen preliminary targets in 1,3-DNB toxicity, followed by molecular, cellular or animal experiments to further confirm.

4.3.3 Microdialysis

Microdialysis should be performed for two purposes. First, microdialysis combined with HPLC/MS can help us obtain an accurate adenosine level before and after 1,3-DNB toxicity. Although getting adenosine concentrations in both sensitive (brain stem) and non-sensitive (cortex) regions is ideal and more relevant in 1,3-DNB study, technique constraints may occur as inserting probes to brain may cause damage and therefore confounding adenosine release. Second, microdialysis can be used to administer different chemicals to brain regions. For example, agonists and antagonists of ARs can be tested to see if individual AR pathways are involved in 1,3-DNB toxicity *in vivo*.

4.3.4 Protein expression

Up- or down- regulation of protein in 1,3-DNB toxicity has not been fully studied. However, study has shown that the expression of certain proteins can affect the

susceptibility to 1,3-DNB (Phelka et al., 2006). Therefore, it is important to study the expression levels (mRNA and protein) of proteins before and after 1,3-DNB exposure. Based on current knowledge, proteins that are involved in energy metabolism pathways are of the most interest, especially mitochondrial proteins and proteins in purinergic pathways.

4.4 REFERENCES

(1989) Toxicology update. Dinitrobenzene. Journal of applied toxicology : JAT 9:199-202.

Allaman I, Belanger M, Magistretti PJ (2011) Astrocyte-neuron metabolic relationships: for better and for worse. Trends Neurosci 34:76-87.

Alunni S, Orru M, Ottavi L (2008) A study on the inhibition of adenosine deaminase. J Enzyme Inhib Med Chem 23:182-189.

Aoyama K, Watabe M, Nakaki T (2008) Regulation of neuronal glutathione synthesis. J Pharmacol Sci 108:227-238.

Aschner M, Costa LG (2005) The role of glia in neurotoxicity. Boca Raton, FL: CRC Press.

Ask K, Decologne N, Asare N, Holme JA, Artur Y, Pelczar H, Camus P (2004) Distribution of nitroreductive activity toward nilutamide in rat. Toxicology and applied pharmacology 201:1-9.

Attwell D, Laughlin SB (2001) An energy budget for signaling in the grey matter of the brain. Journal of cerebral blood flow and metabolism : official journal of the International Society of Cerebral Blood Flow and Metabolism 21:1133-1145.

Ault JG, Lawrence DA (2003) Glutathione distribution in normal and oxidatively stressed cells. Exp Cell Res 285:9-14.

Bagley PR, Tucker SP, Nolan C, Lindsay JG, Davies A, Baldwin SA, Cremer JE, Cunningham VJ (1989) Anatomical mapping of glucose transporter protein and pyruvate dehydrogenase in rat brain: an immunogold study. Brain research 499:214-224.

Bauer A, Holschbach MH, Meyer PT, Boy C, Herzog H, Olsson RA, Coenen HH, Zilles K (2003) In vivo imaging of adenosine A1 receptors in the human brain with [18F]CPFPX and positron emission tomography. Neuroimage 19:1760-1769.

Beauchamp RO, Irons RD, Rickert DE, Couch DB, Hamm TE (1982) A Critical-Review of the Literature on Nitrobenzene Toxicity. Crc Critical Reviews in Toxicology 11:33-84.

Belanger M, Allaman I, Magistretti PJ (2011) Brain energy metabolism: focus on astrocyte-neuron metabolic cooperation. Cell Metab 14:724-738.

Berridge MJ, Bootman MD, Lipp P (1998) Calcium--a life and death signal. Nature 395:645-648.

Berthet C, Lei H, Thevenet J, Gruetter R, Magistretti PJ, Hirt L (2009) Neuroprotective role of lactate after cerebral ischemia. Journal of cerebral blood

flow and metabolism : official journal of the International Society of Cerebral Blood Flow and Metabolism 29:1780-1789.

Betz AL (1985) Identification of hypoxanthine transport and xanthine oxidase activity in brain capillaries. Journal of neurochemistry 44:574-579.

Biaglow JE, Jacobson B, Varnes M (1978) The oxidation of ascorbate by electron affinic drugs and carcinogens. Photochem Photobiol 28:869-876.

Blackburn DM, Gray AJ, Lloyd SC, Sheard CM, Foster PM (1988a) A comparison of the effects of the three isomers of dinitrobenzene on the testis in the rat. Toxicology and applied pharmacology 92:54-64.

Blackburn DM, Gray AJ, Lloyd SC, Sheard CM, Foster PM (1988b) A comparison of the effects of the three isomers of dinitrobenzene on the testis in the rat. Toxicol Appl Pharmacol 92:54-64.

Blondel O, Collin C, McCarran WJ, Zhu S, Zamostiano R, Gozes I, Brenneman DE, McKay RD (2000) A glia-derived signal regulating neuronal differentiation. The Journal of neuroscience : the official journal of the Society for Neuroscience 20:8012-8020.

Bond JA, Chism JP, Rickert DE, Popp JA (1981) Induction of hepatic and testicular lesions in Fischer-344 rats by single oral doses of nitrobenzene. Fundam Appl Toxicol 1:389-394.

Bradley WG (2008) Neurology in clinical practice. Philadelphia: Butterworth-Heinemann/Elsevier.

Brown CD, Miller MG (1991a) Effect of Culture Age on 1,3-Dinitrobenzene Metabolism and Indicators of Cellular Toxicity in Rat Testicular Cells. Toxicol in Vitro 5:269-275.

Brown CD, Miller MG (1991b) Effect of culture age on 1,3-dinitrobenzene metabolism and indicators of cellular toxicity in rat testicular cells. Toxicol In Vitro 5:269-275.

Brown GK, Squier MV (1996) Neuropathology and pathogenesis of mitochondrial diseases. Journal of inherited metabolic disease 19:553-572.

Burnstock G (2006) Historical review: ATP as a neurotransmitter. Trends Pharmacol Sci 27:166-176.

Butina D (1999) Unsupervised data base clustering based on Daylight's fingerprint and Tanimoto similarity: A fast and automated way to cluster small and large data sets. J Chem Inf Comp Sci 39:747-750.

Butterworth RF, Kril JJ, Harper CG (1993) Thiamine-dependent enzyme changes in the brains of alcoholics: relationship to the Wernicke-Korsakoff syndrome. Alcohol Clin Exp Res 17:1084-1088.

Cavanagh JB (1988) Lesion localisation: implications for the study of functional effects and mechanisms of action. Toxicology 49:131-136.

Cavanagh JB (1992) Methyl bromide intoxication and acute energy deprivation syndromes. Neuropathology and applied neurobiology 18:575-578.

Cavanagh JB (1993) Selective vulnerability in acute energy deprivation syndromes. Neuropathology and applied neurobiology 19:461-470.

Cavanagh JB, Harding BN (1994) Pathogenic factors underlying the lesions in Leigh's disease. Tissue responses to cellular energy deprivation and their clinico-pathological consequences. Brain : a journal of neurology 117 (Pt 6):1357-1376.

Cavanagh JB, Nolan CC (1993) The neurotoxicity of alpha-chlorohydrin in rats and mice: II. Lesion topography and factors in selective vulnerability in acute energy deprivation syndromes. Neuropathology and applied neurobiology 19:471-479.

Chandra AM, Qualls CW, Jr., Reddy G (1995) 1,3,5-Trinitrobenzene-induced encephalopathy in male Fischer-344 rats. Toxicol Pathol 23:527-532.

Chaudry IH (1982) Does ATP cross the cell plasma membrane. Yale J Biol Med 55:1-10.

Cody TE, Witherup S, Hastings L, Stemmer K, Christian RT (1981a) 1,3-dinitrobenzene: toxic effects in vivo and in vitro. Journal of toxicology and environmental health 7:829-847.

Cody TE, Witherup S, Hastings L, Stemmer K, Christian RT (1981b) 1,3-dinitrobenzene: toxic effects in vivo and in vitro. J Toxicol Environ Health 7:829-847.

Coligan JE (1996) Current protocols in protein science. pp <1- > (loose-leaf) New York: John Wiley and Sons.

Cossum PA, Rickert DE (1987) Metabolism and toxicity of dinitrobenzene isomers in erythrocytes from Fischer-344 rats, rhesus monkeys and humans. Toxicology letters 37:157-163.

Cristalli G, Costanzi S, Lambertucci C, Lupidi G, Vittori S, Volpini R, Camaioni E (2001) Adenosine deaminase: functional implications and different classes of inhibitors. Med Res Rev 21:105-128.

Cunha RA (2005) Neuroprotection by adenosine in the brain: From A(1) receptor activation to A (2A) receptor blockade. Purinergic Signal 1:111-134.

Dahl HH (1998) Getting to the nucleus of mitochondrial disorders: identification of respiratory chain-enzyme genes causing Leigh syndrome. American journal of human genetics 63:1594-1597.

Davis GW (2006) Homeostatic control of neural activity: from phenomenology to molecular design. Annu Rev Neurosci 29:307-323.

de Mendonca A, Sebastiao AM, Ribeiro JA (2000) Adenosine: does it have a neuroprotective role after all? Brain Res Brain Res Rev 33:258-274.

Dringen R (2000) Metabolism and functions of glutathione in brain. Progress in neurobiology 62:649-671.

Duan Y, Wu C, Chowdhury S, Lee MC, Xiong G, Zhang W, Yang R, Cieplak P, Luo R, Lee T, Caldwell J, Wang J, Kollman P (2003) A point-charge force field for molecular mechanics simulations of proteins based on condensed-phase quantum mechanical calculations. J Comput Chem 24:1999-2012.

Escartin C, Valette J, Lebon V, Bonvento G (2006) Neuron-astrocyte interactions in the regulation of brain energy metabolism: a focus on NMR spectroscopy. J Neurochem 99:393-401.

Facchini V, Griffiths LA (1981) The involvement of the gastro-intestinal microflora in nitro-compound-induced methaemoglobinaemia in rats and its relationship to nitrogroup reduction. Biochemical pharmacology 30:931-935.

Farina C, Aloisi F, Meinl E (2007) Astrocytes are active players in cerebral innate immunity. Trends Immunol 28:138-145.

Fastbom J, Pazos A, Palacios JM (1987a) The distribution of adenosine A1 receptors and 5'-nucleotidase in the brain of some commonly used experimental animals. Neuroscience 22:813-826.

Fastbom J, Pazos A, Probst A, Palacios JM (1987b) Adenosine A1 receptors in the human brain: a quantitative autoradiographic study. Neuroscience 22:827-839.

Ferrara P, Gohlke H, Price DJ, Klebe G, Brooks CL (2004) Assessing scoring functions for protein-ligand interactions. J Med Chem 47:3032-3047.

Foster PM (1989) M-dinitrobenzene: studies on its toxicity to the testicular Sertoli cell. Archives of toxicology Supplement = Archiv fur Toxikologie Supplement 13:3-17.

Fredholm BB (2007a) Adenosine, an endogenous distress signal, modulates tissue damage and repair. Cell death and differentiation 14:1315-1323.

Fredholm BB (2007b) Adenosine, an endogenous distress signal, modulates tissue damage and repair. Cell Death Differ 14:1315-1323.

Fredholm BB, Chen JF, Masino SA, Vaugeois JM (2005) Actions of adenosine at its receptors in the CNS: insights from knockouts and drugs. Annu Rev Pharmacol Toxicol 45:385-412.

Frenguelli BG, Llaudet E, Dale N (2003) High-resolution real-time recording with microelectrode biosensors reveals novel aspects of adenosine release during hypoxia in rat hippocampal slices. J Neurochem 86:1506-1515.

Frick L, Wolfenden R, Smal E, Baker DC (1986) Transition-state stabilization by adenosine deaminase: structural studies of its inhibitory complex with deoxycoformycin. Biochemistry 25:1616-1621.

Gracia E, Cortes A, Meana JJ, Garcia-Sevilla J, Herhsfield MS, Canela EI, Mallol J, Lluis C, Franco R, Casado V (2008) Human adenosine deaminase as an allosteric modulator of human A(1) adenosine receptor: abolishment of negative cooperativity for [H-3](R)-pia binding to the caudate nucleus. Journal of Neurochemistry 107:161-170.

Halldner L, Lopes LV, Dare E, Lindstrom K, Johansson B, Ledent C, Cunha RA, Fredholm BB (2004) Binding of adenosine receptor ligands to brain of adenosine receptor knock-out mice: evidence that CGS 21680 binds to A1 receptors in hippocampus. Naunyn Schmiedebergs Arch Pharmacol 370:270-278.

Harada N, Omura T (1980) Participation of cytochrome P-450 in the reduction of nitro compounds by rat liver microsomes. J Biochem 87:1539-1554.

Haydon PG, Carmignoto G (2006) Astrocyte control of synaptic transmission and neurovascular coupling. Physiol Rev 86:1009-1031.

Hengartner MO (2000) The biochemistry of apoptosis. Nature 407:770-776.

Hockenbery DM, Oltvai ZN, Yin XM, Milliman CL, Korsmeyer SJ (1993) Bcl-2 functions in an antioxidant pathway to prevent apoptosis. Cell 75:241-251.

Holder JW (1999) Nitrobenzene carcinogenicity in animals and human hazard evaluation. Toxicol Ind Health 15:445-457.

Holton JL, Nolan CC, Burr SA, Ray DE, Cavanagh JB (1997) Increasing or decreasing nervous activity modulates the severity of the glio-vascular lesions of 1,3-dinitrobenzene in the rat: effects of the tremorgenic pyrethroid, Bifenthrin, and of anaesthesia. Acta Neuropathol 93:159-165.

Hsu CH, Stedeford T, Okochi-Takada E, Ushijima T, Noguchi H, Muro-Cacho C, Holder JW, Banasik M (2007) Framework analysis for the carcinogenic mode of action of nitrobenzene. Journal of Environmental Science and Health Part C-Environmental Carcinogenesis & Ecotoxicology Reviews 25:155-184.

Hu HL, Bennett N, Holton JL, Nolan CC, Lister T, Cavanagh JB, Ray DE (1999) Glutathione depletion increases brain susceptibility to m-dinitrobenzene neurotoxicity. Neurotoxicology 20:83-90.

Hu HL, Bennett N, Lamb JH, Ghersi-Egea JF, Schlosshauer B, Ray DE (1997a) Capacity of rat brain to metabolize m-dinitrobenzene: an in vitro study. Neurotoxicology 18:363-370.

Hu HL, Bennett N, Lamb JH, GhersiEgea JF, Schlosshauer B, Ray DE (1997b) Capacity of rat brain to metabolize m-dinitrobenzene: an in vitro study. Neurotoxicology 18:363-370.

Ikeda M, Kita A (1964) Excretion of P-Nitrophenol and P-Aminophenol in the Urine of a Patient Exposed to Nitrobenzene. British journal of industrial medicine 21:210-213.

Johansson B, Georgiev V, Fredholm BB (1997) Distribution and postnatal ontogeny of adenosine A2A receptors in rat brain: comparison with dopamine receptors. Neuroscience 80:1187-1207.

Johansson B, Halldner L, Dunwiddie TV, Masino SA, Poelchen W, Gimenez-Llort L, Escorihuela RM, Fernandez-Teruel A, Wiesenfeld-Hallin Z, Xu XJ, Hardemark A, Betsholtz C, Herlenius E, Fredholm BB (2001) Hyperalgesia, anxiety, and decreased hypoxic neuroprotection in mice lacking the adenosine A1 receptor. Proc Natl Acad Sci U S A 98:9407-9412.

Jones BE (2009) Glia, adenosine, and sleep. Neuron 61:156-157.

Kaplan NO (1955) Specific Adenosine Deaminase from Intestine. Method Enzymol 2:473-475.

Kauffman FC, Johnson EC (1974) Cerebral energy reserves and glycolysis in neural tissue of 6-aminonicotinamide-treated mice. J Neurobiol 5:379-392.

Kinoshita T, Nakanishi I, Terasaka T, Kuno M, Seki N, Warizaya M, Matsumura H, Inoue T, Takano K, Adachi H, Mori Y, Fujii T (2005) Structural basis of compound recognition by adenosine deaminase. Biochemistry-Us 44:10562-10569.

Kinoshita T, Tada T, Nakanishi I (2008) Conformational change of adenosine deaminase during ligand-exchange in a crystal. Biochem Biophys Res Commun 373:53-57.

Krieger E, Darden T, Nabuurs SB, Finkelstein A, Vriend G (2004) Making optimal use of empirical energy functions: Force-field parameterization in crystal space. Proteins 57:678-683.

Kumar A, Chawla R, Ahuja S, Girdhar KK, Bhattacharya A (1990) Nitrobenzene poisoning and spurious pulse oximetry. Anaesthesia 45:949-951.

Kurz LC, Moix L, Riley MC, Frieden C (1992) The rate of formation of transition-state analogues in the active site of adenosine deaminase is encounter-controlled: implications for the mechanism. Biochemistry 31:39-48.

Kwan AC (2008) What can population calcium imaging tell us about neural circuits? J Neurophysiol 100:2977-2980.

Latini S, Pedata F (2001) Adenosine in the central nervous system: release mechanisms and extracellular concentrations. Journal of neurochemistry 79:463-484.

Lee HB, Blaufox MD (1985) Blood volume in the rat. J Nucl Med 26:72-76.

Levin AA, Dent JG (1982) Comparison of the metabolism of nitrobenzene by hepatic microsomes and cecal microflora from Fischer-344 rats in vitro and the relative importance of each in vivo. Drug metabolism and disposition: the biological fate of chemicals 10:450-454.

Li H, Wang H, Sun H, Liu Y, Liu K, Peng S (2003) Binding of nitrobenzene to hepatic DNA and hemoglobin at low doses in mice. Toxicol Lett 139:25-32.

Lin MS, Hung KS, Chiu WT, Sun YY, Tsai SH, Lin JW, Lee YH (2011) Curcumin enhances neuronal survival in N-methyl-d-aspartic acid toxicity by inducing RANTES expression in astrocytes via PI-3K and MAPK signaling pathways. Prog Neuropsychopharmacol Biol Psychiatry 35:931-938.

Linden J (1991) Structure and function of A1 adenosine receptors. Faseb J 5:2668-2676.

Logan M, Sweeney MI (1997) Adenosine A1 receptor activation preferentially protects cultured cerebellar neurons versus astrocytes against hypoxia-induced death. Mol Chem Neuropathol 31:119-133.

Lopes LV, Halldner L, Rebola N, Johansson B, Ledent C, Chen JF, Fredholm BB, Cunha RA (2004) Binding of the prototypical adenosine A(2A) receptor agonist CGS 21680 to the cerebral cortex of adenosine A(1) and A(2A) receptor knockout mice. Br J Pharmacol 141:1006-1014.

Lutz PL, Nilsson GE, Prentice HM (2003) The brain without oxygen : causes of failure--physiological and molecular mechanisms for survival. Dordrecht ; Boston: Kluwer Academic Pub.

Martin PR, Singleton CK, Hiller-Sturmhofel S (2003) The role of thiamine deficiency in alcoholic brain disease. Alcohol research & health : the journal of the National Institute on Alcohol Abuse and Alcoholism 27:134-142.

Marzo I, Brenner C, Zamzami N, Jurgensmeier JM, Susin SA, Vieira HL, Prevost MC, Xie Z, Matsuyama S, Reed JC, Kroemer G (1998) Bax and adenine nucleotide translocator cooperate in the mitochondrial control of apoptosis. Science 281:2027-2031.

Mason RP, Holtzman JL (1975) The mechanism of microsomal and mitochondrial nitroreductase. Electron spin resonance evidence for nitroaromatic free radical intermediates. Biochemistry 14:1626-1632.

Mavroudis G, Prior MJ, Lister T, Nolan CC, Ray DE (2006a) Neurochemical and oedematous changes in 1,3-dinitrobenzene-induced astroglial injury in rat brain

from a 1H-nuclear magnetic resonance perspective. J Neural Transm 113:1263-1278.

Mavroudis G, Prior MJ, Lister T, Nolan CC, Ray DE (2006b) Neurochemical and oedematous changes in 1,3-dinitrobenzene-induced astroglial injury in rat brain from a 1H-nuclear magnetic resonance perspective. J Neural Transm 113:1263-1278.

Meyer-Estorf G, Schulze PE, Herken H (1973) Distribution of 3 H-labelled 6-aminonicotinamide and accumulation of 6-phosphogluconate in the spinal cord. Naunyn-Schmiedeberg's archives of pharmacology 276:235-241.

Miller JA, Runkle SA, Tjalkens RB, Philbert MA (2011a) 1,3-Dinitrobenzene-induced metabolic impairment through selective inactivation of the pyruvate dehydrogenase complex. Toxicological sciences : an official journal of the Society of Toxicology 122:502-511.

Miller JA, Runkle SA, Tjalkens RB, Philbert MA (2011b) 1,3-Dinitrobenzene Induced Metabolic Impairment Through Selective Inactivation of the Pyruvate Dehydrogenase Complex. Toxicol Sci.

Morgan KT, Gross EA, Lyght O, Bond JA (1985) Morphologic and biochemical studies of a nitrobenzene-induced encephalopathy in rats. Neurotoxicology 6:105-116.

Morris GM, Goodsell DS, Halliday RS, Huey R, Hart WE, Belew RK, Olson AJ (1998) Automated docking using a Lamarckian genetic algorithm and an empirical binding free energy function. J Comput Chem 19:1639-1662.

Morrison RS, de Vellis J (1983) Differentiation of purified astrocytes in a chemically defined medium. Brain Res 285:337-345.

Mott JL, Zhang D, Freeman JC, Mikolajczak P, Chang SW, Zassenhaus HP (2004) Cardiac disease due to random mitochondrial DNA mutations is prevented by cyclosporin A. Biochem Biophys Res Commun 319:1210-1215.

North RA, Verkhratsky A (2006) Purinergic transmission in the central nervous system. Pflugers Arch 452:479-485.

O'Leary T, Wyllie DJ (2011) Neuronal homeostasis: time for a change? The Journal of physiology 589:4811-4826.

O'Shaughnessy PJ, Morris ID, Huhtaniemi I, Baker PJ, Abel MH (2009) Role of androgen and gonadotrophins in the development and function of the Sertoli cells and Leydig cells: data from mutant and genetically modified mice. Mol Cell Endocrinol 306:2-8.

Pak MA, Haas HL, Decking UK, Schrader J (1994) Inhibition of adenosine kinase increases endogenous adenosine and depresses neuronal activity in hippocampal slices. Neuropharmacology 33:1049-1053.

Pal D, Chakrabarti P (1999) Cis peptide bonds in proteins: residues involved, their conformations, interactions and locations. J Mol Biol 294:271-288.

Parke DV (1961) Studies in detoxication. 85. The metabolism of m-dinitro[C]benzene in the rabbit. Biochem J 78:262-271.

Parkinson FE, Xiong W, Zamzow CR (2005) Astrocytes and neurons: different roles in regulating adenosine levels. Neurol Res 27:153-160.

Pellerin L, Magistretti PJ (2004) Neuroenergetics: calling upon astrocytes to satisfy hungry neurons. The Neuroscientist : a review journal bringing neurobiology, neurology and psychiatry 10:53-62.

Perez-Reyes E, Kalyanaraman B, Mason RP (1980) The reductive metabolism of metronidazole and ronidazole by aerobic liver microsomes. Mol Pharmacol 17:239-244.

Phelka AD, Beck MJ, Philbert MA (2003) 1,3-Dinitrobenzene inhibits mitochondrial complex II in rat and mouse brainstem and cortical astrocytes. Neurotoxicology 24:403-415.

Phelka AD, Sadoff MM, Martin BP, Philbert MA (2006) BCL-XL expression levels influence differential regional astrocytic susceptibility to 1,3-dinitrobenzene. Neurotoxicology 27:192-200.

Philbert MA, Billingsley ML, Reuhl KR (2000) Mechanisms of injury in the central nervous system. Toxicol Pathol 28:43-53.

Philbert MA, Nolan CC, Cremer JE, Tucker D, Brown AW (1987) 1,3-Dinitrobenzene-induced encephalopathy in rats. Neuropathology and applied neurobiology 13:371-389.

Phillips E, Newsholme EA (1979) Maximum activities, properties and distribution of 5' nucleotidase, adenosine kinase and adenosine deaminase in rat and human brain. J Neurochem 33:553-558.

Prinz H (2009) Hill coefficients, dose-response curves and allosteric mechanisms. J Chem Biol.

Ramakers GJ, Moolenaar WH (1998) Regulation of astrocyte morphology by RhoA and lysophosphatidic acid. Exp Cell Res 245:252-262.

Ray DE, Brown AW, Cavanagh JB, Nolan CC, Richards HK, Wylie SP (1992) Functional/metabolic modulation of the brain stem lesions caused by 1,3-dinitrobenzene in the rat. Neurotoxicology 13:379-388.

Reader SC, Shingles C, Stonard MD (1991) Acute testicular toxicity of 1,3-dinitrobenzene and ethylene glycol monomethyl ether in the rat: evaluation of biochemical effect markers and hormonal responses. Fundam Appl Toxicol 16:61-70.

Reddy BG, Pohl LR, Krishna G (1976) The requirement of the gut flora in nitrobenzene-induced methemoglobinemia in rats. Biochemical pharmacology 25:1119-1122.

Reeve IT, Miller MG (2002a) 1,3-Dinitrobenzene metabolism and protein binding. Chem Res Toxicol 15:352-360.

Reeve IT, Miller MG (2002b) 1,3-Dinitrobenzene metabolism and protein binding. Chemical research in toxicology 15:352-360.

Ribeiro JA, Sebastiao AM (2010) Modulation and metamodulation of synapses by adenosine. Acta Physiol (Oxf) 199:161-169.

Rickert DE (1985) Toxicity of nitroaromatic compounds. Washington [D.C.]: Hemisphere Pub. Corp.

Rickert DE (1987) Metabolism of nitroaromatic compounds. Drug Metab Rev 18:23-53.

Rickert DE, Bond JA, Long RM, Chism JP (1983) Metabolism and excretion of nitrobenzene by rats and mice. Toxicology and applied pharmacology 67:206-214.

Romero I, Brown AW, Cavanagh JB, Nolan CC, Ray DE, Seville MP (1991) Vascular factors in the neurotoxic damage caused by 1,3-dinitrobenzene in the rat. Neuropathology and applied neurobiology 17:495-508.

Romero IA, Lister T, Richards HK, Seville MP, Wylie SP, Ray DE (1995) Early metabolic changes during m-Dinitrobenzene neurotoxicity and the possible role of oxidative stress. Free Radic Biol Med 18:311-319.

Romero IA, Ray DE, Chan MW, Abbott NJ (1996) An in vitro study of m-dinitrobenzene toxicity on the cellular components of the blood-brain barrier, astrocytes and endothelial cells. Toxicology and applied pharmacology 139:94-101.

Rouach N, Koulakoff A, Abudara V, Willecke K, Giaume C (2008) Astroglial metabolic networks sustain hippocampal synaptic transmission. Science 322:1551-1555.

Salmowa J, Piotrowski J, Neuhorn U (1963) Evaluation of exposure to nitrobenzene. Absorption of nitrobenzene vapour through lungs and excretion of p-nitrophenol in urine. Br J Ind Med 20:41-46.

Schneider H, Cervos-Navarro J (1974) Acute gliopathy in spinal cord and brain stem induced by 6-aminonicotinamide. Acta Neuropathol 27:11-23.

Sealy RC, Swartz HM, Olive PL (1978) Electron spin resonance-spin trapping. Detection of superoxide formation during aerobic microsomal reduction of nitro-compounds. Biochem Biophys Res Commun 82:680-684.

Sedel F, Challe G, Mayer JM, Boutron A, Fontaine B, Saudubray JM, Brivet M (2008) Thiamine responsive pyruvate dehydrogenase deficiency in an adult with peripheral neuropathy and optic neuropathy. Journal of neurology, neurosurgery, and psychiatry 79:846-847.

Seidler J, McGovern SL, Doman TN, Shoichet BK (2003) Identification and prediction of promiscuous aggregating inhibitors among known drugs. J Med Chem 46:4477-4486.

Shao JL, Wan XH, Chen Y, Bi C, Chen HM, Zhong Y, Heng XH, Qian JQ (2011) H2S protects hippocampal neurons from anoxia-reoxygenation through cAMP-mediated PI3K/Akt/p70S6K cell-survival signaling pathways. J Mol Neurosci 43:453-460.

Silver J, Miller JH (2004) Regeneration beyond the glial scar. Nat Rev Neurosci 5:146-156.

Song JH, Narahashi T (1996) Modulation of sodium channels of rat cerebellar Purkinje neurons by the pyrethroid tetramethrin. J Pharmacol Exp Ther 277:445-453.

Sperlagh B, Vizi ES (2011) The role of extracellular adenosine in chemical neurotransmission in the hippocampus and Basal Ganglia: pharmacological and clinical aspects. Current topics in medicinal chemistry 11:1034-1046.

Squier MV, Thompson J, Rajgopalan B (1992) Case report: neuropathology of methyl bromide intoxication. Neuropathology and applied neurobiology 18:579-584.

Steiner SR, Philbert MA (2011) Proteomic identification of carbonylated proteins in 1,3-dinitrobenzene neurotoxicity. Neurotoxicology 32:362-373.

Stevenson D, Jones AR (1985) Production of (S)-3-chlorolactaldehyde from (S)-alpha-chlorohydrin by boar spermatozoa and the inhibition of glyceraldehyde 3-phosphate dehydrogenase in vitro. Journal of reproduction and fertility 74:157-165.

Stone TW, Ceruti S, Abbracchio MP (2009) Adenosine receptors and neurological disease: neuroprotection and neurodegeneration. Handb Exp Pharmacol 535-587.

Sweeney MI (1997) Neuroprotective effects of adenosine in cerebral ischemia: window of opportunity. Neurosci Biobehav Rev 21:207-217.

Takahashi T, Otsuguro K, Ohta T, Ito S (2010a) Adenosine and inosine release during hypoxia in the isolated spinal cord of neonatal rats. British journal of pharmacology 161:1806-1816.

Takahashi T, Otsuguro K, Ohta T, Ito S (2010b) Adenosine and inosine release during hypoxia in the isolated spinal cord of neonatal rats. Br J Pharmacol 161:1806-1816.

Tjalkens RB, Ewing MM, Philbert MA (2000a) Differential cellular regulation of the mitochondrial permeability transition in an in vitro model of 1,3-dinitrobenzene-induced encephalopathy. Brain research 874:165-177.

Tjalkens RB, Ewing MM, Philbert MA (2000b) Differential cellular regulation of the mitochondrial permeability transition in an in vitro model of 1,3-dinitrobenzene-induced encephalopathy. Brain Res 874:165-177.

Tjalkens RB, Phelka AD, Philbert MA (2003) Regional variation in the activation threshold for 1,3-DNB-induced mitochondrial permeability transition in brainstem and cortical astrocytes. Neurotoxicology 24:391-401.

U.S. Department of Health and Human Services (1995) Toxicological profile for 1,3-dinitrobenzene and 1,3,5-trinitrobenzene.

U.S. Environmental Protection Agency (1997) 1,3,5-Trinitrobenzene support documents.

U.S. Environmental Protection Agency (2009) Toxicological review of nitrobenzene.

Vasquez GB, Reddy G, Gilliland GL, Stevens WJ (1995) Dinitrobenzene induces methemoglobin formation from deoxyhemoglobin in vitro. Chemico-biological interactions 96:157-171.

Vijayaraghavan S (2009) Glial-neuronal interactions--implications for plasticity and drug addiction. AAPS J 11:123-132.

Wang SH, Wang SF, Xuan W, Zeng ZH, Jin JY, Ma J, Tian GR (2008) Nitro as a novel zinc-binding group in the inhibition of carboxypeptidase A. Bioorg Med Chem 16:3596-3601.

Wang YP, Liu X, Schneider B, Zverina EA, Russ K, Wijeyesakere SJ, Fierke CA, Richardson RJ, Philbert MA (2012) Mixed Inhibition of Adenosine Deaminase Activity by 1,3-Dinitrobenzene: A Model for Understanding Cell-Selective Neurotoxicity in Chemically-Induced Energy Deprivation Syndromes in Brain. Toxicological Sciences 125:509-521.

Williams ES, Phelka A, Ray DE, Philbert MA (2005) Astrocytes in Acute Energy Deprivation Syndromes: CRC Press.

Wolfenden R, Snider MJ (2001) The depth of chemical time and the power of enzymes as catalysts. Acc Chem Res 34:938-945.

Xu J, Nolan CC, Lister T, Purcell WM, Ray DE (1999a) Pharmacokinetic factors and concentration-time threshold in m-dinitrobenzene-induced neurotoxicity. Toxicol Appl Pharmacol 161:267-273.

Xu J, Nolan CC, Lister T, Purcell WM, Ray DE (1999b) Pharmacokinetic factors and concentration-time threshold in m-dinitrobenzene-induced neurotoxicity. Toxicology and applied pharmacology 161:267-273.

Xu Y, Venton BJ (2010a) Rapid determination of adenosine deaminase kinetics using fast-scan cyclic voltammetry. Phys Chem Chem Phys 12:10027-10032.

Xu YD, Venton BJ (2010b) Rapid determination of adenosine deaminase kinetics using fast-scan cyclic voltammetry. Phys Chem Chem Phys 12:10027-10032.

Zamzami N, Susin SA, Marchetti P, Hirsch T, Gomez-Monterrey I, Castedo M, Kroemer G (1996) Mitochondrial control of nuclear apoptosis. The Journal of experimental medicine 183:1533-1544.

4.5 FIGURES

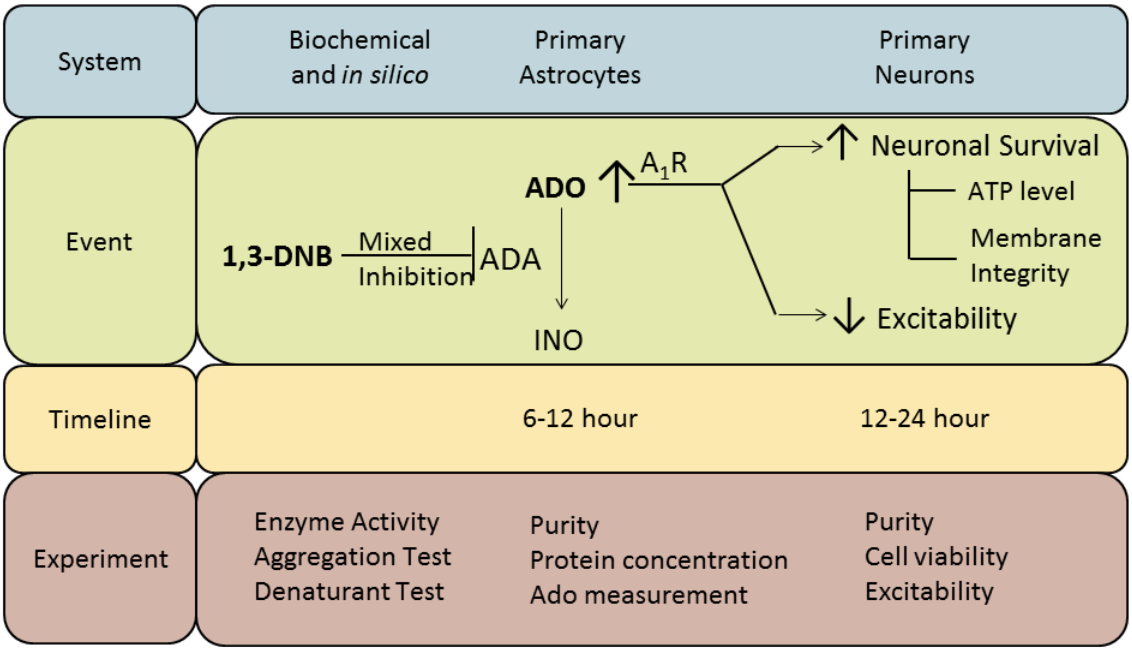

Figure 4.1. Results summary.

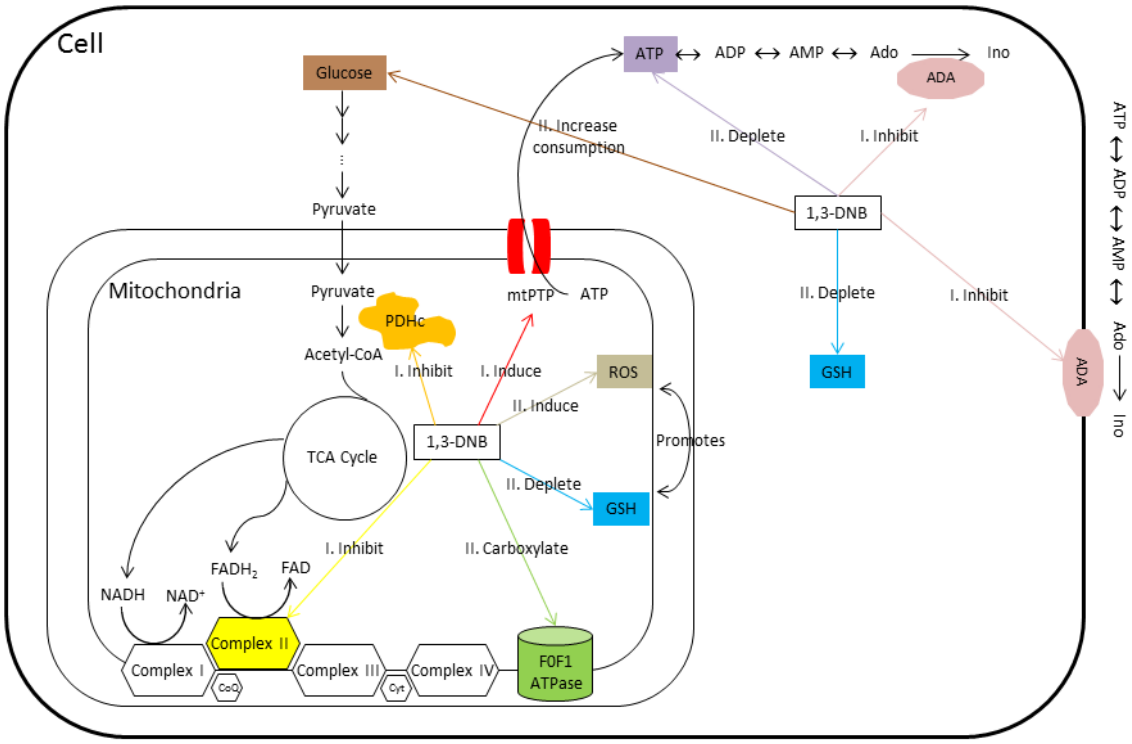

Figure 4.2 Targets in 1,3-DNB toxicity.

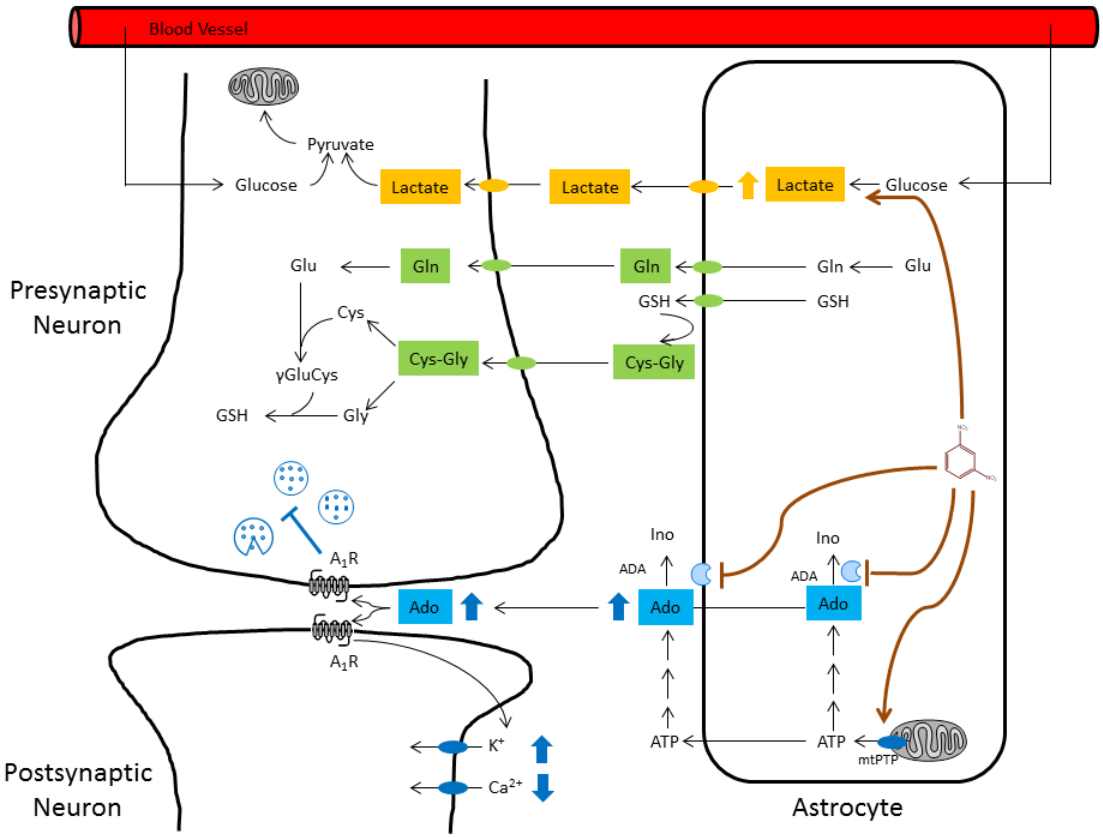

Figure 4.3. Proposed neuroprotection mechanism of adenosine in 1,3-DNB toxicity.

Oval shape located on the cell membrane indicates transporters and ion channels. Oval shape locate on mitochondrial membrane indicates mtPTP. Blue circles with dots in presynaptic neurons represent vesicles containing neurotransmitters, in this case, glutamate. Blue Pacmans in the cytoplasm and on the cell membrane of astrocyte show cytoplasmic and membrane ADAs, respectively.